THE UNIVERSITY OF MICHIGAN

INDUSTRY PROGRAM OF THE COLLEGE OF ENGINEERING

THE EFFECT OF NUCLEAR RADIATIONS ON BENZENE-WATER SYSTEMS

Terry Robert Johnson

A dissertation submitted in partial fulfillment
of the requirements for the degree of
Doctor of Philosophy in the
University of Michigan
1959

February 1959

IP-352

TABLE OF CONTENTS

TABLE OF CONTENTS (CONT'D)

LIST OF FIGURES

LIST OF FIGURES (CONT'D)

I. INTRODUCTION

Interest in the field of radiation chemistry has grown at a rapidly increasing rate in the last ten years. Impetus for this growth is the availability of high level radiation sources and the possible application of radiation to produce chemicals commercially. Nuclear reactors make available artificial isotope sources such as cobalt, cesium, and fission products. The use of particle accelerators has become more widespread. Now most large industrial laboratories have some kind of accelerator capable of producing radiation with energies of one million electron volts or more.

At the present time actual commercial applications of radiation to the promotion of chemical reactions are few and are limited to the field of polymers. The limiting factors today are the small size of the sources even though kilocurie sources are available, the costs involved partly because of the uncertainty of the economics, and the lack of understanding of the fundamental processes of radiation chemistry. The next few years should see these factors partly overcome, resulting in the increased commercial application of radiation chemistry.

Nuclear reactors are a source of ionizing radiation that is orders of magnitude larger than present isotope and machine sources. There is interest today in constructing a reactor for a chemical manufacturing plant. The reactor would supply the heat and power requirements and the ionizing radiation that would be used to catalyze reactions. Since a power reactor is still economically marginal, it is imperative that the "by-products" of the reactor be used advantageously. One of

these by-products is the radiation emitted mainly in the form of gammas and neutrons. In present reactor designs this radiant energy is absorbed in thick shields and dissipated as heat. If this energy could be absorbed usefully in a chemical system, it would favorably influence the economics of the reactor.

The study reported in this paper investigated the effect of the radiation from the Ford Nuclear Reactor on benzene dissolved in water solutions. This system was selected even though it has no commercial importance. The principal consideration in its selection was that it would possibly yield significant basic results. Much of the work in the past few years has been in the field of dilute aqueous solutions. Some success has been achieved in developing a theory of the radiation chemistry of aqueous solutions. It is hoped that this study will add to this theory.

The effect of several variables on the radiation chemistry of aqueous benzene were studied in cobalt-60 and pile radiation. These were dose, dose rate, benzene concentration, and oxygen concentration. The yield of phenol in the pile radiation was compared to the yield in cobalt radiation in order to detect the effect of neutrons. Solutes with high neutron absorption cross-sections were added to the benzene solutions in order to increase the energy released by neutrons. These solutes were cadmium sulfate, boric acid, and lithium metaborate.

Water saturated with benzene has several important advantages as a dosimeter over the standard ferrous dosimeter. This is pointed out in this paper and work was done to develop this system as a quantitative gamma dosimeter.

A discussion of the many problems associated with the irradiation of chemical samples in a nuclear reactor is presented. Most of these are problems met in this program and some are unique to a swimming pool reactor. The problems are discussed in this paper because they may be of some general interest. The choice of an experimental system was made after some preliminary work with other reactions. These included the copolymerization of n-hexene-1 and sulfur dioxide, and the decomposition of chlorinated hydrocarbons.

II. THEORETICAL BACKGROUND

A. Interaction of Radiation and Matter

Ionizing radiation can be divided conveniently into two general classes: (1) photons and fast electrons; (2) heavy charged particles. Photons and electrons ionize and excite atoms but cannot move atoms. Heavy particles can move[1] atoms by collision as well as cause ionizations and excitations. The average energy loss per unit path length (linear energy transfer) for photons and electrons is generally much lower than that of heavy ions. The linear energy transfer (LET) of the particle is directly related to the ionization density. Neutrons may be considered in class 2 even though they do not ionize matter directly. Fast neutrons cause ionizations by scattering from nuclei, thereby accelerating the nucleus and causing it to lose some or all of its orbital electrons. Neutron captures by nuclei result in the emission of one or more types of ionizing radiation.

Photons lose[37] energy to matter through interaction with orbital electrons, the photoelectric and Compton effects, or with the nuclear fields, pair production. The Compton effect is the most important in the range of photon energies (0.1 - 5 Mev) used in most chemical studies. In a Compton interaction the photon behaves like a particle striking an electron. The result is a photon with a lower energy and an energetic electron. The photon cannot lose all its energy in a Compton encounter, and each collision yields an energetic electron. For 1 Mev gamma photons, the average energy of the recoil electrons is 440 kev.[110]

As the photon energy is degraded through one or more Compton scatters, the probability for a photoelectric event is increased. In such

an event the photon is completely absorbed. An orbital electron is ejected with a kinetic energy equal to the energy of the incident photon less the ionization potential of that electron.

Heavy charged particles transfer[102] their energy to the electrons by means of the Coulomb forces between the charged particles. They are characterized by very dense ionization and rapid dissipation of their energy. The path of a heavy particle is a fairly straight line. The electrons are given sufficient energy to be freed from the atomic orbits but they have a low average kinetic energy.

A high energy electron moving through a medium will interact many times, and because of its small mass will be deflected so that its path will not be straight. Ionization results from the same mechanism as that of alpha particles, but other effects[59] are important. Photons are produced by the accelerated electrons and the electrons are scattered elastically by the electron and nuclear fields of the atoms.

The effect of all ionizing radiation in matter is the formation of electrons, ions and excited molecules. Any differences in the chemical effect of particles must be related to differences in the ionization density and to the ability of heavy particles to move atoms. The actual charge or mass input of the ionizing beam is negligible in most chemical studies.

B. Primary Events

1. The Fate of Electrons

The Compton electrons formed by the initial action of the radiation are too energetic to be captured by any molecule or positive ion.

The fast electrons ionize other molecules forming secondary electrons. The process may be represented as:

$$(1) \qquad e_1^- + R \rightarrow R^+ + e_1^- + e_2^-$$

A maximum of one half of the original energy of the electron is transferred in each interaction. However, the average fraction of initial energy lost per interaction is 3% to 10%.[68] Less than one thousandth of the energy transferred is absorbed by the molecule itself. The initial ionizing events involve any electron in the atomic orbit randomly, but electrons with low energies will prefer certain orbitals and transitions. The slowing down process of the Compton electrons is repeated until the electron has an energy lower than the lowest excitation energy of the system molecules.

For the most part, the electrons produced by the primary Compton recoil electrons or directly by high energy charged particles have energies below 100 ev. These electrons can penetrate less than 20 Å in liquids and produce[59] in this small region from 1 to 5 additional ionizations and approximately the same number of excitations. Thus a small region around the point of original formation of the secondary electron contains several ions and excited molecules. Fast electrons create these secondary electrons at widely spaced intervals. Each cluster of excited species surrounding a secondary ionization is isolated from every other cluster. Heavy particles form these clusters so close to one another that the clusters form a continuous cylinder of excitation.

The slowing process of the secondary electron is extremely rapid ($<10^{-13}$ sec.).[85] The thermalized electron can neutralize a positive

ion yielding an excited molecule with approximately 10 ev of excess energy. The probability of a radiative capture is negligible.(67)

(2) $$R^+ + e^- \rightarrow R^*$$

The capture of an electron by a neutral molecule is unlikely and can be ignored(68,85) in most chemical systems unless one species has a high electron affinity. Secondary ionization processes have been postulated in the gas phase. A particular example(35) is the ionization of hydrogen bromide by alphas:

(3) $$HBr \rightarrow HBr^+ + e^-$$

$$HBr^+ + HBr \rightarrow H_2Br^+ + Br$$

Secondary ion reactions have been postulated in water solutions where the ions may be stabilized(24) by the polar water molecule. However, these reactions seem to have little effect on the final chemical product. They must occur very rapidly since the ions are generally supposed to be very short lived, ($<10^{-12}$ sec.).(91) Charge transfer reactions in the liquid phase are also unimportant. It is generally assumed that ions have no importance in the mechanism of reactions in the liquid phase. This is not true(74) in low pressure gas phases.

The actual fate of electrons is of great importance to radiation chemistry as pointed out by R. L. Platzman.(85) The fate of thermal electrons is unknown and is a basic point of contention in radiation chemistry today. Thermal electrons have energies below the lowest excitation energy of the system molecules. Samuel and Magee(91) have developed a classical model of secondary electron formation that indicates that slow daughter

electrons never leave the Coulomb field of the parent ion. The electrons are eventually recaptured in a very short time ($<10^{-12}$ sec.) by the same ion from which they were formed. Platzman has suggested that electrons may have a long lifetime and will escape the attractive field of the parent ion. The contribution of these electrons can be significant. It is estimated that these subexcitation electrons can dissipate 15-20% of the total absorbed energy. Effects on a dissolved solute generally attributed to the "indirect action" of energy absorbed in the solvent might be explained by subexcitation electrons. If the solute had the lowest excitation energy, the electrons will excite[12] these molecules preferentially. One result is fluorescence caused by an excited electron falling to the ground state as observed in some solutions. It will be pointed out later that the lifetime of the electrons, and therefore the ions, is important to the theory of aqueous solutions.

2. Fate of the Activated Species

Activated molecules are also produced from the direct action of radiation. It is not known how many energetic molecules are formed and what their energies are. It is estimated that half the absorbed energy yields activated molecules directly. Measured values of the energy absorbed per ion pair formed are approximately twice the ionization energy of the molecule for several gases. This is assumed for the liquid phase as no experimental measurements have been reported.

The activated molecules, formed by the direct action of radiation and the neutralization of ions, transfer energy to other molecules through collisions; suffer rearrangement to reach a stable state; or decompose into free radicals. The energy transfer process is of basic importance but is poorly understood.

Burton[17,18,20] has pointed out a trend in the radiation effects in the liquid phase of the members of an organic homologous series. As the size of the molecule increases, the products of the radiation-induced reactions become more specific, and in some cases the larger molecules are more stable.[92] Actual fragmentation of a molecule can occur at a point remote from the original point of impact. The reasons for these observed facts may be due to the Franck-Rabinowitsch cage effect and the size and configuration of the molecule. The ionic configuration of a larger molecule is more similar to that of the uncharged molecule. Less rearrangement is necessary after neutralization. The energy of excitation can be more evenly distributed in a large molecule, increasing the probability of deactivation. Decomposition by the lowest energy route, favoring certain specific decompositions, is more likely in larger molecules.

The energy is initially concentrated at the atom involved in the neutralization step. However, the energy is transferred in preferred ways to other parts of the molecule and probably appears in all modes of molecular energy. If the molecule is large the energy can be shared and dissipated in such a way that the breaking energy of any single bond is not exceeded. In smaller molecules energy distribution without bond rupture is more unlikely. Polarizing groups such as carbonyl, carboxyl, or amine may weaken adjacent bonds or prevent the effective energy transfer. The predominant effect is then the breaking of bonds adjacent to these groups. The radiolysis of aliphatic acids yields[99] principally hydrogen and carbon dioxide indicating decomposition of the carboxyl group.

Electrons may be involved in this intramolecular energy transfer. The radiation stability of the benzene ring has been attributed[20,71] to

the non-localized bonding orbitals allowing a more rapid and uniform distribution of energy over the entire molecule.

The Franck-Rabinowitsch[39] "cage effect" qualitatively explains radiation effects in liquid systems. Two energetic radicals formed from the dissociation of a single activated molecule collide with the neighboring molecules and lose kinetic energy. In the dense liquid phase the neighboring molecules are closely packed and form the walls of a cage. Unless the radicals escape the cage or react with the wall molecules before losing their kinetic energy, they will react with one another again.

Noyes[81] has discussed the cage effect in more quantitative terms. He postulated that a primary recombination of radicals takes place in a time greater than a molecular vibration (10^{-13} sec.), but less than the time required for the molecule to diffuse a distance equal to a molecular diameter (10^{-11} sec.). The probability of reacting with the cage walls is extremely low even in solutions with high concentrations of "radical traps" or scavengers. Radicals escaping the primary recombination, may suffer secondary recombination after diffusing for times between 10^{-11} - 10^{-9} seconds. The probability of secondary recombination in the cage decreases rapidly with time after dissociation.

The probability of a radical escaping from the cage depends on the energy of the radical and its diffusive properties. High energy radicals suffer more collisions before slowing down and consequently have a higher escape probability. Small radicals may carry away a larger share of the total energy of the activated molecule and will be able to penetrate the walls more easily. For the radiolysis of liquid hydrocarbons, the yields of hydrogen are much larger than the yields of methane, which are larger than the yields of ethane, etc.

It is not known what energy states an activated molecule occupies or what energy states are important to the final reaction. It is also not known if the energy is contained in the molecule by rotational, translational, or vibrational energy states. In at least one case it was found(95) that the molecular state that led to reaction had an energy of a fraction of an electron-volt. This was inferred from a similar photochemical reaction of the substance. Considering the large amounts of energy originally transferred to the molecule by the neutralization event, the low energy of the reactive molecule is surprising.

The important excited state in the polymerization of acetylene by radiation to form benzene also has been identified. The main product was cuprene but 21% of the acetylene reacted to form benzene. Dorfman and Shipko(32) have identified an excited state of acetylene that has almost exactly the same molecular dimensions, bond lengths, and angles as the benzene molecule. The formation of benzene and cuprene are not competing processes. Different excited states produce specific products in this system.

3. Free Radicals

Free radicals are molecules with an odd number of electrons. Because of this unpaired electron, they are very reactive and are consequently short-lived in chemical media. Ghormley(43) using pulsed radiation has estimated that an intermediate in the formation of hydrogen peroxide in irradiated water has a mean lifetime of the order of 10^{-3} seconds. There are numerous reports of the production of stable free radicals by the irradiation of solid polymers. Radicals have been immobilized(69,76) and preserved by freezing the irradiated medium. Free

radicals are short-lived under most circumstances not because they are unstable but because they are highly reactive.

Radical-radical reactions are generally assumed to have zero activation energy. Radical-molecule reactions generally have very low but non-zero activation energies. Many radiation induced reactions show little or no dependence of reaction rate on temperature indicating that they may be radical reactions.

Modern theories explaining the chemical effects of ionizing radiation invariably involve free radicals as reaction intermediates. The observed chemical products are the direct result of radical reactions and are not due to primary events, ions, and excited molecules. Considerable success has been achieved in the orderly and logical explanation of the observed results from the radiolysis of many systems. One of the most complete theories has been developed for the radiolysis of pure water and dilute aqueous solutions.

C. Chemical Effects of Radiation

Radiation chemistry has been defined as the study of the chemical effects (as opposed to the nuclear effects) of ionizing radiation. It differs from photochemistry in several respects. Photochemistry deals with low energy electromagnetic radiation. The primary photon event is invariably absorption by a photoelectric interaction between the photon and an orbital electron. The yield of excited molecules in photochemistry is always one for each quanta of light absorbed. Photochemical yields are reported as molecules reacted per light quanta absorbed. The quantum yield is less than one, except for chain reactions, indicating that some activated molecules do not react. However, there are similarities between

photochemistry and radiation chemistry. The same chemical products are often found, and similar cage effects can be expected. It is hoped that photochemistry can aid in ascertaining what energy states are responsible for radiolytic reactions, but little success has been achieved.(103,112)

1. History

Radiation chemistry was put on a firm basis forty years ago by the systematic studies of Lind.(61-65) From the study of many reactions induced by alpha bombardment, he postulated that the ions formed were the important species leading to the final reaction. He correlated the data in terms of the ionic yield, M/N, the number molecules reacted per ion pair formed. This picture of the reaction process involved "ion-clusters" to explain ion yields greater than one. An ion formed by a primary event would be stable long enough to attract neutral atoms and form an ion cluster. As many as 20 molecules might comprise an ion cluster. Electrons might be captured by neutral molecules and negative clusters formed analogous to the positive clusters. Neutralization of the clusters would yield activated complexes which would rearrange or dissociate to form the final product. Alyea(6) showed that the cluster theory could not explain chain reactions and reactions with high ionic yields.

Modern theory places importance on the radicals rather than ions. Yields are reported in terms of a G value, the number of molecules reacted per 100 ev absorbed. The G value and the M/N value are related by W, the energy required to produce on ion pair in the system.

Eyring, Hirschfelder and Taylor[35,48] laid the groundwork for the modern theory in their classic papers. They emphasized that the free radicals resulting from the dissociation of ions and excited molecules are important in the reaction mechanisms. This involves some mechanism for the transformation of electronic ionization and excitation energy into molecular vibrations which result in dissociation and production of free radicals. Burton[19] modified the modern theory by postulating that the electronic energy can be transferred from its initial locus to the molecule as a whole. This theory is discussed in more detail in Section II, B.

2. Radiation Chemistry of Pure Compounds

Radiation chemistry can be classified according to type of radiation used and composition and state of the chemical system irradiated. The radiation chemistry of pure compounds is the most fundamental system for study. However, the usual results derived from pure compounds are of little value in discovering the basic mechanisms. The observed products are the results of a wide variety of radical-radical and radical-molecule reactions. The probability of back reaction of the radicals to form the original compound is high. Undetectable traces of impurities may drastically influence the observed effect. The products of the radiation may cause undesirable effects and the chemistry of the compound will change as the concentration of the products increases.

There are two excellent reviews of the radiation chemistry of pure organic compounds. McDonell[71] has published a general introduction to the subject. Collinson and Swallow[22] have assembled the reported data.

3. Radiation Chemistry of Solutions

In order to prevent radical-radical and back reactions to obscure the immediate effect of radiation, an efficient radical trap may be added to the pure compound. This type of study may be classified under the radiation chemistry of dilute solutions. Important information can be gained not only on the radiation chemistry of the solution but also on the chemistry of the pure solvent. Radical traps can be any one of several species. In this study benzene was used.

The radical traps compete efficiently with solvent molecules and radicals for other solvent radicals. At a relatively low concentration(10^{-5}- 10^{-1}M) of the radical acceptor, essentially all available solvent radicals react with the acceptor. The acceptor generally cannot compete[81] with the back reaction of radicals in the solvent cage. Since the solute is present in small amounts, the radiation absorbed in the solute is negligible with respect to that absorbed in the solvent. It is assumed that the proportion of the radiation absorbed in each substance is proportional to the electron fraction of that component. It is further assumed that the effect of the radiation absorbed directly in the solute, the radical trap, is negligible. Therefore, the effect noted in the solute is due entirely to the action of solvent radicals.

Most of the work to date in the area of dilute solutions has been with aqueous solutions. Theories of the radiolysis of non-aqueous solutions have not been developed[86] in any detail, but there are interesting differences noted. The hydrogen yield from water is a function of the linear energy transfer of the radiation. For hydrocarbon systems[45], the hydrogen yield is a function only of the total energy absorbed.

D. Theory of Dilute Aqueous Solutions

1. Primary Events

There is a large body of experimental data on the final chemical products produced by the action of ionizing radiation in water solutions. The direct physical effect of the radiation on water molecules is well understood. However, the processes that occur between the initial physical event and the final products remain partly unknown. It is felt that hydrogen and hydroxyl radicals are the agents responsible for the chemical action of irradiated water. The reaction schemes postulated by which H and OH radicals react to form the final product are open to speculation. It is not known how these radicals are formed but several theories have been proposed. These are reviewed in a general way in this and later sections of this paper

It is thought by some authorities[25] that information on the primary effects can be derived from electron bombardment studies of water in a mass spectrograph. However, the conditions prevailing in a mass spectrograph do not exist[22] in actual experiments. The results from electron bombardment are of limited value to ordinary aqueous systems. The reactions listed in Table I have been observed.[25]

It is perhaps more significant to study the relative amounts of the ions and radicals produced at higher voltages corresponding to the energies of typical secondary electrons in irradiated systems. It can be seen from Table II that the relative yields change greatly with voltage but that the reactions yielding the pairs OH^+ and H; H^+ and OH; and H_3O^+ and OH are the most important. More than 95% of all positive ions formed at voltages below 100 v are H_2O^+, H_3O^+, H^+ and OH^+.

TABLE I

IONS FROM ELECTRON IMPACT ON WATER

Voltage	Reaction	Notes
5.6	$H_2O + e^- \rightarrow H + OH^-$	first current
12.8	$H_2O + e^- \rightarrow H_2O^+ + 2e^-$ $H_2O^+ + H_2O \rightarrow H_3O^+ + OH$	ionization potential
18.5	$H_2O + e^- \rightarrow HO^+ + H + 2e^-$	small amounts of O^-
19.5	$H_2O + e^- \rightarrow H^+ + OH + 2e^-$	at 18.6 and 28.1 v

TABLE II

RELATIVE ABUNDANCE OF IONS FROM ELECTRON IMPACT ON WATER

Voltage	Relative Abundance (arbitrary values)					
	H_2O^+	OH^+, H	H^+, OH	H_3O^+, OH	H_2, 2H, O^-	H_2^+, O^+, O
50	1000	200	200	200	20	5
100	-	230	50	?	20	1

The primary electron ionization processes in liquid water may be represented[46] by the reactions listed in Table III. Reaction 4 is the primary ionization due to Compton scatter. The ionization of a molecule can be caused by a charged particle but the average energy of the ejected electron would be much lower. Figures 1, 2 and 3 show the fraction of relatively high energy electrons ejected[59,68] by the passage of alpha particles and fast electrons in water. The transfer of energy from a charged particle to an orbital electron is an inefficient process. The energy of the secondary electron is almost independent of the energy and type of the incident particle.

Reaction 5 is the series of secondary ionizations caused by the Compton scatter electron. These reactions occur at widely separated independent sites since the energy of the recoil electron is relatively high. The average distance between primary ionizations sites for 440 kev electrons is 4600 Å. Reaction 6 is the series of ionizations caused by secondary electrons. Only 8%[68] of the secondary electrons from 440 kev electrons have energies over 40.6 ev. Thus the number of ionizations caused by the secondary electrons is less than 5 and the average is estimated as 2.5.[59] These ionizations are formed very close together since the range of 40 ev electrons in water is 12 Å. This cluster of closely spaced ionizations is referred to as a spur or hot spot. Reaction 7 is the dissociation of the positive water ion and may be thought of simply as:

(7a) $$H_2O^+ \rightarrow H^+ + OH$$

However, the water molecule is necessary to satisfy kinetic theory. According to some authors[115] the water molecule must be oriented for the reaction to take place. The reaction time must be of the order of the

TABLE III

PRIMARY REACTIONS IN IRRADIATED WATER

4.	$H_2O + \gamma \rightarrow H_2O^+ + e_c + \gamma'$
5.	$H_2O + e_c \rightarrow H_2O^+ + e_{c1} + e_s$ $H_2O + e_{cn} \rightarrow H_2O^+ + e_{cn+1} + e_s$
6.	$H_2O + e_s \rightarrow H_2O^+ + e_{s1} + e_s$ $H_2O + e_{sm} \rightarrow H_2O^+ + e_{sm+1} + e_s$
7.	$H_2O^+ + H_2O \rightarrow H_3O^+ + OH$
8.	$H^+ + e_{sm} \rightarrow H + 13.6$ ev.
9.	$H_2O^+ + e_{sm} \rightarrow H_2O + 12.8$ ev $\rightarrow H + OH$
10.	$H_2O + e_{sm} \rightarrow H_2O^- \rightarrow H + OH^-$
11.	$H_2O \rightarrow H + OH$ (Net Reaction)

Where:

e_c = Compton electron

e_{cn} = Compton electron after n ionizations

e_s = secondary scatter electron

e_{sm} = secondary scatter electron after m ionizations

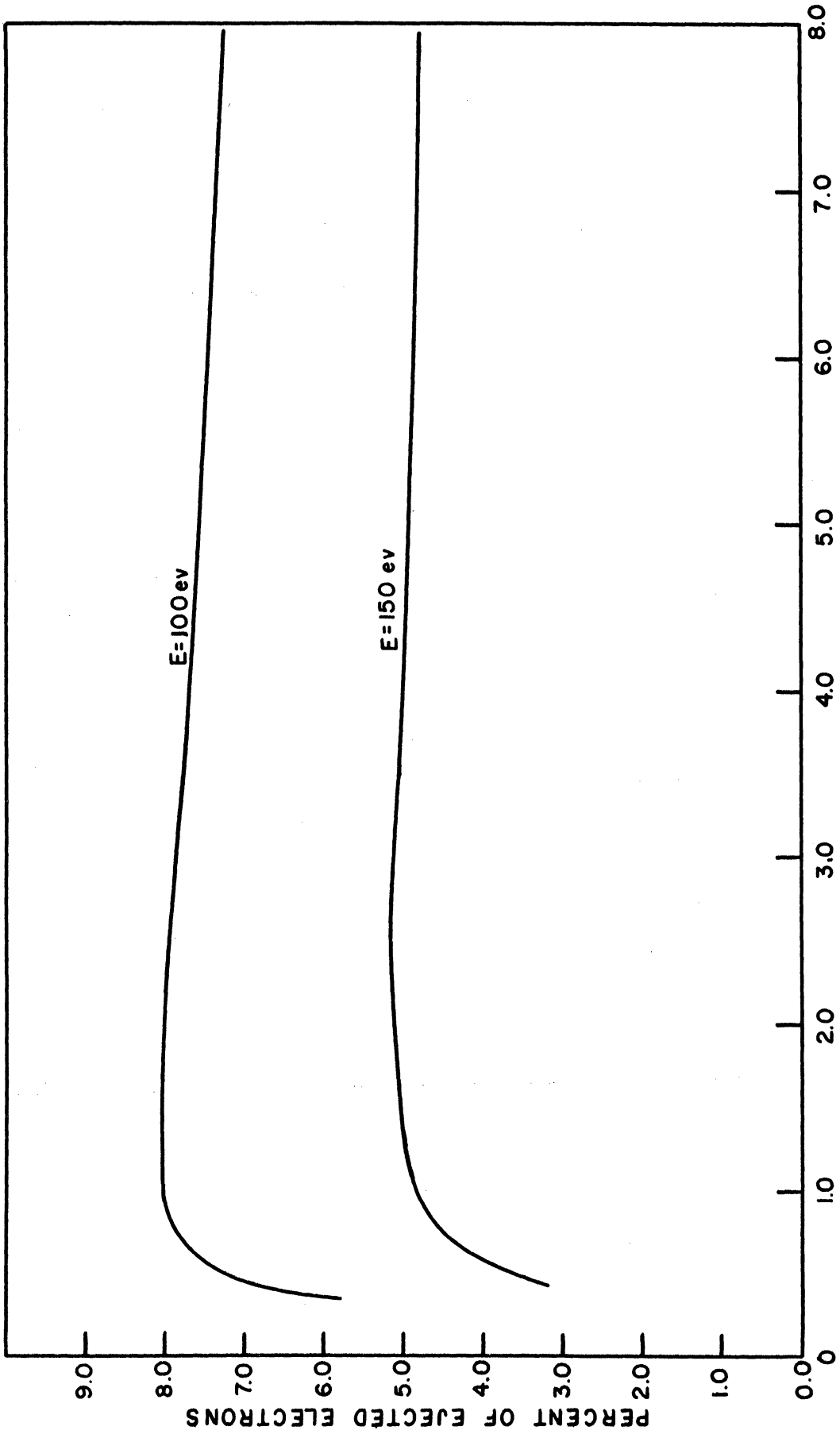

Figure 1. Percent of Electrons Ejected in Water with Energies Greater than 100 and 150 ev as a Function of the Energy of the Incident Alpha.

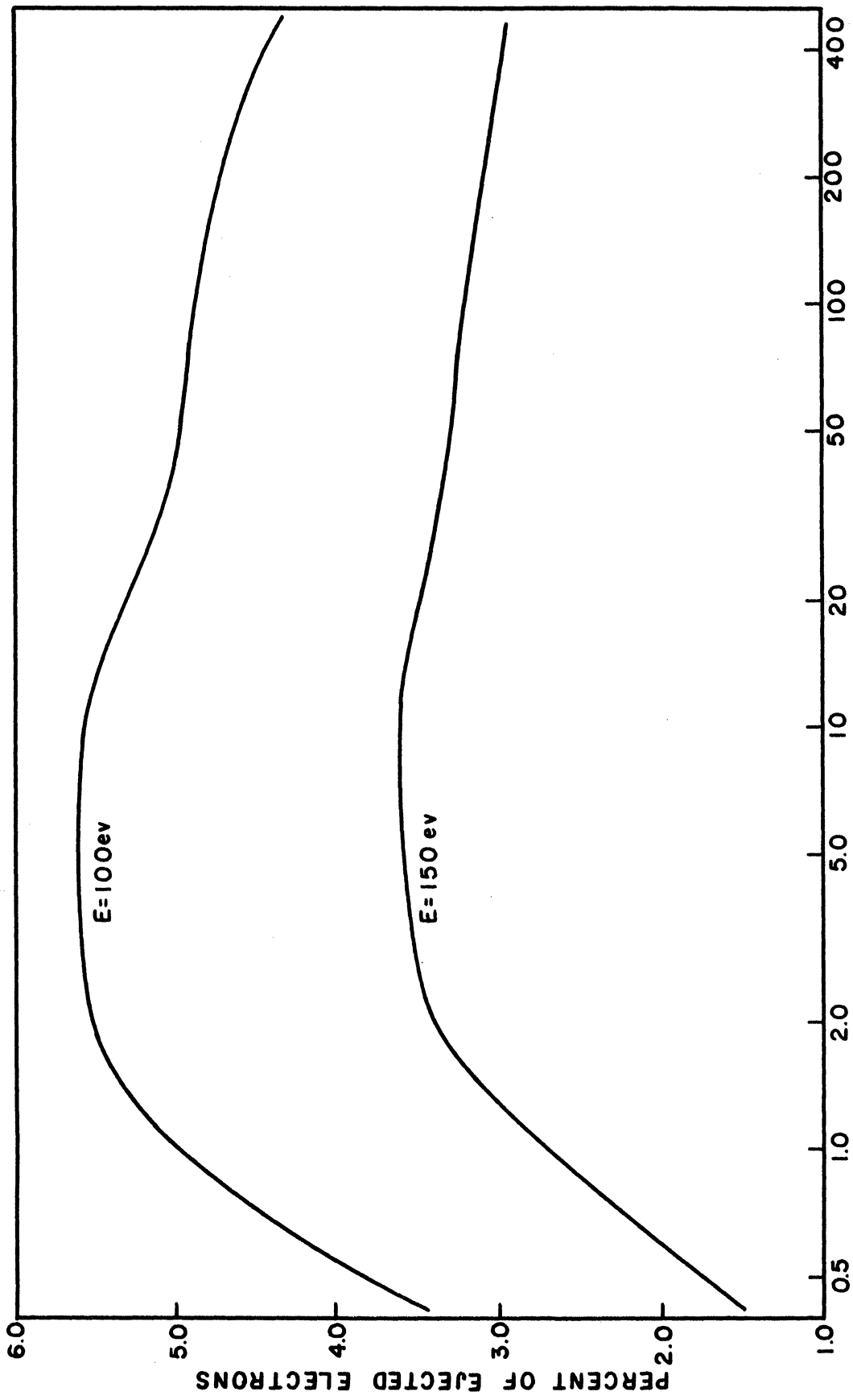

Figure 2. Percent of the Secondary Electrons in Water with Energies Greater than 100 and 150 ev as a Function of the Energy of the Incident Electron.

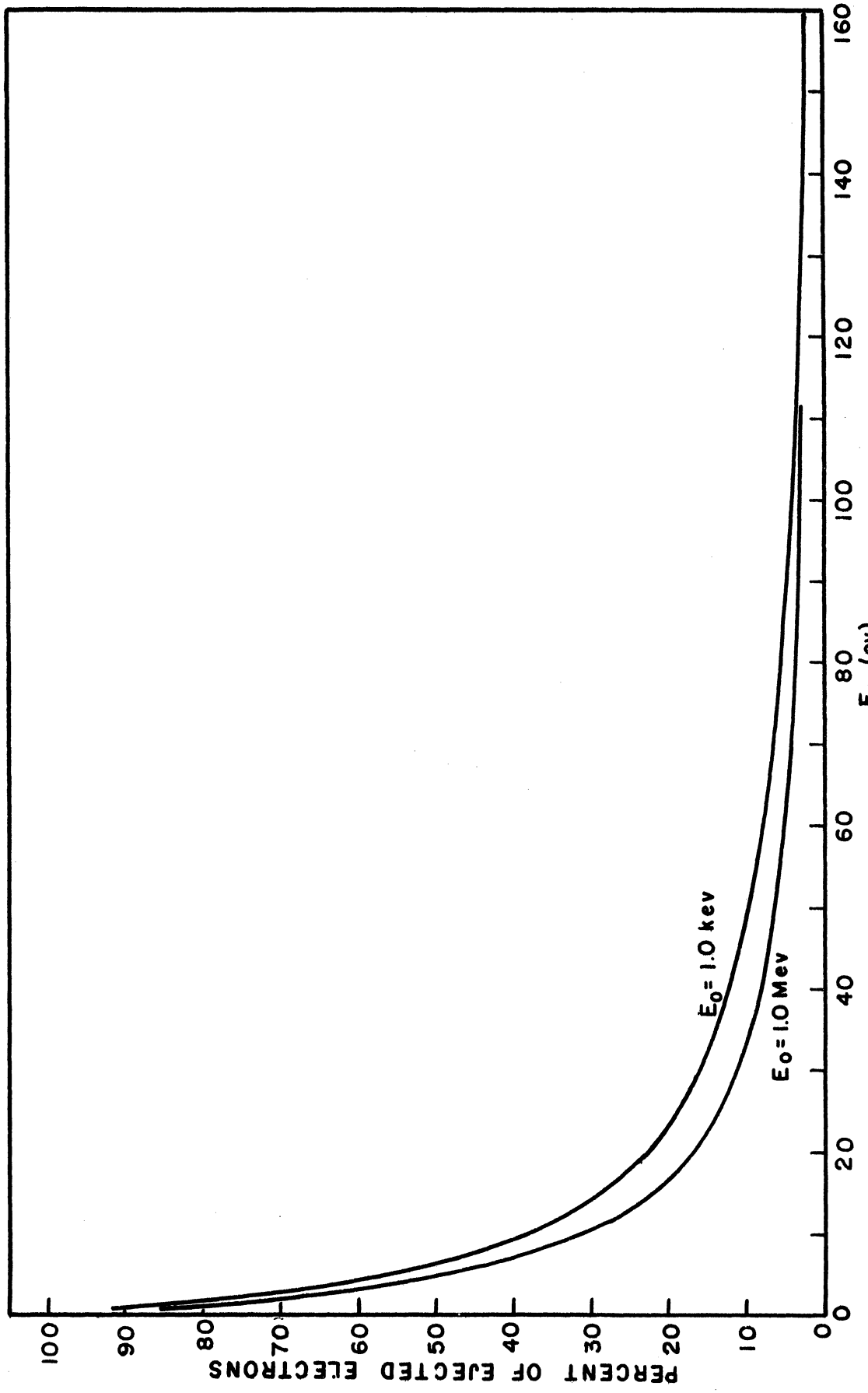

Figure 3. Percent of Electrons Ejected in Water with Energies Greater than E_p as a Function of E_p for Incident Electrons with Initial Energy of 1 kev and 1 Mev.

relaxation time of the water dipole, about 10^{-11} seconds. But there is indication that the lifetime of ions is less than 10^{-12} seconds. This casts doubt on the importance of this reaction, but there is some strong evidence that the H radical is formed at some diatance from the OH radical. This can be explained by Reactions 7 and 8, providing Reaction 7 occurs. The hydrogen ion and the hydroxyl radical are formed together, but in the time before the hydrogen ion is neutralized, the ion and radical diffuse apart escaping the solvent cage. There is a basic contradiction here. This point is discussed more fully below in connection with radical diffusion models.

Reaction 9 is the neutralization of a water molecule yielding an excited water molecule resulting in the decomposition into free radicals. These radicals are formed in the same solvent cage so the probability of their recombination is high. However, they are formed with a large excess energy (presumably translational energy) so they may be able to escape the cage easily.

Reaction 10 is the capture of a low energy electron by a water molecule. The negative ion may dissociate analogous to the reaction observed in the mass spectrograph. This reaction has only a small amount of excess energy so the negative water ion may not dissociate. Negative ion formation is usually considered an unimportant event. Reaction 11 is the net reaction.

Superimposed on these primary ionic reactions are reactions due to the excitation of the water molecules by the ionizing particles. The reaction may be represented as:

(12) $\qquad H_2O \rightarrow H_2O^* \rightarrow H + OH$

The radicals are formed in the same radical cage, but with lower excess energy than radicals resulting from neutralization. Therefore, the probability of escape is less. There is reason to believe that the cage effect in water is less important because of the high probability that the hydrogen radical will react with the cage walls as shown by reaction 13.

(13) $H + HOH \rightarrow HOH + H$

Other intermediates have been suggested(31) to explain effects in aqueous media. Rigg(89) has postulated the ionic radical H_2^+. This species should be stable(24) in aqueous solution. Its electron spends most of the time between the protons so its hydration power is only slightly less than that of a proton. Its action would be similar to the hydrogen radical. Dainton(26) has postulated the existence of the OH^+ ion to explain the high equivalent redox potential of irradiated water (-0.95 v). However, this ion has a low hydrating power and would be destroyed(24) by the very favorable reaction,

(14) $H_2O + OH^+ \rightarrow H_2O^+ + OH + 1.0$ ev

2. Radical-Molecule Theory

If it is assumed that the important products of ionizing radiation in water are the hydrogen and hydroxyl free radicals, a theory explaining observable chemical effects can be constructed without consideration of the primary events by which these radicals are formed. A simplified picture of the primary event would be:(49)

(15) $H_2O \rightarrow (\text{intermediates}) \rightarrow aH + bOH + cH_2 + dH_2O_2$

The molecules are formed by fast reactions of like radicals in the spur.

These radicals have been observed[82] as the predominant species in electron discharges in water vapor. Dainton and Collinson[21] have shown that OH and H free radicals are present in water by the polymerization of acrylonitrile in dilute solutions. Hydroxyl groups were identified on the product polymer. When the polymerization was carried out in heavy water, the characteristic C-D bond vibration frequencies were found.

The radiolysis of pure water was difficult to understand until a few years ago. It was not fully appreciated that trace impurities in water alter the decomposition effects observed. If the impurity is an oxidizing agent, oxygen is the principle product, but if the substance is a reducing agent, hydrogen is formed.[31] Some organic compounds exhibit[29] a catalytic effect in certain solutions.

Hydrogen peroxide is formed in the liquid. The concentration reaches an equilibrium value depending on the solute concentration, and the radiation intensity and ionization density. Absolutely pure water is not dissociated by x-rays or fast electrons, but is decomposed by heavy particles into hydrogen and oxygen. Stoichiometric amounts of the gases are produced after an induction period during which the hydrogen peroxide equilibrium is reached. The equilibrium hydrogen peroxide concentration in X-irradiated water is very low and was thought to be zero by many investigators. It is[13] much higher for heavy particle irradiation.

Allen[23] has proposed the following primary reactions to account for all reactions in aqueous media.

(F) $2H_2O \rightarrow H_2 + H_2O_2$ forward or molecular reaction

(E) $2H_2O \rightarrow 2H + H_2O_2$

(R) $H_2O \rightarrow H + OH$ radical reaction

The yield of each species is related to the reaction yields by:

$$\begin{aligned} G(H_2) &= G(F) & G(OH) &= G(R) \\ G(H) &= G(F) + 2G(E) & G(H_2O_2) &= G(F) + G(E) \end{aligned} \qquad (1)$$

A material balance relates these G values;

$$G(H_2O_2) + 2G(OH) = G(H_2) + 2G(H) \qquad (2)$$

The total decomposition of water molecules is given by;

$$-G(H_2O) = 2G(F) + 2G(E) + G(R) \qquad (3)$$

The relative amounts of each reaction varies with the ionization density of the radiation. High ionization densities increase the yield of reaction F and decrease R. For a wide range of low LET particles, the relative yields are constant. The total number of water molecules decomposed per 100 ev decreases for high values of linear energy transfer (LET) and is a function of pH. In 0.8N sulfuric acid $-G(H_2O)$ is 4.5 molecules/100 ev for gammas and fast electrons and decreases to about 3.8 for heavy particle irradiation. In pure water it is 3.8 for low LET radiation.[2,3,47,60] The yields of each reaction in 0.8N sulphuric acid and pure water are shown in Table IV.

Allen[2] discusses experimental evidence supporting Reactions F, E, and R. Their use in explaining chemical results observed is demonstrated by the oxidation of ferrous sulphate in aerated 0.8N sulphuric

TABLE IV

YIELD OF RADIATION REACTIONS IN WATER

Radiation	System	G(F)	G(E)	G(R)
Co-60 or fast e^-	0.8N H_2SO_4	0.39	0.39	2.92
" " "	pH~7	0.43	0.3	2.15
8 Mev deut.	0.8N H_2SO_4	1.05	0.10	1.50

acid solutions which is the standard Fricke dosimeter. The proposed reaction mechanism is Reactions F, E, and R and;

(16) $OH + Fe^{2+} \rightarrow Fe^{3+} + OH^-$

(17) $H + O_2 \rightarrow HO_2$

(18) $H_2O_2 + Fe^{2+} \rightarrow Fe^{3+} + OH^- + OH$

(19) $H^+ + HO_2 + Fe^{2+} \rightarrow Fe^{3+} + H_2O_2$

(20) $HO_2 + Fe^{3+} \rightarrow Fe^{2+} + O_2 + H^+$

Therefore, G (Fe) = 2G (F) + 8G (E) + 4G (R) = 15.5.

In deaerated solutions the process is:

(21) $Fe^{2+} + H_2 \rightarrow H_2 + Fe^{3+}$

(22) $Fe^{2+} + OH \rightarrow Fe^{3+} + OH^-$

(23) $Fe^{2+} + H_2O_2 \rightarrow Fe^{3+} + OH^- + OH$

and G (Fe^{3+}) = 2G (F) + 4G (E) + 2G (R) = 8.18 which agrees well with experimentally determined values of 8.22 and 8.13.

The change in the relative amounts of each reaction with ionization density is shown by Allen and Saeland[90] as the change in

the yield of the Fricke dosimeter. Figure 4 shows the instantaneous G value for the oxidation of ferrous ions as a function or ionization density. The line is an empirical equation given by Allen.[3,4,5]

Allen's equation is:

$$G_i(Fe^{3+}) = 3.4 + \frac{12.1}{1 + 0.38\ (dE/dx)} \qquad (4)$$

Where G_i is the instantaneous 100 ev yield and is related to the observed overall yield by:

$$G\ (Fe^{3+}) = \left(\int_{E_f}^{E_0} G_i\ (E)\ dE \right)/(E_0 - E_f) \qquad (5)$$

E_0 = initial energy of particle

E_f = final energy of particle

$\frac{dE}{dx}$ = LET, linear energy transfer in ev/Å

The radiolysis of pure deaerated water can be qualitatively explained. The OH radicals oxidize the hydrogen and the H atoms reduce the hydrogen peroxide in chain Reactions 24 and 25,

(24) $OH + H_2 \rightarrow H_2O + H$

(25) $H + H_2O_2 \rightarrow H_2O + OH$

and the reactions:

(26) $OH + H_2O_2 \rightarrow H_2O + HO_2$

(27) $HO_2 + HO_2 \rightarrow H_2O + O_2$

(28) $H + O_2 \rightarrow HO_2$

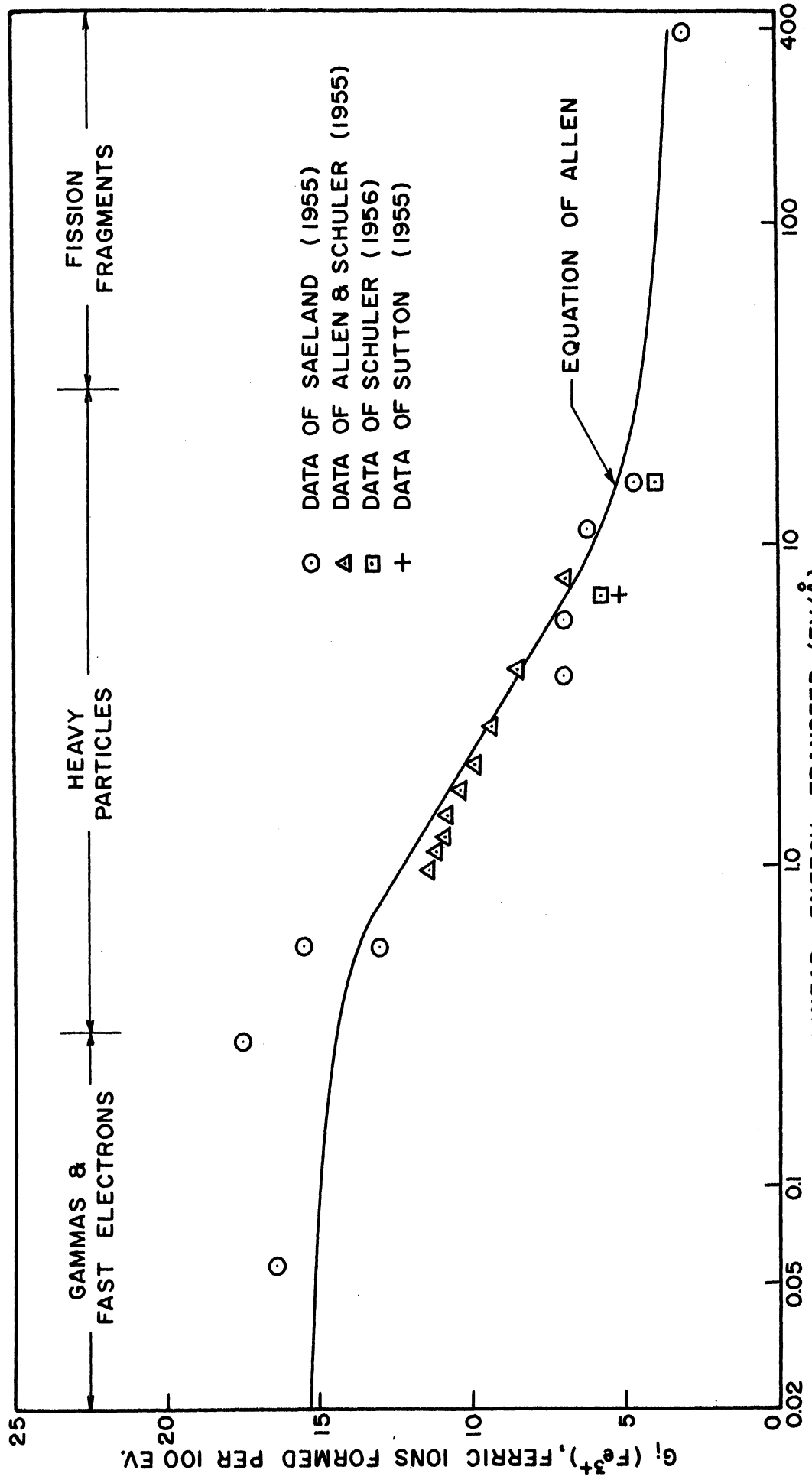

Figure 4. Yield of Fricke Dosimeter as a Function of Linear Energy Transfer

Since radiations of low LET produce high yields of radicals, the molecular products are completely destroyed by the radicals. Heavy particle radiations yield few radicals so the molecules produced are not all destroyed. Reactions 26, 27, and 28 explain the stoichiometric yields of oxygen and hydrogen in high dosage heavy particle irradiations.

3. Radical Diffusion Models

The ionic processes are important because they shed light on the spatial distribution of hydrogen and hydroxyl radicals at the moment of their formation. The basic question is whether the radicals are formed at the same instant, therefore in the same radical cage, or by different events, therefore at some distance from one another. Are they formed near one another by Reaction 29,

(29) $H_2O^+ + e^- \rightarrow H_2O^* \rightarrow H + OH$

or at a distance from one another by Reaction 30?

(30) $H_2O^+ \rightarrow H^+ + OH$: $H^+ + e^- \rightarrow H$

or

$H_2O^- \rightarrow H + OH^-$

If some information on the initial distribution of radicals is available or assumptions are made, a mathematical model can be constructed that describes the competing processes of radical diffusion away from the spur and radical reactions within the spur. Then the yields of the Reactions F, E, and R can be calculated and the efficiency of radical traps can be estimated. There are several theoretical treatments of the kinetics of the aqueous radicals formed by ionizing radiations. Only a general

outline of the assumptions, results, and implications of these theories will be presented in this paper. The exact results are not pertinent here.

Lea(58,59) assumed that the two types of radicals are formed at a distance from each other (Reactions 30). Samuel and Magee(91) postulated that the spatial distribution of the H and OH radicals about a spur is the same (Reaction 29). The two theories treat similarly the diffusion of the radicals away from the spur or ionizing track into the homogeneous solution. During this diffusion process there are complementary probabilities that the radicals will be lost by reaction with other radicals and that the radical will escape into the solution.

Lea's model is based on a theory proposed by Jaffé(52) to explain saturation conductivity in irradiated liquids. The distance that the hydrogen atom is formed from the hydroxyl radical depends on the distance traveled by the hydrogen ion before it attaches an electron or undergoes a charge transfer with a negative ion. The distribution of H and OH radicals is the same as the original distribution of the negative and positive ions. The original distribution of radicals is represented by a Gaussian distribution with cylindrical symmetry about the path of the ionizing particle.

$$n = \frac{N_o}{\pi b^2} e^{-r^2/b^2} \qquad (6)$$

where

n = number of radicals of one kind / cm^3

N_o = $\frac{\text{total number of radical pairs formed}}{\text{centimeter of particle path length}}$

b = measure of the radius of the column, cm

r = radial distance from path of particle, cm

After a time t, the radicals have diffused randomly. If there is no loss of radicals due to combination or recombination:

$$n = \frac{N_o}{\pi(4Dt + b^2)} \exp\left(-\frac{r^2}{4Dt + b^2}\right) \tag{7}$$

D = diffusion coefficient of the radical, cm^2/sec. The assumption that the H radicals are formed on the average farther from the axis than the OH radicals is accounted for by assuming a larger value for b_H than b_{OH}. It is also reasonable that D_H will be larger than D_{OH}.

To include the effect of radical recombination, differential Equations (8) and (9) must be solved.(59)

$$\frac{\partial n_H}{\partial t} = \frac{D_H \partial}{r \partial r}\left(r \frac{\partial n_H}{\partial r}\right) - k n_H n_{OH} \tag{8}$$

$$\frac{\partial n_{OH}}{\partial t} = \frac{D_{OH} \partial}{r \partial r}\left(r \frac{\partial n_{OH}}{\partial r}\right) - k n_H n_{OH} \tag{9}$$

k = reaction rate constant for radical recombination.

It is assumed in these equations that recombination of unlike radicals is the only important reaction.

Lea obtained an approximate solution to the equations keeping the same form of solutions as the case of no radical loss.

$$n_H = \frac{N(t)}{\pi(4D_H t + b_H)^2} \exp\left[-\frac{r^2}{(4D_H t + b_H)^2}\right] \tag{10}$$

$$n_{OH} = \frac{N(t)}{\pi(4D_{OH} t + b_{OH})^2} \exp\left[-\frac{r^2}{(4D_{OH} t + b_{OH}^2)^2}\right] \tag{11}$$

Where: N(t) is a function of time only.

$$-\frac{dN(t)}{dt} = 2\pi \int_0^\infty kn_H n_{OH} r\,dr \qquad (12)$$

Then:

$$\frac{N_o - N(t)}{N(t)} = \frac{kN_o}{4\pi(D_H + D_{OH})} \ln \frac{(4D_H t + b_H)^2 + (4D_{OH} t + b_{OH})^2}{b_H^2 + b_{OH}^2} \qquad (13)$$

Reasonable values for the constants in the expressions can be estimated and the extent of the expansion of the track can be calculated. Lea concluded from such calculations that the radicals formed by a heavy charged particle do not diffuse far before they recombine. The radicals formed by electrons will diffuse long distances (distances of the order of microns) before they have recombined. However, Lea's formulae apply only where the distance between primary ionizations is smaller than the parameter b. This is a good approximation for heavy charged particles, but is very poor for fast electrons. Values of b_H and b_{OH} assumed by Lea are 150 Å and 20 Å respectively, derived from some results of Jaffé. The distance between primary ions in the track of a 1 Mev alpha is 1.0 Å, but that of 440 kev electrons is 4600 Å. The tertiary ionizations around a secondary ionization in the path of a fast electron are within 20 Å of the point of initial ionization. Instead of a cylindrical symmetry as in the case of alpha irradiation, spherical symmetry would be a better representation.

Samuel and Magee[91] have developed theoretical treatments for both the cylindrically and spherically symmetrical cases. They postulated that both radicals form at a site close to the original ionization or excitation. The radicals then diffuse randomly until the spurs or tracks

merge into the homogeneous radical concentration of the solution. During this diffusing process, the radicals react with one another. The probability of radical-radical encounters can be computed with every encounter assumed to lead to reaction. The radicals that escape recombination in the spur or track are free to react with solute molecules or radicals from other spurs.

The Samuel-Magee equation for the case of isolated spurs of radicals is:

$$\frac{N_o}{N_\infty} = N_o - (N_o - 1)e^{-xN_o^{1/3}} \tag{14}$$

Where:

$$x = \sigma/[2\pi^3)^{1/2}\ L\bar{r}_o'] \tag{15}$$

N_o = number of radicals originally present

N_∞ = number of radicals after spur is dissipated, i.e. at infinite time

σ = collision cross-section of radicals

L = mean free path of radicals

$\bar{r}_o' = \bar{r}_o/N_o^{1/3}$ (the initial volume of the spur is assumed proportional to the number of radicals)

$\bar{r}_o$ = initial radius of spur

For the case of columnar ionization:

$$N_o/N(t) = 1 + \left(\frac{N_o\sigma}{2\pi ZL}\right)\ \ln\ \left[\frac{t+\tau}{\tau}\right] \tag{16}$$

Where

Z = length of column

$N(t)$ = radicals remaining after time t

τ = measure of initial path diameter

By assuming reasonable values of the physical parameters in the above equations, Samuel and Magee calculated values of the ratio $G(F)/[G(F) + G(R)]$ for low and high LET radiations that are in agreement with experiments. This should not be taken as proof of the theory as there is great uncertainty in the values of the physical parameters. Improvements in the theory of radical diffusion have been made recently. Ganguly and Magee[42] include the effect of solute-radical reactions during the expansion of the spur. Fricke[41] and Monchick, et al,[80] have also made improvements in the theory.

These theories are at best only first approximations of actual events. Lea's theory predicts that the radicals are formed and move considerable distance from the particle track before they react. The extension of Lea's theory to fast electron irradiation is incorrect and leads to false conclusions. The electric field produced along the track of an ionizing particle is very large. The field may have an influence on the motion of electrons and ions such that the original distribution of ions will not be Gaussian. Reed[88] has suggested that the distribution of radicals after diffusion will not be normal. The high concentration of radicals along the axis will make the probability of reaction there high. This will tend to depress the radical concentration at the center.

Samuel and Magee's theory predicts that the dimensions of the spur are a magnitude smaller than that predicted by Lea's work. It is incorrect to assume that the mobility of the H and OH radicals are the same. In agreement with Lea's hypothesis, a reasonable interpretation of experimental results indicates that the distribution of the two radical

types is different. No account in either theory is given to any kinetic energy that a radical may be given at the moment of formation.

It is not possible to decide from the theories and experiements how the radicals and molecules are formed. If both kinds of radicals had the same initial distribution, recombination to form water would be a probable reaction. It is expected that $-G(H_2O)$ would decrease for high ionization densities. Data for 0.8N sulfuric acid show this effect but the decrease is not as large as is expected.(60) The presence of sulfuric acid probably changes the mechanisms of the radical reactions from those of pure water. The yield of OH radicals is greater than that of H radicals in acidic solutions for high LET radiations. This may be explained by electron capture by a hydronium ion.(60)

(31) $$H_3O^+ + e^- \rightarrow H_2 + OH$$

Data in pure water is not complete enough to show the decrease in water decomposition with increasing LET.

Recently results have been published(23,97) that indicate that the formation of hydrogen peroxide and molecular hydrogen are not primary events. They are formed by reaction of the radicals. Previously it was assumed that these reactions were so fast that radical scavengers could not compete with them and for practical purposes they were primary events. Weiss(114) had suggested that the combination of hydroxyl radicals may have a high activation energy due to the dipole force. Therefore, he postulated(56) that the molecular products are the result of the reaction of two excited water molecules.

(32) $H_2O^* + H_2O^* \rightarrow$ 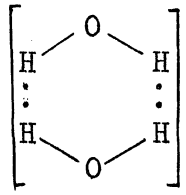 $\rightarrow H_2 + H_2O_2$

The yields for the Reactions F, E, and R are constant[54] for a variety of radical scavengers and a wide range of concentrations. However, some recent work[23,97] has shown that the yield of aqueous radicals is a function of the solute type and concentration for some radical scavengers. The yield of molecules decreases with scavenger concentration and the yield of radicals increases proportionately. Schwarz[97] has described the decrease in molecular yield for several scavengers by a radical diffusion model similar to that of Samuel and Magee. Apparently there is competition between scavengers and radicals in the spur and the yields of F, E, and R are not basic quantities. However, some radical scavengers cannot compete with these radical reactions within the spur and the yields measured using these solutes are the same. Among the class of inefficient or slow scavengers are the bromide, iodide, and ferrous ions, hydrogen peroxide and oxygen. Benzene used in this study behaves like this class of scavenger.

Some workers[60] feel that the radicals may never reach the homogeneous solution. All reactions observed take place within 100 Å of the point of original ionization. Experiments with very high gamma dose rates indicate that the yield of the Fricke dosimeter is independent of dose rate up to 10^{-10} rads/sec.[55] Overlapping of spurs is not important and the size of the spurs is much less than previously thought. If every reaction took place in isolated regions, no effect of radiation intensity would be noted, but scavenger concentration would be important. For a spur of 100 Å radius, there are about 5 scavenger molecules in the spur

for a bulk scavenger concentration of 0.001 M. The reaction is limited to a few acceptor molecules which may be entirely consumed within the individual spur. It has not been noted that the net decomposition of water increased with radical acceptor concentration. The back reaction of radicals, therefore, is either a very rapid reaction with which the acceptors cannot compete or it does not occur.

It is the purpose of this section to point out the basic dilemma of the radiation chemistry of dilute aqueous solutions. Is the lifetime of the thermal electrons and ions long enough to allow the ions to decompose, or are the H and OH radicals formed in the same solvent cage? Existing contradictions could be explained by proposing new radical diffusion models, new reaction intermediates and perhaps denying the importance of hydrogen and hydroxyl radicals, or altering the reaction kinetics between radicals and molecules. However, more data on different systems is needed rather than new diffusion models. There is a shortage of reliable results on which to base unequivocal interpretations. Most of the work to date has been with 0.8N sulfuric acid solutions. Experiments with neutral water solutions would be of interest.

E. Effect of Neutrons

Neutrons impart their energy to the matter through which they are passing by elastic collision with nuclei and by absorption in nuclei. On the average, thermal neutrons impart no energy to nuclei by scattering events. The maximum fraction of the initial energy that a neutron can impart to a hydrogen nucleus is one. It is less for heavier elements. Since the C-H bond energy is about 4.3 ev, neutrons with energies below about 5 ev cannot give a hydrogen nucleus enough energy to rupture the

bond. From the standpoint of chemical effect, 5 ev is an approximate dividing line between slow and fast neutrons.

1. Estimated Effect of Fast Neutrons

The maximum fraction of the neutron energy that can be lost in a single scattering collision is related[44] to the atomic weight of the struck nucleus.

$$1 - \left(\frac{E_f}{E_o}\right)_{min} = 1 - \left(\frac{A - 1}{A + 1}\right)^2 \qquad (17)$$

where:

E_o is the initial energy of the neutron.

E_f is the final energy of the neutron.

A is the atomic weight of the struck nucleus.

The average fraction of energy lost per collision is expressed as the average logarithmic energy decrement per collision, ξ .

$$\xi = \ln \frac{1}{x} \approx \frac{2}{A + 2/3} \qquad (18)$$

where x = average fraction of the initial energy lost per collision

The approximation holds for all elements except hydrogen for which $\xi = 1.00$. These formulae are derived from a classical model but are adequate for neutron energies from nuclear reactors (<10 Mev). Because of the high average energy loss per collision and the high scatter cross-section of hydrogen, it is a good approximation for hydrogen containing systems to consider only the energy release due to scattering from hydrogen nuclei.

Number of collisions/unit volume and time =

$$M_H \left\{ \int_{E_f}^{E_o} \sigma_H(E) \frac{d\phi_F(E)}{dE} \right\} \tag{19}$$

Total neutron energy absorbed/volume/time =

$$\left(\frac{dE_n}{dt}\right)_a = M_H \left\{ \int_{E_f}^{E_o} \sigma_H(E) \frac{d\phi_F(E)}{dE} dE \right\} \bar{E}\, x \tag{20}$$

Where x is the average fraction of the neutron energy lost per collision = 0.368 for hydrogen

ϕ_F is the fast neutron flux, neutron/cm^2/sec

$\bar{E}$ is the average energy of the neutron flux (ev) determined by:

$$\bar{E} = \frac{\int_{E_f}^{E_o} E(\phi)\, d\phi}{\phi_F} \tag{21}$$

σ_H = scatter cross-section of hydrogen

M_H = the number of hydrogen atoms/cm^3

$= \rho\, w_H\, a$

ρ = density of the system

a = Avagodro's number

w_H = weight fraction of hydrogen in the system

The recoil protons with energies of the order of thousands of electron-volts move through the system causing ionizations and excitations. The chemical effect of fast neutrons is then the effect of the recoil protons.

$$\frac{dM}{dt} = G_p \left(\frac{dE_n}{dt}\right)_a \qquad (22)$$

$\frac{dM}{dt}$ = molecules reacting/sec./cm^3

G_p = 100 ev yield for a given reaction for protons.

Fast neutrons may be captured by nuclei causing the emission of ionizing radiation but this is of second order importance compared to the scattering energy in most aqueous systems.

2. Estimated Effect of Thermal Neutrons

The thermal neutrons release energy only by capture in a nucleus with subsequent emission of energy. The energy appears as prompt gammas and as kinetic energy of nucleus fragments. The prompt energy release occurs within 10^{-16} sec. after the neutron enters the nucleus. The product nucleus may or may not be radioactive. If the half life of the product nucleus is short, its decay radiation may add appreciably to the chemical yield.

The absorption of one neutron can produce many free radicals as a result of the several subsequent events. These include:(86)

1. Szilard-Chalmers effect:

(33) $$RA + n \rightarrow (RA')^* \rightarrow R^\cdot + A'^\cdot + \gamma$$

These primary radicals can account for only 1% to 2% of the total produced.

2. The gamma photons emitted immediately after neutron capture are absorbed.

3. A' may decay emitting gammas or betas which are then absorbed.

4. The excess energy (over that required to break the R-A bond) of the radicals is carried off as kinetic energy. It is dissipated in collisions with surrounding molecules causing ionizations and excitations.

5. The capture of a neutron by A may cause the nucleus to decompose completely producing gammas and energetic heavy ions.

6. If A' is captured and then decays it may rupture a bond, creating new radicals. If A' decays by beta emission, it will change valence creating a new radical.

Prevost-Bernas(86) et al, estimated that each neutron absorption leads to the formation of 500-2000 reactive radicals and molecules. Let S be the neutron utilization defined as the number of molecules reacted per absorption. The number of reacted molecules in a given system of j atomic components is:

$$\frac{dM}{dt} = \phi_T \sum_{i=1}^{j} \sigma_i m_i S_i = \frac{\phi_T}{(MW)_{avg}} \sum_{i=1}^{j} \sigma_i m_i S_i \qquad (23)$$

Where: ϕ_T = thermal neutron flux, neutron-cm/cm^3 sec.

σ_i = capture cross-section for the i-th component.

m_i = mole fraction of the i-th component.

If the major portion of the energy from a capture event is released as ionizing radiation, the chemical effects of slow neutrons can be described better on the basis of the energy released. For a system

with one important absorber, the chemical reaction rate is:

$$\left(\frac{dM}{dt}\right) = G(M)\ \left(\frac{dE}{dt}\right)_a \tag{24}$$

$G(M)$ = 100/ev yield of M for the particular radiation emitted

$\left(\frac{dE}{dt}\right)_a$ = energy absorbed/sec/cm^3

The energy released/sec/cm^3 = $(dE/dt)_r = \phi_T \Sigma_a \rho$

Σ_a = macroscopic capture cross-section

$\phi_T \Sigma_a$ = number of neutron captures/sec cm^3

ρ = energy released per neutron capture

The energy absorbed in the reacting system

$$y\left(\frac{dE}{dt}\right)_r = \left(\frac{dE}{dt}\right)_a \tag{25}$$

y = fraction of the emitted energy that is absorbed in the system

Then:

$$\left(\frac{dM}{dt}\right) = G(M)\,\phi_T \Sigma_a \rho\, y \tag{26}$$

For heavy ions $y \approx 1.0$ because of the very short path of the heavy charged particles. For gammas and fast electrons y is less than one. It can be approximated as:

$$y = 1 - e^{-\mu \bar{R}} \tag{27}$$

$\bar{R}$ = average path length in the reaction system

An analytical expression has been derived for the average path traveled by a particle in a (spherical) reaction vessel. The details of the derivation are given in Appendix A.

The number of neutron captures in a reaction system is given above as $\Sigma_a \phi_T$. This assumes that the flux is uniform over the system volume. The exact expression is:

$$\frac{dn}{dt} = \Sigma_a \int_V \phi_T(V)dV \qquad (28)$$

The expression for neutron flux in a cylinder as a function of solute concentration for various aqueous systems is discussed in Appendix B.

III. INITIAL STUDIES

A. Radiation Sources

1. Cobalt-60 Gamma Source

Two cobalt-60 sources located in the Phoenix Memorial Laboratory at the University of Michigan were used in this study. The first was a nominal 10 kilocurie source. It was more than one half life old when this study was made so that its actual power was approximately 2200 curies. It consisted of 120 aluminum clad cobalt rods arranged in a cylindrical holder. The holder had an internal diameter of four inches. Maximum intensity at the center of the source was approximately 0.9 megarep/hour.

A second source of 5000 curies was received from Chalk River, Canada in April, 1958. It consisted of 350 aluminum covered slugs of cobalt. Each slug was about 3/4 inch long and 3/8 inch in diameter. The slugs were placed in thirty-five 1/2 inch aluminum tubes closed at the top and bottom with cotter pins. These tubes were placed in a 4 inch ID cylindrical holder similar to the first source. The activity of the individual slugs varied by a factor of 10. In assembling the source no attempt was made to balance the activity of each rod so that the gamma field around the source was not radially symmetrical.

The source was raised and lowered by a remotely operated elevator. The source room, where experiments were placed, could only be entered when the source was at the bottom of a 16 foot well filled with water.

2. Ford Nuclear Reactor

The Ford Nuclear Reactor was located adjacent to the Phoenix Memorial Laboratory on the North Campus of the University of Michigan. It was a swimming pool heterogeneous reactor using highly enriched uranium 235 as fuel. It was reflected on four sides with graphite. The pool water served as a reflector, a moderator, a coolant and a radiation shield. The maximum power was 1 megawatt.

The reactor and its facilities were housed in a four story windowless structure having 12 inch thick reinforced concrete walls. Precautions had been taken to make the building air tight. The building could be maintained at two inches of water vacuum so that any active gases could be contained within the building. Exhaust gases were monitored before being vented to the atmosphere.

The pool was a U-shaped tank constructed of barytes concrete 6-1/2 feet thick at the lower levels. The tank was about 10 feet wide by 20 feet long (north-south direction) by 26 feet deep. A thermal column was located on the west side of the pool. Several beam ports focused on the core at the north end of the pool. The pool was divided into two sections with a removable water-tight gate between the sections. The pool water was filtered and demineralized in mixed bed ion exchangers. The water was continuously recirculated to remove any possible contamination. A primary water system, separate from the deionizing system, containing a pump and a heat exchanger provided cooling at high power levels by forced circulation down through the core lattice. A secondary water system supplied cooling water from a cooling tower to the tube side of the heat exchanger.

The core was suspended below a mobile bridge which was mounted on rails running above the east and west edges of the tank. The reactor could be operated either in front of the thermal column, or, to the north, in front of the beam ports. The core itself was made up of fuel and reflector elements held in a grid plate. Fuel elements were 3 inches square in cross section and 35 inches long. The uranium fuel was contained in 18 curved plates held in an aluminum frame forming the outside of the element. Each plate was 3 inches wide by 0.06 inches thick and 24 inches long and consisted of 0.02 inches of aluminum cladding over 0.02 inches of uranium-alluminum alloy. Each element contained 140 grams of U-235. The reflector elements were 3 by 3 by 42 inches and consisted of pure high density graphite canned in aluminum. A lifting lug was provided on all elements so that the core configuration could be changed as desired.

The assembled critical core generally consisted of 21 fuel elements (some partial elements to allow the insertion of the control rods), and about 55 graphite reflector elements. Figure 5 shows the core configuration used for the majority of experiments in the study. Control was achieved by raising or lowering three boron carbide safety rods and one hollow control rod.

There were four methods available at the Ford Reactor for performing irradiations. Twelve aluminum beam ports penetrated the north end of the pool wall. Four of these formed two "throughports" passing through the pool a few inches from the north face of the core. The remaining eight were set radially focusing on the center of the

A, B, C: Safety-Shim Rods (5 Plate Elements)
CR: Control Rod (5 Plate Element)
S: Po-Be Source
F.C: Fission Chamber

Fuel Element No. 18 in Core Position 48

Graphite Reflector Element No. 4 in Core Position 50

Loading: 2539 gms
Critical Mass: 2497 ± 5 gms

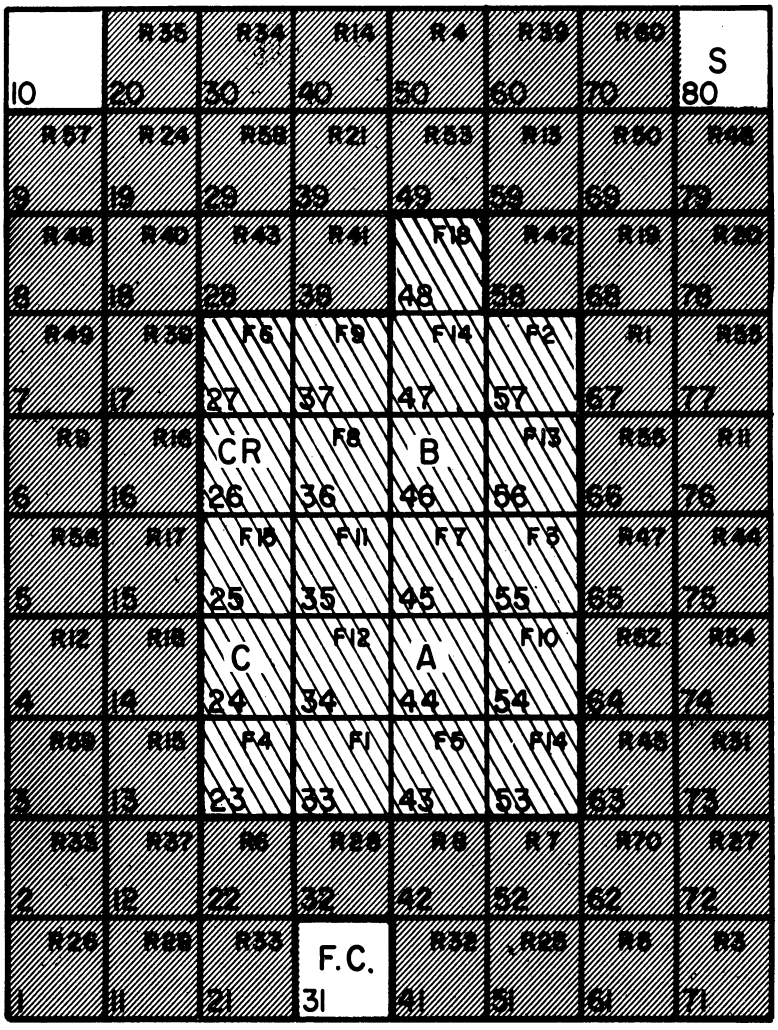

Figure 5. Typical Core Configuration of Ford Nuclear Reactor.

core and abutting it. Each port was equipped with concrete plugs that served as holders for experiments and as shielding. The ports were closed to the pool. They were filled with either deionized water or the concrete plug to provide a radiation shield. A portable steel coffin was provided to facilitate the safe removal of active samples from the beam ports.

A graphite thermal column was located on the west wall of the pool. The column consisted of a large number of long 4 inch square graphite blocks stacked in such a manner that certain ones could be withdrawn and experiments inserted. The facility was intended mainly to supply thermal neutrons.

A system of pneumatic tubes ran from the face of the core to laboratories in the Phoenix Building. Four tubes were located a few inches from the west face. Samples, in sample carriers or "rabbits", were dispatched from any one of seven stations and were returned automatically after a preset time. The rabbits returned in a few seconds from the core so that short life time isotopes could be studied.

In-pool or "fishing" experiments were also possible with this type of reactor. Samples to be irradiated were lowered through the pool down to the core. For this study, in-pool irradiations were chosen as the most suitable. The beam ports were not adapted for the short term exposure of a large number of batch samples. It was difficult to remove active samples from the ports. It was felt that it was better for this exploratory study to use batch irradiations rather than a flow apparatus requiring the use of a beam port.

The pneumatic tubes were not used because the size of the sample was limited, and the gamma and neutron flux were fixed by the power level. Changing the power level would change the fluxes but in the same ratio. Since it was intended to study the effect of varying the gamma and neutron fluxes independently, the in-pool experiment was better. Different gamma and neutron fluxes could be obtained at one power level by changing the position in the pool.

At the far south end of the pool, there was a 12 inch gate valve through which highly active samples could be lowered safely from the pool into one of the hot cells in the Phoenix Laboratory. During this transfer personnel were shielded by ten feet of water or four feet of high density concrete. The gate valve was large enough to pass equipment about 10 inches in diameter and 40 inches long. The two hot cells in Phoenix were equipped with master-slave manipulators and cerium stabilized lead glass windows three feet thick. Exhaust gases and liquid wastes from the cells were monitored before disposal. Numerous lead filled plugs in the walls allowed electrical and process lines to be led out of the cells.

A more detailed description of the Ford Nuclear Reactor and its radiation facilities can be found in the Ford Reactor Handbook[118] and in "Initial Calibration of the Ford Nuclear Reactor"[119]. Figure 6 is an isometric view of the reactor showing many of the associated facilities. Figure 7 is a photograph of the reactor core looking toward the south face. The reactor is operating at 100 kilowatts and is illuminated by the Cerenkov radiation.

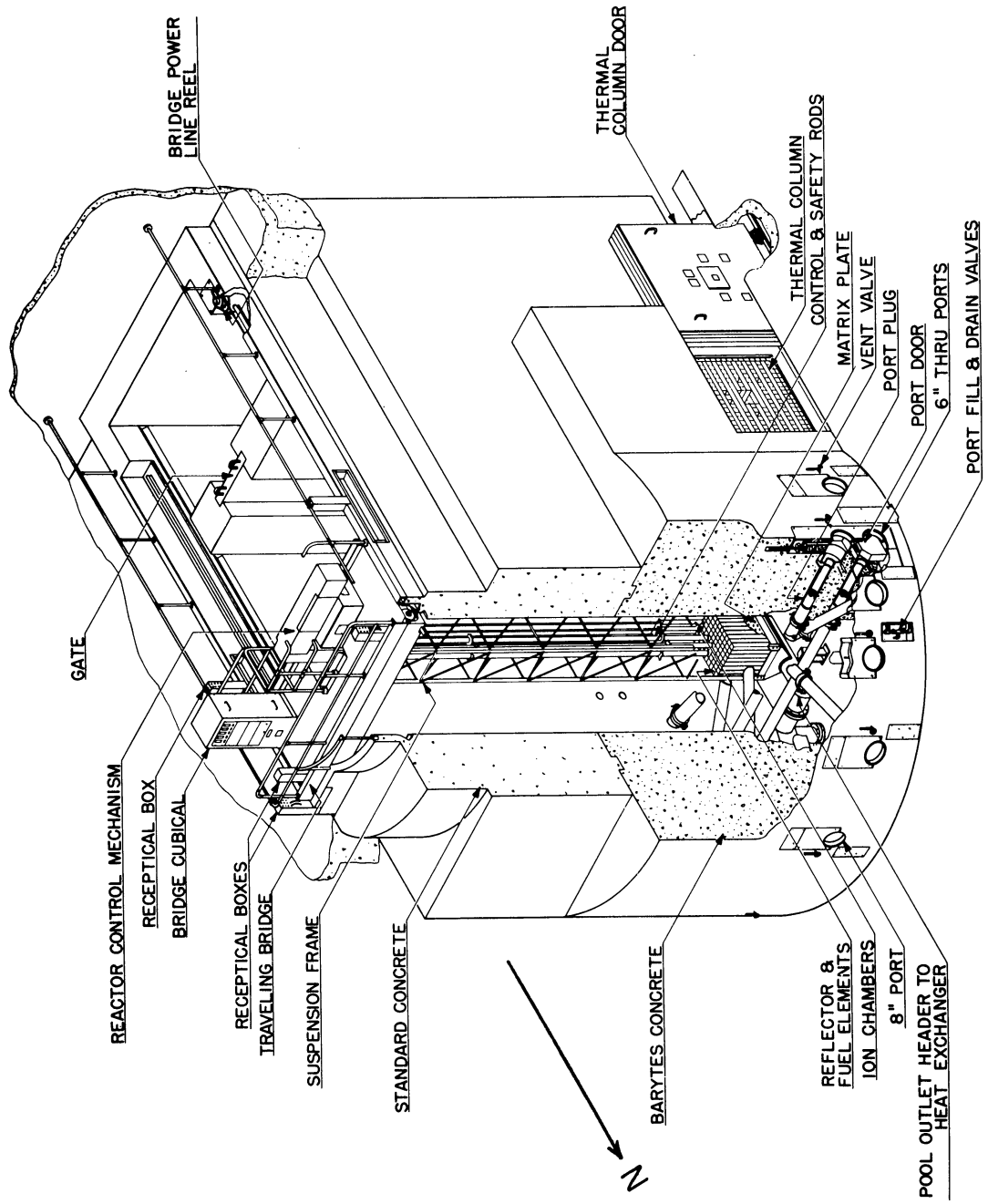

Figure 6. Isometric of Ford Nuclear Reactor

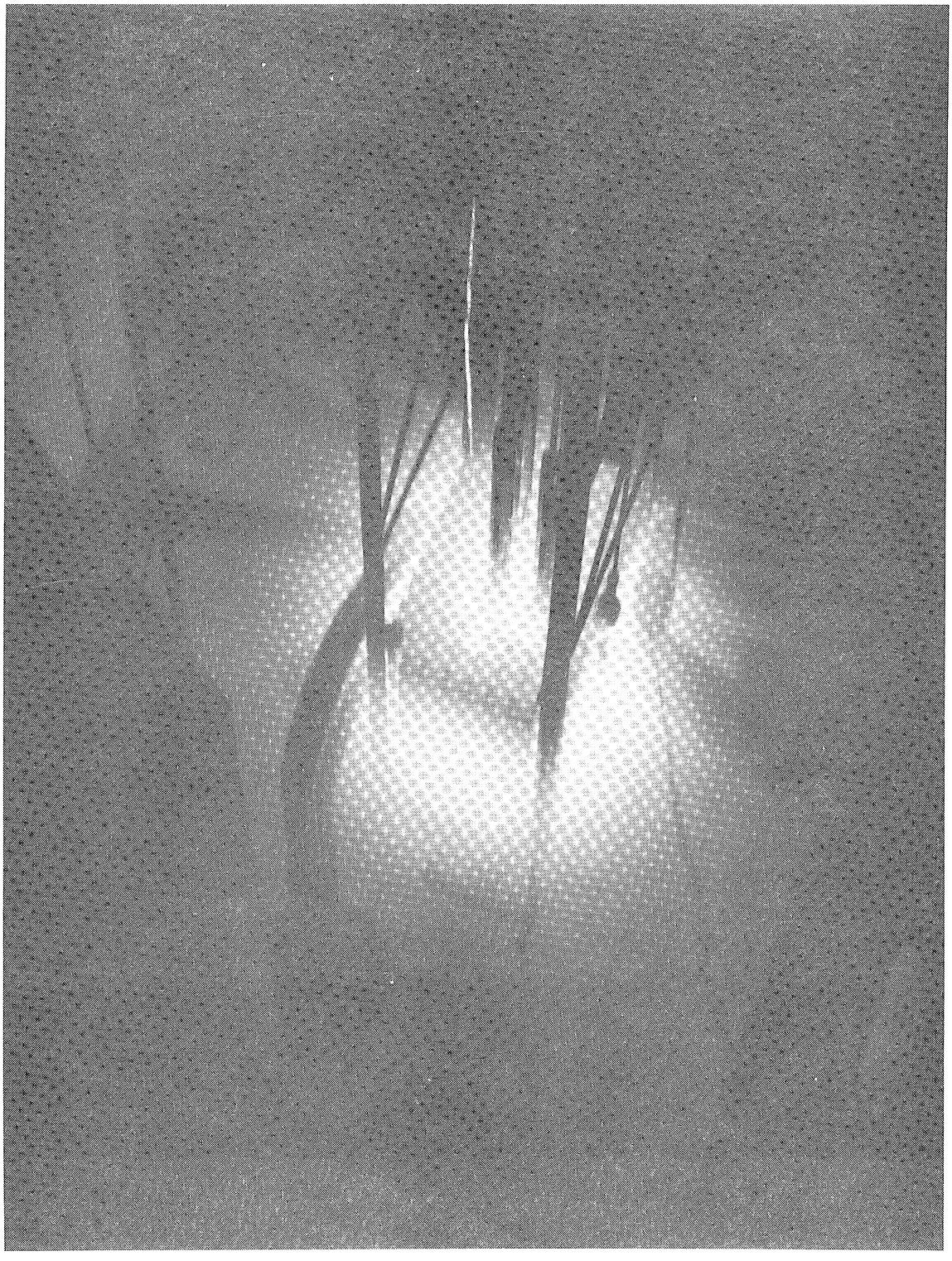

Figure 7. Reactor Core at 100 Kilowatts

B. Problems of Reactor Irradiations

1. Radiation Hazard

The radioactivity induced in equipment exposed to neutrons is a serious hazard. A preliminary study of the problem was made for this study to determine methods of reducing the hazard. Highly active materials can be handled remotely behind heavy shielding or at a distance from the operator. The equipment necessary for this is expensive, and limits the operations that can be performed on the sample.

A second method to avoid the radiation hazard is the proper selection of the materials of construction so that the induced activity has a low level or a short half life. Manipulations of the sample can be made directly after a short cooling period. There are few useful materials of construction that meet these requirements. The best metals are aluminum and magnesium. However, available commercial alloys of these metals contain alloying elements with high neutron cross-sections and long half lives. A small quantity of such an alloying element or impurity will make the metal useless for this purpose. Pure aluminum and magnesium are expensive and have low strengths and very poor workability. Comparisons of the best available alloys of these metals are shown in Figures 8 and 9. The comparison is made by the dose rate (roentgens/hour) expected 10 cm. from a 5000 gram point source of the alloy exposed to a thermal neutron flux of 10^{12} neutron-cm./cm^3/sec. The radiation level is expressed as a function of exposure and cooling time. The calculations were based on empirical relations published by Bopp and

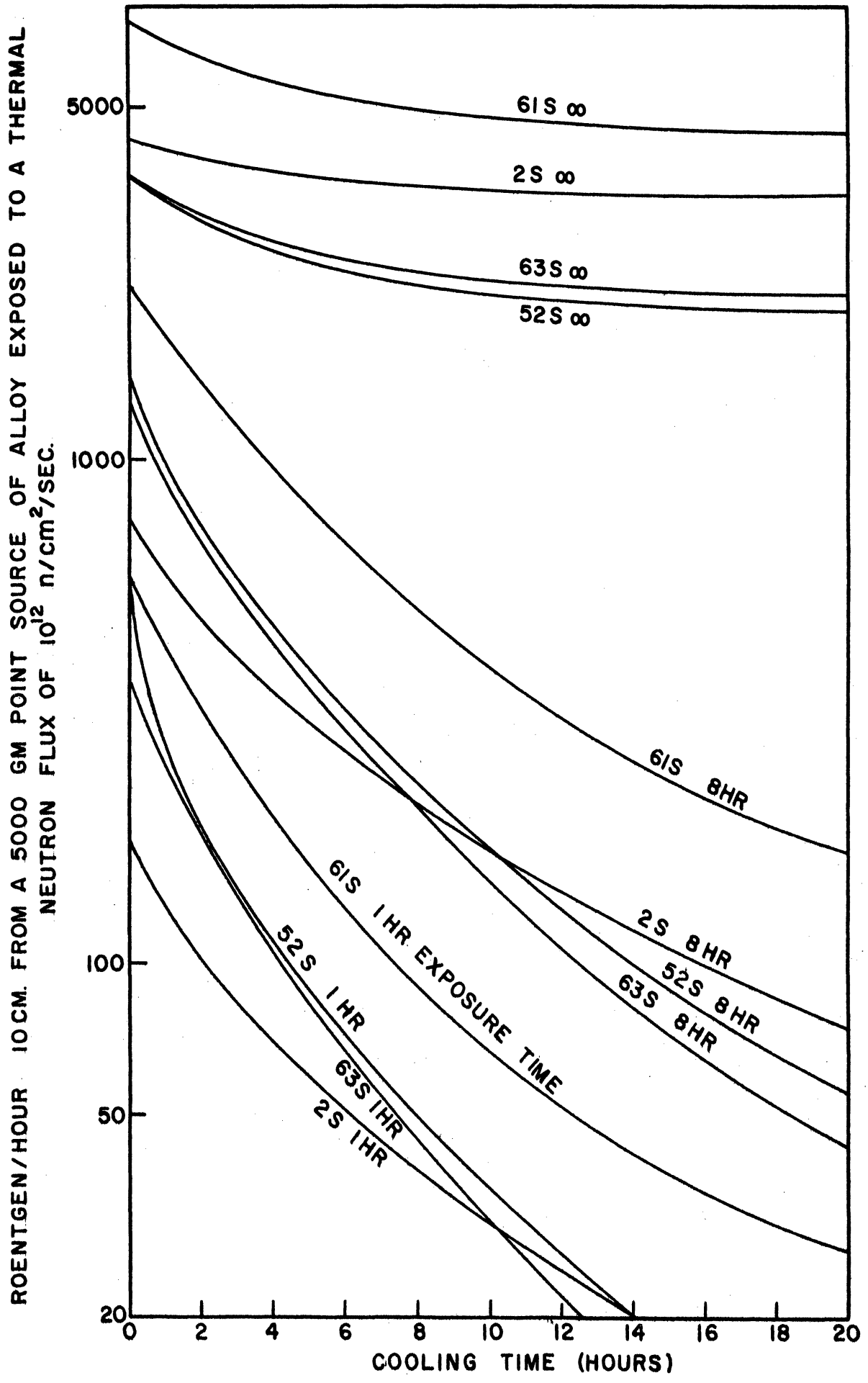

Figure 8. Comparison of the Activity of Aluminum Alloys.

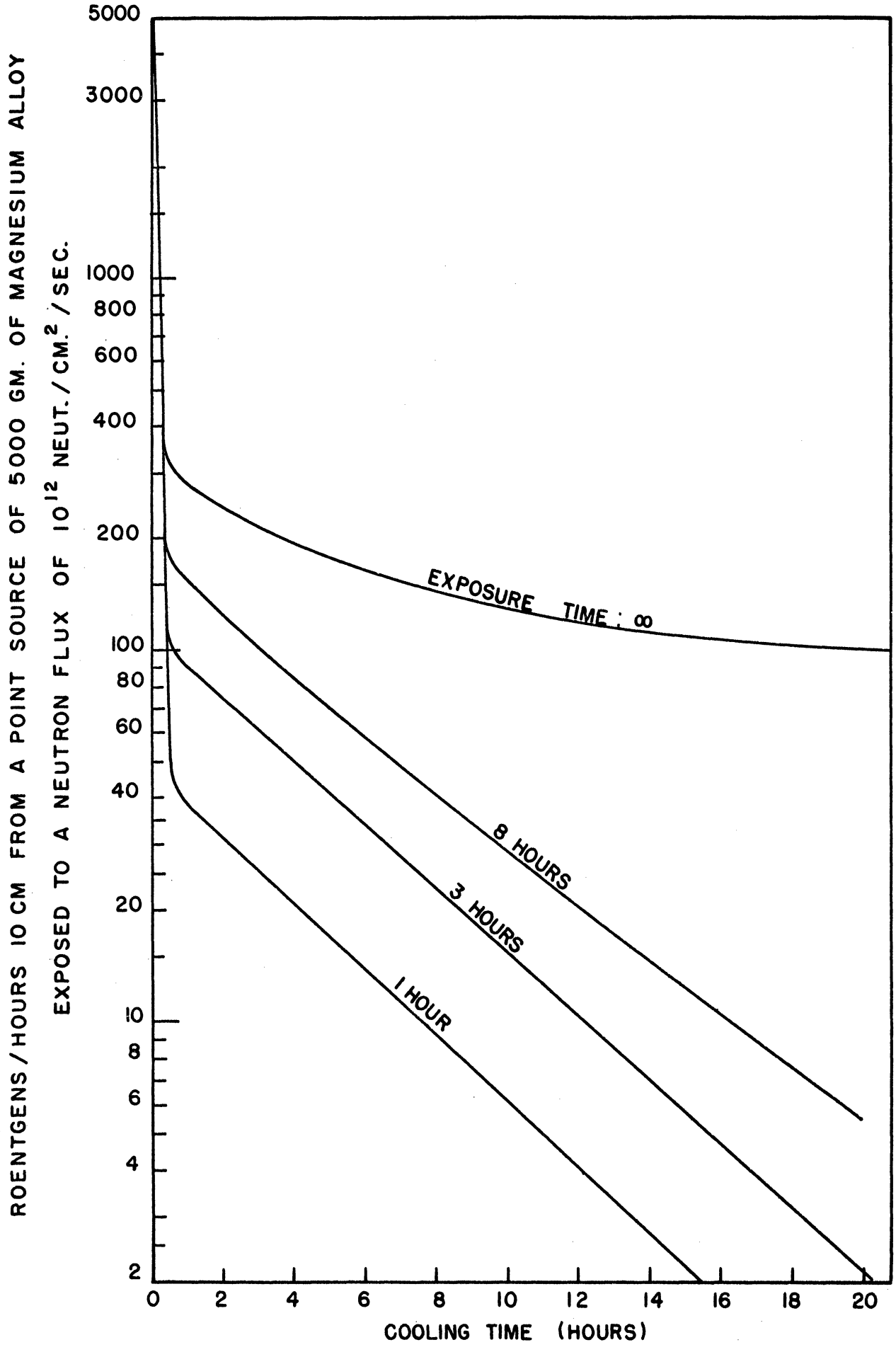

Figure 9. Activity of Magnesium Alloy 58135

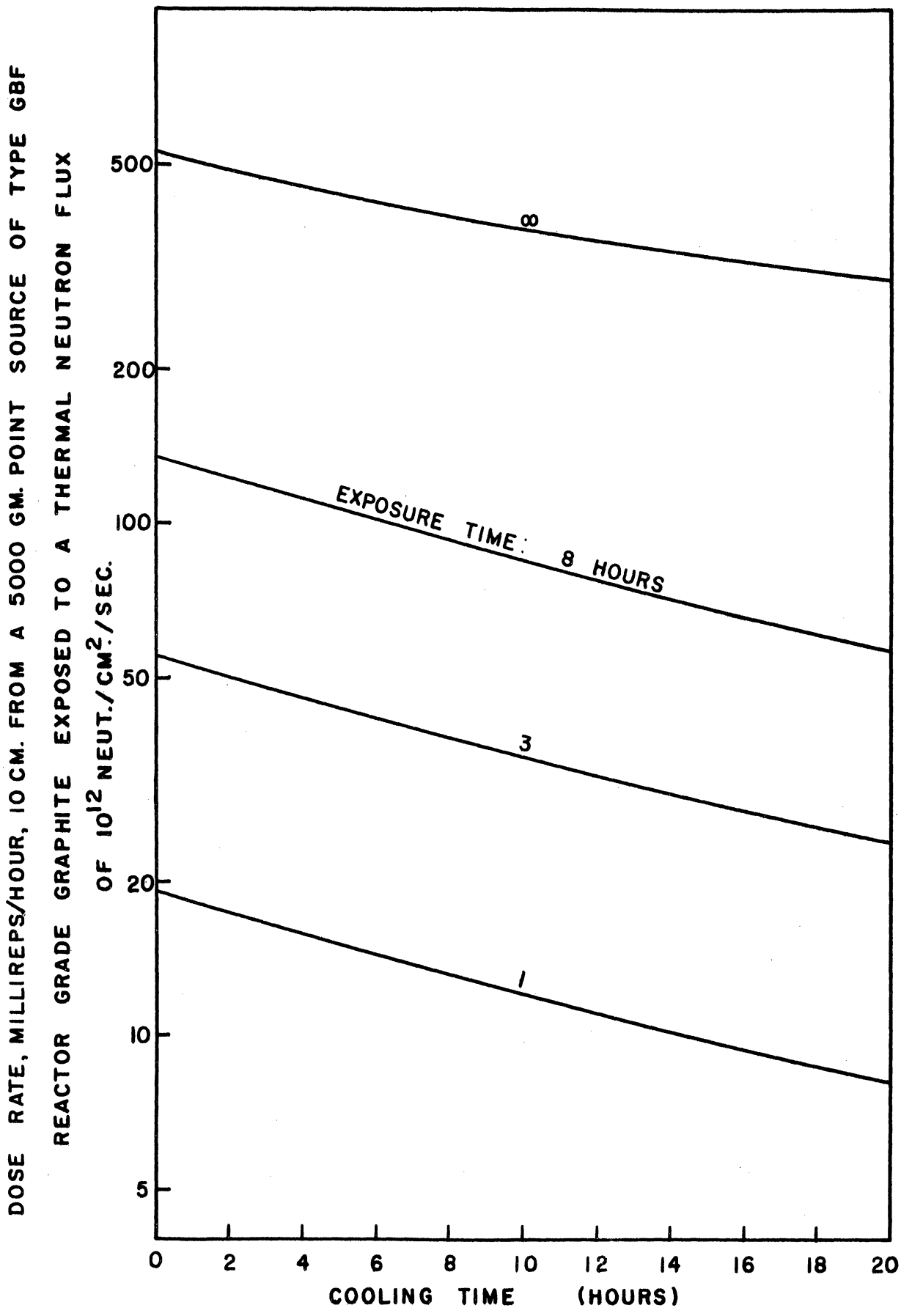

Figure 10. Activity of Graphite (Type GBF)

Sisman[14] and on the compositions of the alloy[100,116] using known cross-section and lifetime data.[116] Both methods gave about the same results if an accurate analysis of the alloy was available. The results obtained agreed within an order of magnitude with experimental observations with 2S and 52S aluminum. Because a point source was assumed for the calculations, the observed values were lower. The long lived activity of these alloys is due mainly to zinc, manganese, iron and chromium.

Extremely high purity graphite is available commercially as "Reactor Grade Graphite". Figure 10 shows the radiation level expected from irradiated graphite.[14] This graphite has a high density and a reasonably high tensile strength. Its high porosity is a drawback for some applications.

2. Dangers to the Reactor.

A chemical experiment can create serious dangers to a nuclear reactor by influencing the reactor controls or by causing physical damage to the reactor system. An experiment that changes the reactivity of the critical assembly significantly should not be moved while the reactor is in operation. However, the effect of equipment outside the reflector is small even for large quantities of material with a high absorption cross-section. Experiments in the Bulk Shielding Facility[53] and the Ford Nuclear Reactor showed that large quantities of saturated boric acid solution adjacent to the reflector had a measurable but small effect on the reactivity. The solutions used in this study had no noticeable effect on the reactivity of the core.

Explosions and fires in apparatus near the reactor are much more hazardous than under ordinary circumstances. Liberal safety factors were used in the design of the pressure vessels to prevent failure. All vessels were designed and tested according to ASME Boiler Code[117] specifications for working pressures twice those expected.

3. Other Hazards

The internal heating caused by absorption of gamma energy can be appreciable. However, for the small vessels used, no temperature rise greater than 20°C was noted. This rise occurred in the aluminum vessel in air at a gamma flux of 10^6 rep/hour.

Possible physical damage to the equipment due to neutrons was investigated. The flux-times contemplated in this study would not cause any appreciable decrease in the physical strength of the pressure vessels. The polyethylene bottles used became less pliable but stronger after long irradiations.

Leakage of chemical reactants must be more carefully controlled than under usual circumstances. The reactant may be radioactive and must not be released to the atmosphere. Leakage into the reactor pool may cause activity in the pool water, excessive corrosion of the reactor components immersed in the water, and overloading and fouling of the deionizing system.

4. Reactor as a Radiation Source.

The reactor was not as convenient a source of radiation as a cobalt-60 source. The dose rate at any point near the core was a function of the neutron population ("power level"), core configuration, position of control rods, past history of the core, and reactor control circuits. The most serious of these and the most nebulous was the power level. Initially, the power level was determined[119] by integrating the measured flux and fuel concentration over the fuel volume. The instruments indicating the power level were then calibrated at the known level with a standard fission chamber set at an arbitrary location near the core. Higher power levels were estimated by a linear extrapolation of the output of this fission chamber.

The power level was considered to be only a reference number. The dose rates were determined experimentally for a given level indication. Fluctuations in the indicated power from minute to minute were negligible ($< 2\%$). They would average out for irradiations longer than a few minutes. However, day to day fluctuations and trends in the actual power level may be large. The neutron population may change even though the power level indicators show the same reading. A slow rise in the neutron population for a power reading of "100 kilowatts" was definitely noticed[119] in the first month of reactor operation.

Essentially one core configuration was used throughout this study so no effects of this variable could be determined. A large fission plate placed on the east face seemed to have little effect on the gamma doses near the south face. Position of the control rods had no observable effect on the dose rates outside the reflector ele-

ments. However, the variation in control rod positions was not large. The 9-inch reflector on the south face minimized effects of these parameters.

The residual activity of the core due to long lived isotopes varied depending on the past history of the core. At 100 kilowatts, this residual activity was a negligible (< 1%) fraction of the activity of the core due to fission gammas and short lived isotopes. This will increase as the number of megawatt-hours of operation increases. At 100 kilowatts a significant increase in gamma activity was noted during the first 15-30 minutes of operation each time the reactor was started. Experiments were not commenced for at least thirty minutes after startup. This rise was due to the short lived isotopes reaching equilibrium activities.

During the initial period of reactor operation, the electronic circuits were altered several times to achieve optimum performance. It was felt that some alterations resulted in changes in flux levels due to changing responses of the instruments. The standard fission chamber failed at times and was replaced or repaired.

Other minor variables could affect the dose rates received by an experiment. Variations in the water temperature would change the absorption of the gammas and scattering of the neutrons. The pool was always $90 \pm 3°F$ for this study. There were usually several other experiments near the core and samples in the pneumatic tubes which were moved during runs. Early runs were difficult because of frequent accidental control rod drops.

To avoid many of these difficulties, gamma dosimetry was performed at least once every day before any experiments were run.

To achieve accurate gamma and neutron dose rates, position in the pool had to be accurately reproduced. The neutron flux decreased by approximately a factor of ten for every four inches moved horizontally away from the south face. The gamma flux fells a decade for every 18 inches. Thus an error of one inch in reproducing a position constituted an error of about 35% in neutron flux and 10% in gamma flux. In this study, samples were hung on the end of a 30 foot cable held by a bridge. Position was not determined relative to the core but relative to a fixed position on the floor where the bridge supports stood. The reproducibility of positioning with the equipment used was considered satisfactory.

During this study, the reactor was operated at 100 $\pm$ 5 kilowatts (nominal rating) as indicated by the linear level recorder. A power level of 100 kilowatts gave convenient dose rates. At higher powers the forced circulation pump was operated which caused swaying of the in-pool experiments. The slight convection currents created at 100 kilowatts caused no visible motion of the samples.

C. Dosimetry

1. Gamma Dosimetry.

The standard Fricke dosimeter[113] (ferrous sulfate in 0.8N H_2SO_4) was used to determine the gamma dose rates in the reactor pool and cobalt-60 source. It was felt that the neutrons in the reactor radiation would yield a negligible amount of energy compared to

the gamma energy absorbed. Neutron capture by the hydrogen in the pool water may have added significantly to the gamma flux from the core.

A stock ferrous solution was prepared by dissolving reagent grade chemicals in triple distilled water to obtain the following final concentrations:

Ferrous ammonium sulfate	0.1M
Sodium chloride	0.02M
Sulfuric acid	0.8N

To prepare the dosimetry solution, the stock solution was dissolved 1 part to 200 parts of aerated 0.8N sulfuric acid in triple distilled water. The stock solution could be kept a few weeks but the dosimetry solution deteriorated after a few days. The sodium chloride minimized [30] the catalytic effect of organic impurities on the yield of ferric ions in this solution.

The dose received by a sample was calculated using G(Fe) = 15.6. This value was reported[50,57] as determined by calorimetric calibrations. A large number of determinations using cavity measurements have been reported.[45,78] However, the theory of the Bragg-Gray principle is still being revised.[101] Dyne[33] has shown that geometric corrections for divergent radiation could explain the higher values of $G(Fe^{3+})$ calibrated by a Bragg-Gray chamber. Therefore, the calorimetrically determined yields are more reliable. It has been shown that the yield of the dosimeter is independent of dose rate up to 2×10^6 rep/sec[93] and perhaps up to 10^{10} rad/sec.[55] This more than adequately covers the range of dose rates encountered in this study.

The yield of ferrous ions was determined on a Beckman spectrophotometer at 3050 Å with a slit width of 0.5 mm. A molar extinction coefficient of 2040 liters/mol/cm. was used. The total gamma dose was calculated by the formula:

$$E_\gamma = \frac{10^6(\Delta D)}{\epsilon p A(Fe)} = 31.7\ (\Delta D) \qquad (29)$$

ϵ = molar extinction coefficient for ferrous ions

p = cell path length = 1.009 cm.

$A(Fe)$ = 15.4 μ mols ferric ions formed/liter/kilorep

ΔD = change in optical density of ferrous solution

E_γ = gamma dose in kiloreps

Figure 11 shows the gamma dose rate versus distance from the south face of the core at a nominal power level of 100 kilowatts. The two lines show the increase in actual neutron population for the period from April 3 to April 31, 1958. At high powers the gamma dose rate from the core is proportional to the actual power of the reactor. The third line is a comparison of reported data taken at the Bulk Shielding Reactor[119] at 100 kilowatts. After April 31, the actual power remained reasonably constant for a given reading of the linear level recorder.

Figure 12 shows typical dosimetry data taken in the sample holder at approximately 9 and 4 inches from the south face in the vertical midplane of the core. The curve is not symmetrical about the center line of the core, because of the scattered radiation from the bottom of the pool.

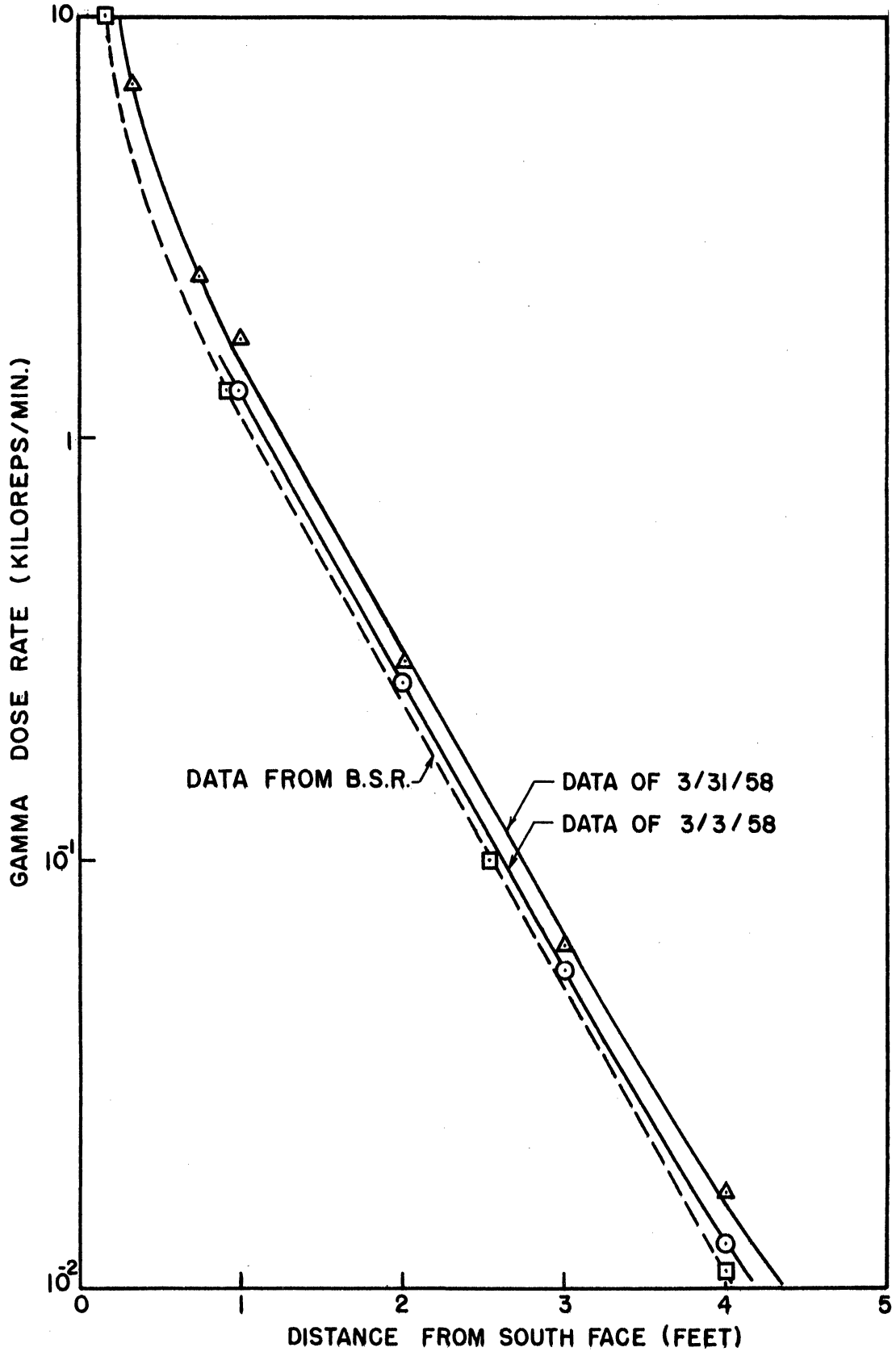

Figure 11. Gamma Dose Rate as a Function of Distance from South Face of Reactor along Center Line of Core.

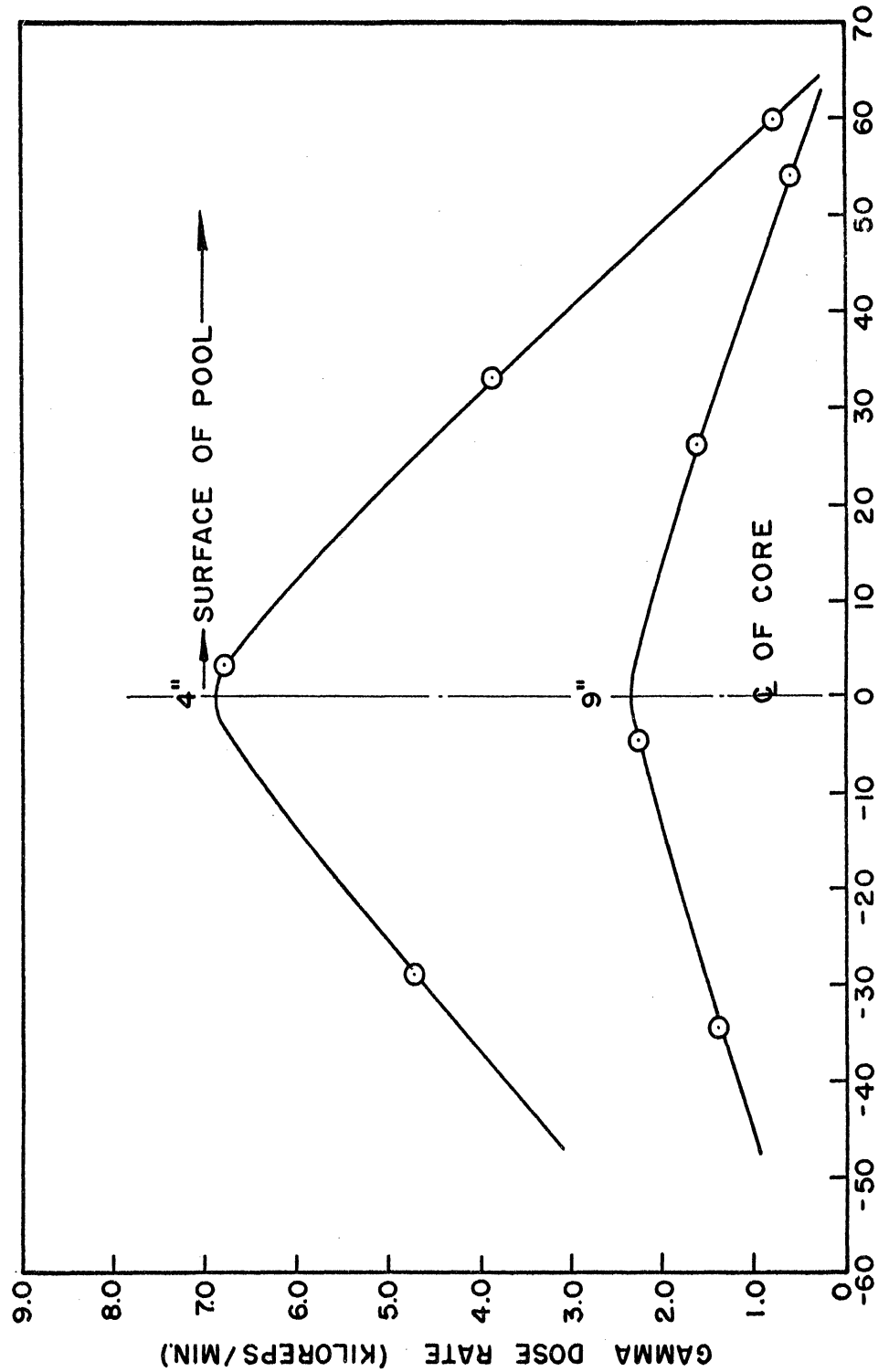

Figure 12. Gamma Dose Rates in Vertical Midplane of Core at 4 and 9 Inches from South Face of Reactor as a Function of Vertical Distance from Horizontal Midplane of Core.

2. Neutron Dosimetry.

The neutron flux was measured as a function of distance from the south face and at the sample positions in the sample rack. A standard gold foil technique[51] was used. The flux and cadmium ratio versus distance data were taken by W. Wegst of the Laboratory staff. The fluxes in the sample bottles were determined by taping small gold foils (~100 mg and 3-5 mils thick) to the front and back of polyethylene bottles filled with water. The bottles were irradiated in the pool by the standard procedure(Sec. IV, C1). The foils were allowed to cool until the activity was at a convenient level for counting in a calibrated scintillation well counter. The measured activity of the foils was then corrected to saturation activity at the time of the exposure. The "total" neutron flux was calculated by multiplying the saturation activity by an empirical factor which included the counter calibration. The activity due to fast neutrons was subtracted by:

$$\phi_T = \phi_t \left(1 - \frac{1}{CR}\right) \qquad (30)$$

ϕ_t = "total" neutron flux

CR = cadmium ratio = $\frac{\text{activity of bare gold foil}}{\text{activity of cadmium covered foil}}$

ϕ_T = thermal flux

The flux in the sample bottles was estimated by taking the geometric mean of the activities of the foils on the front and back of the bottles. The estimated accuracy of these thermal flux measurements is 20%. Table V is a summary of the neutron measurements made in this study.

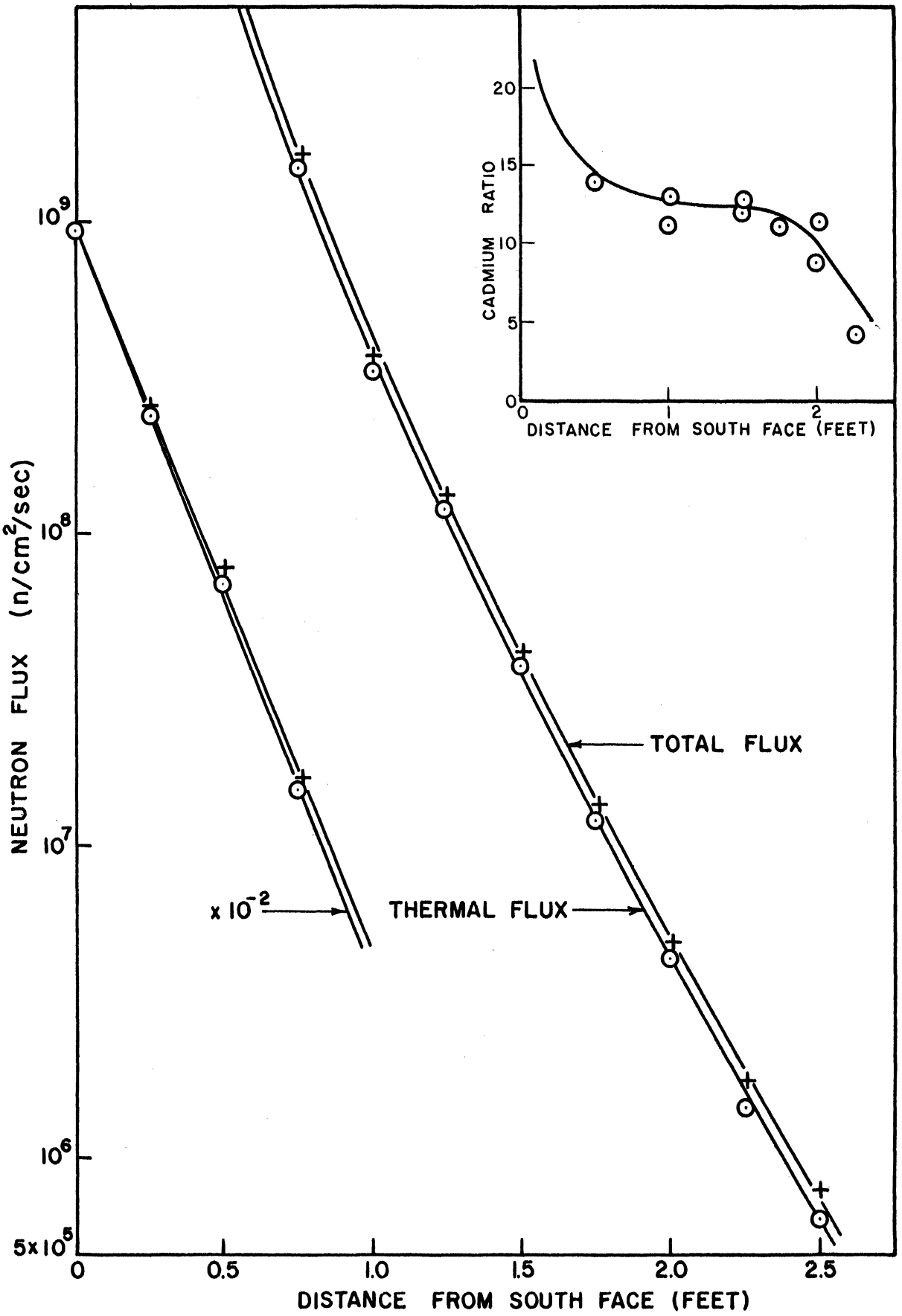

Figure 13. Thermal Neutron Flux as a Function of Distance from South Face of Reactor Along Center Line of Core.

Figure 14. (Upper Corner) Cadmium Ratio as a Function of Distance from South Face of Reactor Along Center Line of Core.

TABLE V

SUMMARY OF NEUTRON FLUX MEASUREMENTS

Date of Irrad.	Sample Position	Date of Count	Actual Counts -BKGD (cps)	Wt. of Foil (mg)	Sat. Count A_s ($\frac{cps}{100\ mg}$)	Total Flux ϕ_t (neut/cm^2/sec)	Thermal Flux ϕ_T (neut/cm^2/sec)
					x10^{+7}	x10^{+9}	x10^{+9}
5/15/58	1f	5/15/58	422	24.1	.0689	.0595	.056
	2f		502	32.9	.0860	.0743	.069
	4f		1902	11.0	.672	.580	.54
	6f		2382	7.9	1.18	1.02	.95
	7f		1141	8.5	.552	.451	.42
	4b		826	8.4	.384	.332	.31
	6b		1373	8.2	.650	.561	.52
5/15/58	3f	6/5/58	23.2	21.7	.635	.548	.51
	4f		11.2	11.0	.601	.520	.49
	5f		50.0	22.1	1.34	1.16	1.08
	6f		13.9	7.9	1.03	.890	.83
	7f		6.7	8.5	.470	.406	.38
	8f		22.4	26.3	.505	.436	.41
	4b		4.55	8.4	.312	.270	.25
	6b		8.7	8.2	.622	.538	.50
5/19/58	1f	6/5/58	8.8	37.2	.0502	.0434	.040
	2f		8.0	41.2	.0419	.0362	.034
	3f		123.2	46.8	.560	.484	.45
	4f		101.5	36.1	.597	.516	.48
	5f		226.3	39.2	1.24	1.07	1.00
	6f		284.7	45.1	1.53	1.32	1.23
	8f		99.7	40.5	.526	.455	.42
	1b		19.9	125.0	.0338	.0292	.027
	2b		14.8	108.0	.0293	.0253	.024
	3b		160.0	118.4	.293	.253	.24
	4b		182.2	124.8	.314	.271	.25
	5b		350.1	125.5	.601	.520	.49
	6b		307.3	122.6	.540	.466	.44
	7b		130.5	122.5	.228	.197	.184
	8b		144.4	116.5	.270	.233	.22

Notes: f = foil taped to front of bottle
b = foil taped to back of bottle
All irradiations were 10 minutes long.

$\phi_t = 86.3\ A_s$

$\phi_T = .933\ \phi_t$

Average cadmium ratio = 15

3. Discussion of Dosimetry

It has been assumed that the Fricke dosimeter measured only the absorbed energy contributed by the incident gammas. The incident neutrons contributed a negligible fraction of the total energy absorbed. Thermal neutrons were captured in the pool water by hydrogen. The 2.23 Mev prompt photon[15] emitted by such capture added to the gamma photons emanating from the reactor core. There would be no experimental difference between these gammas. This addition by the neutrons to the gamma flux was considered as part of the total gamma flux. Calkins[122] has estimated that the gammas resulting from neutron capture by hydrogen may contribute 30% of total gamma flux. In this paper, the chemical effects due to that portion of the gamma flux originating from neutron capture in the pool water was not considered an effect of the neutrons, but as an effect of the gammas. Any reference to gamma energy from reactor radiation implicitly means the total gamma flux resulting from both origins.

The only significant capture cross-section in the dosimeter was 0.26 barns for sulfur-34. The prompt gammas emitted with almost equal intensity have energies of 0.84 and 2.34 Mev.[15] The thermal neutron capture energy absorbed in the dosimeter was negligible.

The fast neutrons scattered principally from hydrogen nuclei as described in Section II-F of this paper. In order to estimate the fast neutron energy released in the dosimeter, some assumptions about the energy spectrum of the neutrons had to be made. At a point in the pool 4 inches from the south face, the thermal neutron flux was 1.6×10^{10} neutrons-cm/cm^3/sec. and the gamma dose rate was 6900 reps/min.

1. Assume the epithermal flux (0.1-10^4 ev) was 1/10 the thermal flux. This was based on a reported measurement in the Bulk Shielding Reactor[111] which was similar to the Ford Reactor. The cadmium ratio could not be used to obtain this ratio since the absorption cross-section of gold is not constant over the energy range.

2. The fast flux (10^4-10^7 ev) was 1/10 of the thermal flux. This was also based on observations at the Bulk Shielding Reactor.[111]

Other assumptions are tabulated in Table VI.

TABLE VI

NEUTRON SPECTRUM - ASSUMPTIONS FOR CALCULATIONS

	Thermal	Epithermal	Fast
Energy Range (ev)	0 - 0.1	0.1 - 10^4	10^4 - 10^7
Average Energy (ev)	--	10^3	10^6
Flux (cm^{-2} sec^{-1})	1.6 x 10^{10}	1.6 x 10^9	1.6 x 10^9
Average hydrogen[44] scatter cr.-sec.	--	20 barns	5

The assumed average energy of the fast neutrons did not correspond to average energy of fission neutrons (2.3 Mev) since the assumed energy range included .01 to 1 Mev neutrons.

From Equation (20)

$$\left(\frac{dE_n}{dt}\right)_a = \rho a \omega_H \chi \left[(\bar{\sigma}_H \phi \bar{E})_{Epi} + (\sigma_H \phi \bar{E})_{Fast}\right]$$

$\cong$ 2.06 x 10^{14} ev/sec/cm^3 = 210 rep/min. due to fast neutrons.

Compared to a gamma flux of 6900 rep/minute, it was about 3% of the total energy. The assumptions were made on the high side so that 4 inches from the south face the neutrons would contribute less than 3% of the total energy absorbed. This would decrease as the distance from the reactor increased because the neutron flux fell faster than the gamma flux. The effect of the fast neutrons on the Fricke dosimeter would be less than the estimated 3% because of the conservative estimates. The yield of ferrous ions for the fast protons which dissipated the fast neutron energy is 1/3 of that for gammas. The effect of the neutrons on the Fricke dosimeter would be less than 1% of the total. Thus, the radiation dose as measured by the ferrous solutions was effectively only the total gamma dose.

The neutron flux and gamma dose rate measured at the same point in the pool at a reactor power of 100 kilowatts are correlated in Figure 15. The neutron flux received by an experiment irradiated in the pool can be calculated from the total gamma dose rate at that point. An empirical equation for the line drawn through the points in Figure 15 is:

$$\phi_T = 0.23 \left(\frac{dE_\gamma}{dt}\right)_a^{2.97} \qquad (30)$$

$\left(\frac{dE_\gamma}{dt}\right)_a$ = total gamma dose rate (reps/min)

ϕ_T = thermal neutron flux (neut cm/cm^3/sec)

The empirical equation was not good near the reflector where the total gamma flux increased rapidly.

The same correlation should apply at any high power level. Since both the neutron and gamma flux were directly proportional to

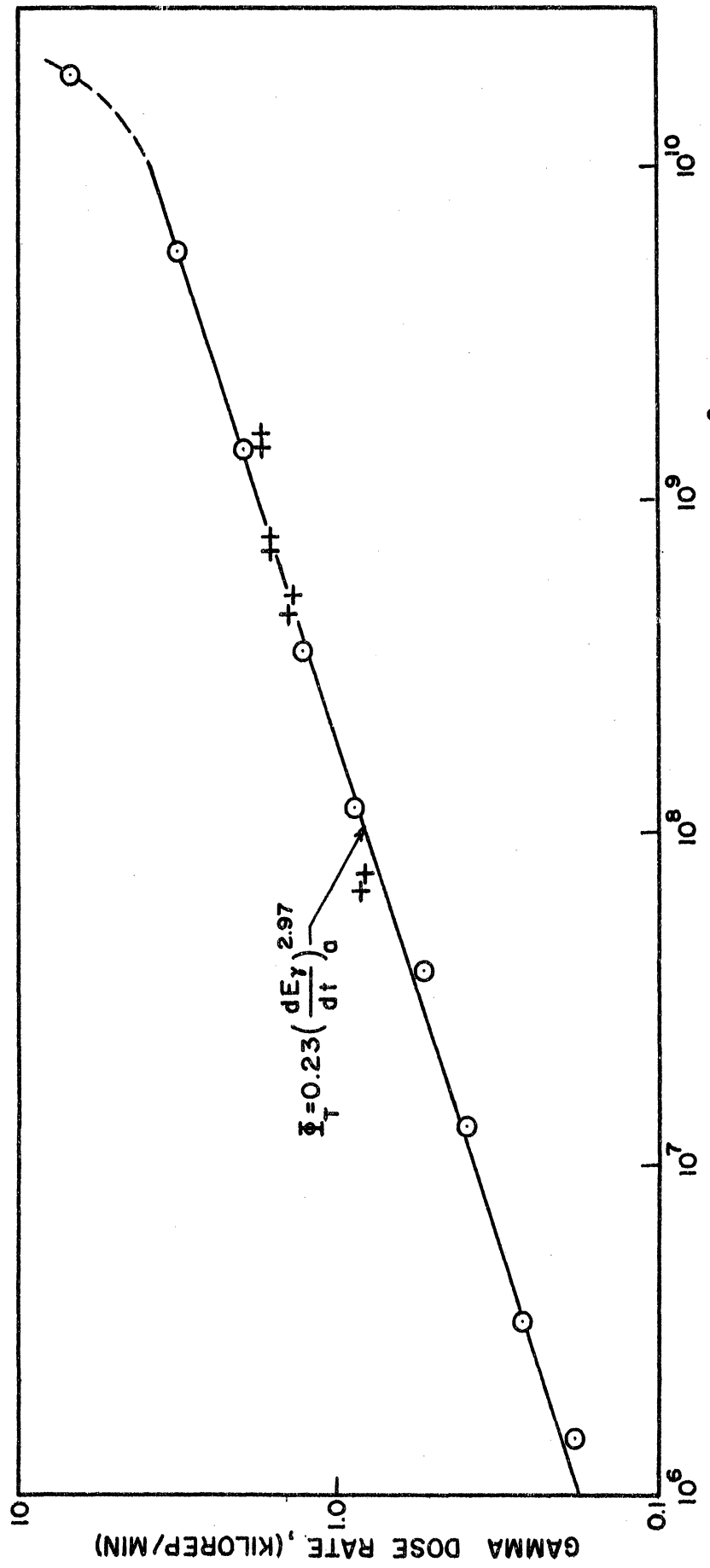

Figure 15. Gamma Dose Rate as a Function of Thermal Neutron Flux near South Face of Reactor Core.

the power level

$$\phi_T = 0.23 \left(\frac{100}{P}\right)^{1.97} \left(\frac{dE_\gamma}{dt}\right)_a^{2.97} \qquad (31)$$

P = power level in kilowatts.

D. Preliminary Experimental Investigations

1. Reactions Studied

Several reactions were considered before the selection of the benzene-water system. These were briefly investigated to determine their suitability for this study. They were:

1. The copolymerization of olefins and sulfur dioxide.
2. Chlorinated hydrocarbon-water systems.
3. Acid solutions of ferrous and ceric sulfate.

Bray[16] has studied the gamma induced polysulfone reactions. A ceiling temperature phenomenon was found, ie., above a certain temperature no reaction occurred. The only olefin with a ceiling temperature above room temperature was n-hexene-1. Trichloroethylene was chosen as the chlorinated hydrocarbon for this preliminary study.

2. Apparatus for Preliminary Investigations.

Two small pressure vessels were designed and constructed for the preliminary investigations.

Aluminum alloy (52-S) was selected for one vessel because its strength and working properties were superior to other alloys with comparable induced activity level. Alloys 2-S and EC have the lowest induced activity but they have low strength and very poor workability. The vessel was designed according to the ASME Boiler

Construction Code[117] with increased safety factors because of the hazard to the reactor and the cobalt-60 source. The working design pressure was 400 psi, but the highest expected pressure was 200 psi. The vessel was hydrostatically tested successfully at 700 psi. Closure was made by an "O" ring seal compressed by 6-1/8 inch Allen head bolts that screwed directly into threads in the flange. The absence of nuts facilitated the removal of the bolts remotely. A 1/4 inch aluminum Hoke needle valve (#372) was attached to allow the filling and emptying of the reactor. The vessel is shown in Figure 16. It was machined from a single 2 inch bar. No welds were used.

Another vessel was constructed of high density graphite. The level of its induced activity was lower than that of the best metals. The vessel was designed by application of the A.S.M.E. Boiler Code.[117] The Code does not strictly apply. It was intended to design the vessel as closely as possible and then to test to failure. The breaking pressure used for the design was 200 psi using an ultimate strength of 700 psi. The vessel was hydrostatically tested to 300 psi without failure. However, the graphite was very porous. The #30 weight motor oil used in the tester oozed through the walls so rapidly that the pressure could be kept at 300 psi for only a few seconds.

Solvents were forced through the walls in an attempt to flush out the oil that saturated the walls. It was hoped that the pore spaces could be filled by polymerizing a monomer in the walls by gamma radiation. If a pure hydrocarbon polymer were used, the low neutron activation properties of the graphite could be preserved. Several attempts were made to polymerize styrene, butene-1 and ethylene in the

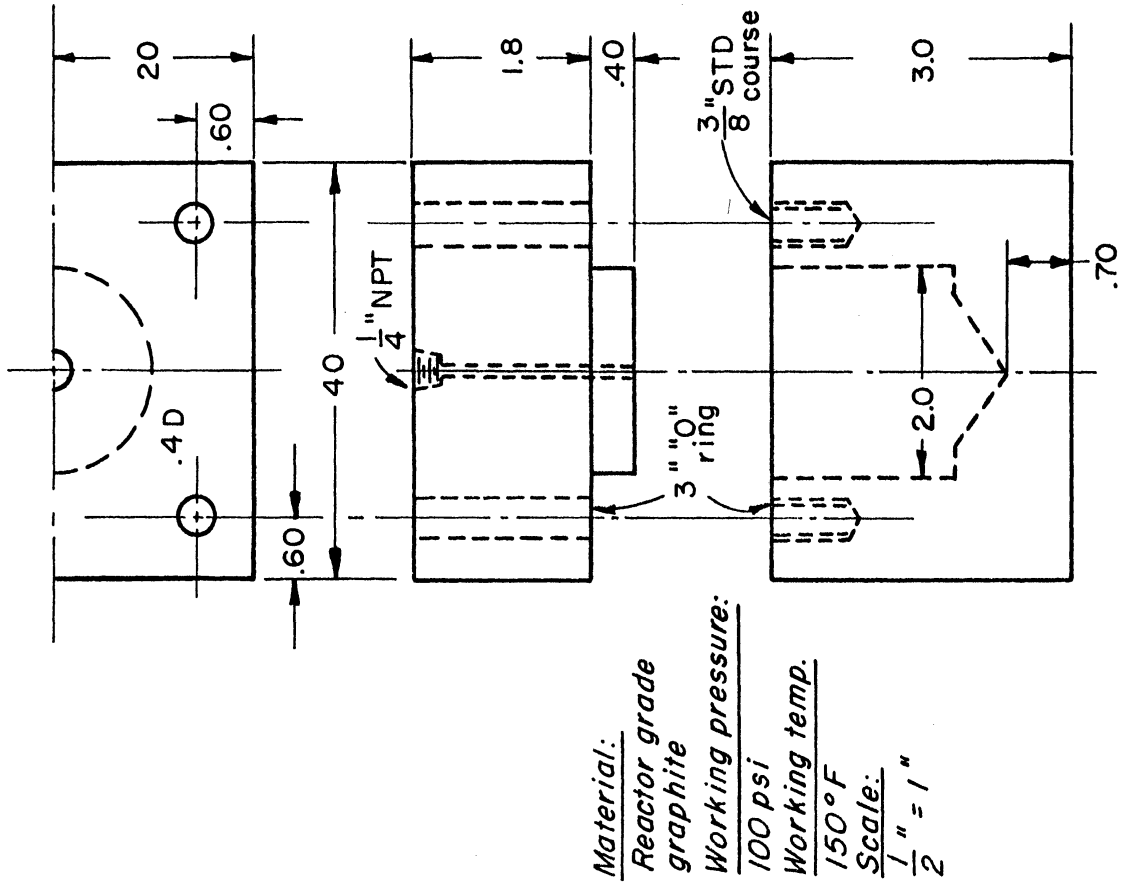

Figure 17. Graphite Pressure Vessel

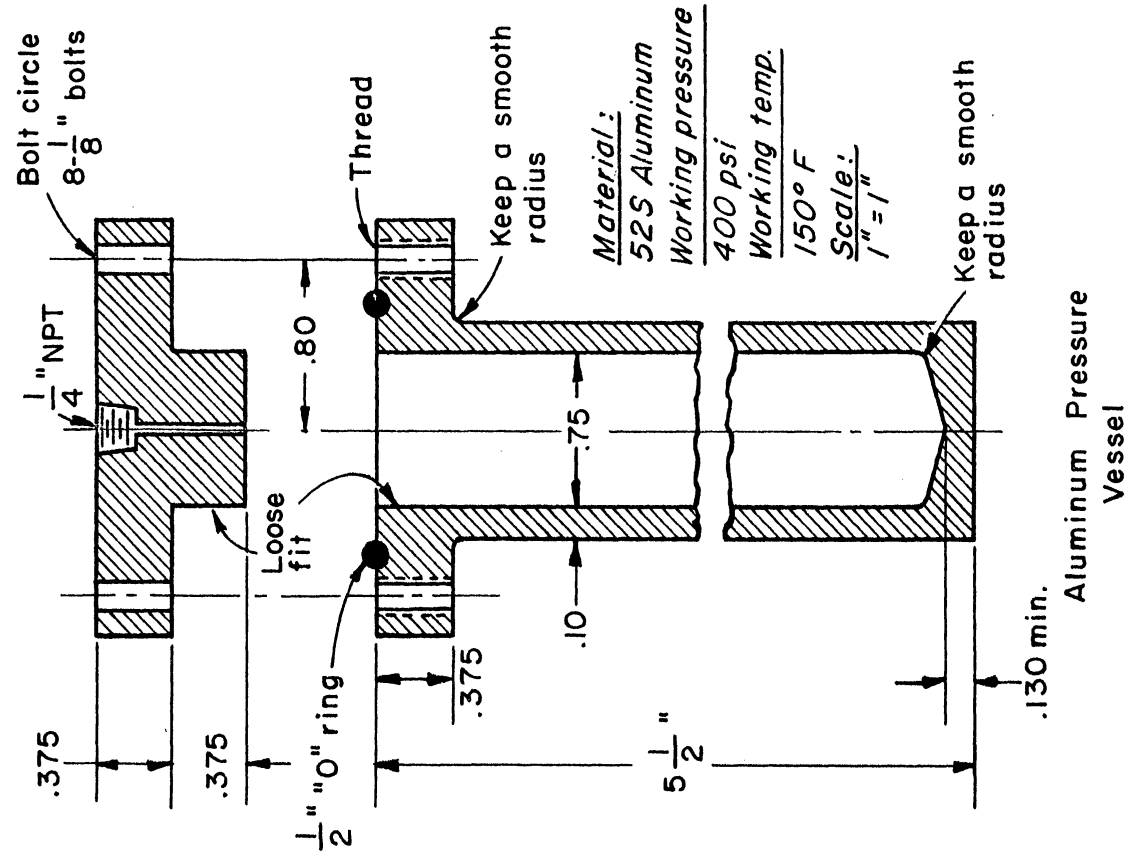

Figure 16. Aluminum Pressure Vessel

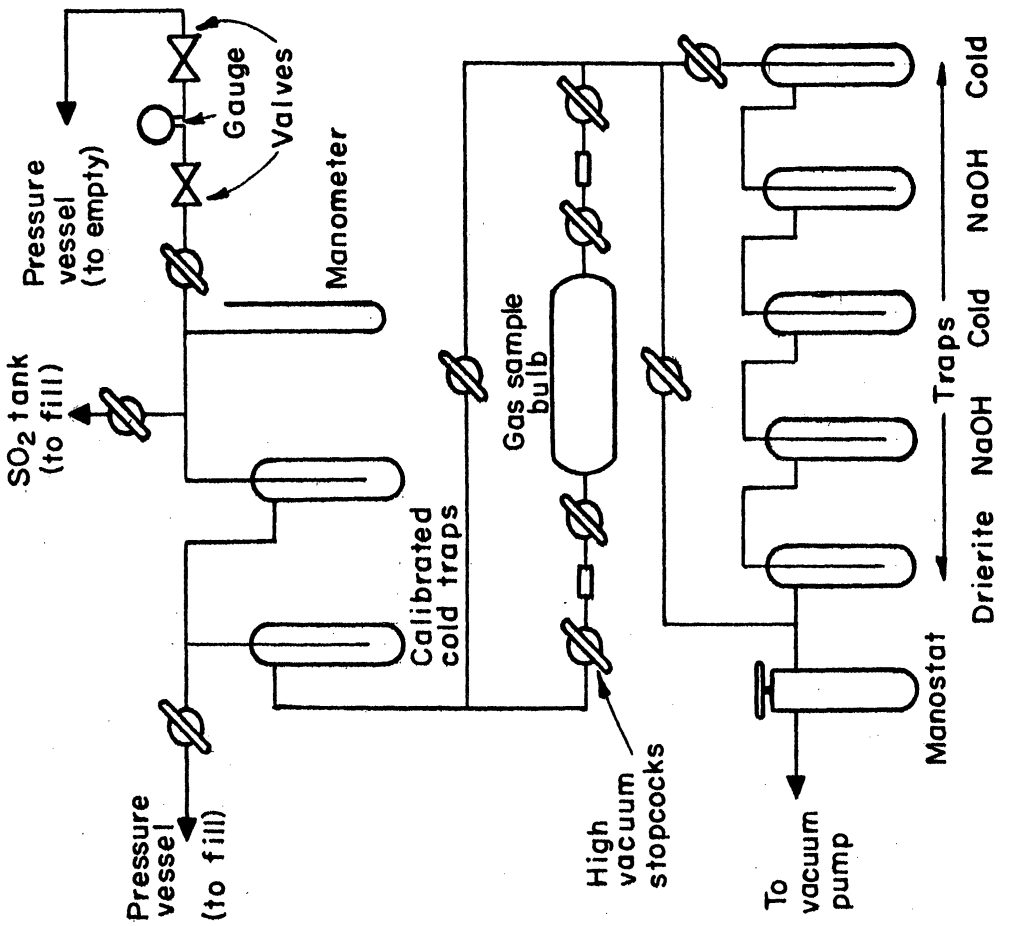

Figure 19. Gas Handling Apparatus

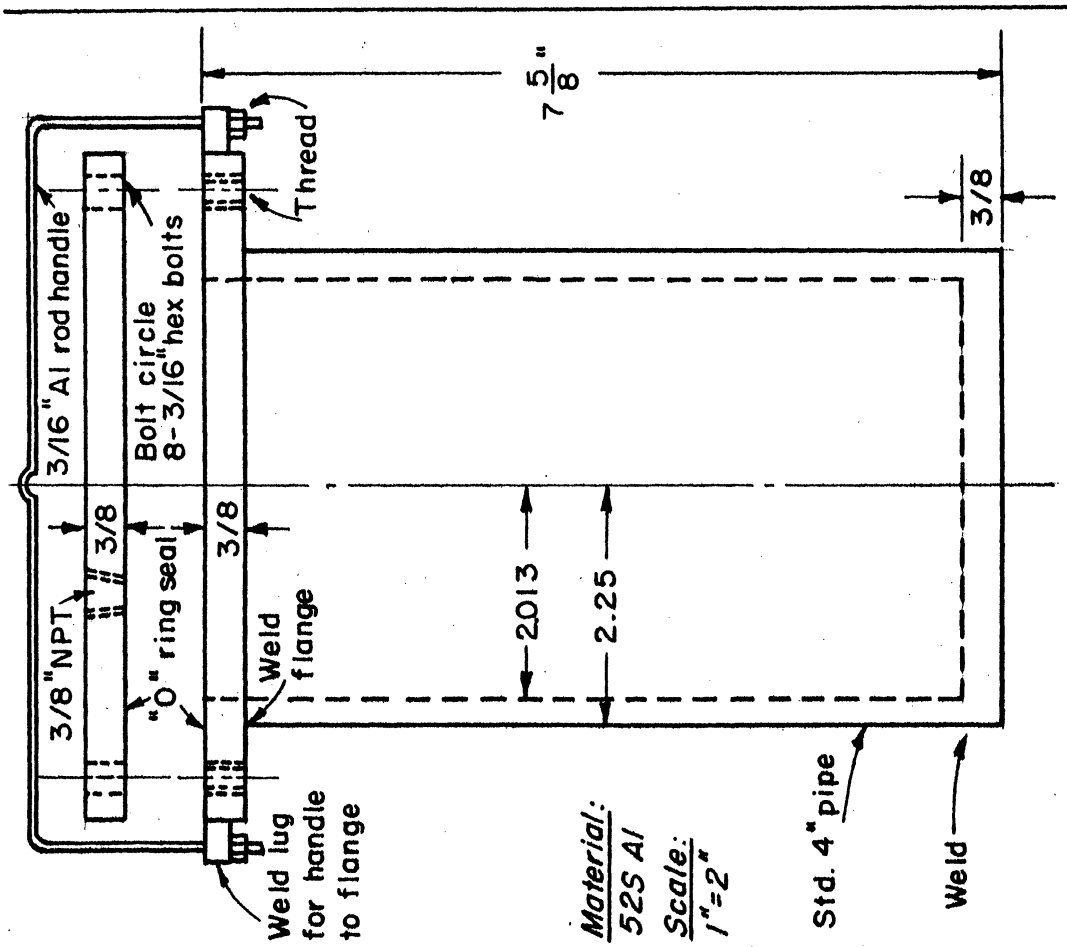

Figure 18. Aluminum Container for Pressure Vessel

walls by forcing the monomer through the walls while in a high gamma flux. All attempts failed, probably because of the low pressures that could be attained and the oil that remained in the walls.

The vessel is shown in Figure 17. It was machined from a single square block of graphite. An "O" ring seal was compressed by 4-3/8 inch by 2-3/8 inch iron stove bolts screwed into the body of the reactor. The reactor grade graphite machined well but was very dirty to work with. It was fragile and chipped easily.

An aluminum container (Figure 18) was constructed to hold the vessels. It was intended to contain any leaks from the vessels and to protect the vessels from damage during passage through the 12 inch gate valve.

A gas handling apparatus was constructed to fill the pressure vessels with the reactants for the polysulfone reactions, and to collect the gaseous products (Figure 19). In anticipation of removing radioactive sulfur dioxide from the vessels, precautions were taken to prevent exhausting the gases into the air. Two cold traps and two sodium hydroxide traps were provided before the vacuum pump. A connection would be made remotely to the Hoke valve on the top of the vessel by using the master slave manipulators in the hot cell. The connection would lead through a lead filled plug in the cell wall to the handling apparatus outside the cell. The vacuum pump, inside the cell, would keep a vacuum in the system at all times.

3. Experimental Procedures.

The procedure for the polysulfone reactions closely followed those of Bray.[16] Pure grade n-hexene-1 was purified by fractionation on a Podbielniak column (L/D ~ 20) by taking the middle one-half fraction. This fraction was poured into the pressure vessel. The vessel was sealed and weighed. The vessel was attached to the filling apparatus, cooled in a bath of dry ice and isopropyl alcohol, and evacuated. Sulfur dioxide was condensed directly from the cylinder in a calibrated cold trap. The sulfur dioxide was then recondensed in the pressure vessel. The valve on the vessel was closed and the vessel allowed to come to room temperature and reweighed.

After irradiation, the vessel was again attached to the gas apparatus. The remaining gases were allowed to boil off and be condensed in a calibrated cold trap. A vacuum was applied for several hours to remove the last traces of volatile gases. The vessel was weighed to determine the weight of the polymer formed. The vessel was then opened and the polymer removed.

Trichloroethylene was purified on a Podbielniak column (L D ~ 20) by taking the middle one-half fraction. This fraction was carefully protected from light since the stabilizer added to the commercial chemical had been largely removed during the fractionation. Measured amounts (~ 10 ml) of the purified chemical were pipetted into 25 ml glass vials with constricted necks. The vials were flame sealed.

After the irradiation, the outside of the vial was carefully washed with distilled water. In a hood, the vial was broken

by a hot wire technique into a 400 ml beaker containing 25 ml of standard 0.1 M NaOH to extract the acids from the organic phase and 3 ml of 30% H_2O_2 to decompose organic peroxides. The mixture was agitated and titrated with standard 0.1 N H_2SO_4 to the methyl orange end point.

4. Results and Discussion.

The results from the quantitative polysulfone runs are summarized in Table VII. The calculations follow the methods used by Bray.[16] The product was a tough, hard, foam-like plastic, similar to that observed by Bray. The plastic frequently stuck to the pressure vessel and was difficult to remove. It was quite soluble in trichloroethylene. Upon evaporation of the solvent, the polymer formed a very hard, transparent, colorless plastic that was inert to acids and bases. Reaction rate and percent conversion were the only experimental parameters observed. The results were very erratic. This was possibly caused by the reaction temperature being close to the ceiling temperature (57°C.) and by impurities in the reactants.

The aluminum pressure vessel became highly active. The gases could be removed remotely but a cooling period of several days would be required before the polymer could be removed. The activity of the reactants and polymer would be due mainly to sulfur-35 (87 day half life) which emits a weak beta particle (0.17 Mev). It is not hazardous unless ingested. Analyses of the product were difficult to perform and interprete. The difficulty of the experiments, the hazards, and the erratic data ruled out this system as a possible system for this study.

TABLE VII

SUMMARY OF DATA FROM PRELIMINARY INVESTIGATIONS

Polysulfone -- n-Hexene-1 and Sulfur Dioxide

Average Reaction Temperature: 90°F.

Gms of Hexene	Gms of SO_2	Gms of Polymer Formed	Total Dose, Mrep	Gm-mols Reacted / liter (1)	Time, Min.	Average Rate, Gm mols / lit.-hr.
19.91	12.69	10.0	0.205	1.71	15.0	6.84
23.25	7.85	9.93	0.273	1.63	20.0	4.89
22.71	25.48	4.41	0.12	0.56	18.5	1.83
21.33	10.79	17.0	0.240	2.85	17.5	9.75

Trichloroethylene

Volume of Trichloroethylene sample; 9.9 ml

Total Dose, Megarep	HCl Formed, millimols / liter	A(HCl) micromols / (krep)(lit.)	HCl Formed, millimols / liter	A(HCl) micromols / (krep)(lit.)
0.572	215 (2)	376	285 (3)	498
0.572	228	398	283	495
0.572	234	408	295	516

Notes:

(1) Mols of hexene reacted equals mols of SO_2 reacted.

(2) Titrated the same day the irradiation ended.

(3) Titrated the next day after the irradiation ended.

The results from the gamma irradiations of trichloroethylene are summarized in Table VII. The principal product was hydrochloric acid and, if water or oxygen was present, other organic acids.[96] Many other minor products were formed. These acids were extracted from the organic phase with a known amount of base and were determined by back titration with acid. After irradiation, the organic phase was extremely sensitive to light. The titration end point drifted rapidly as the solution became more acid. Unirradiated trichloroethylene showed no sensitivity to light. The radiation either destroyed the remaining stabilizer or produced a substance that induced photosensitivity. The sensitivity to light persisted after several weeks. The principal radioactivity is caused by chlorine-38 which emits energetic betas and gammas but has only a 37 minute half life.

The system was not studied further because of the photosensitivity of the irradiated trichloroethylene. Because the reaction was carried out in pyrex vials, a cooling period of several days was required for reactor runs. Pyrex contains a large quantity of boron. Thus, a large fraction of the thermal neutrons would be absorbed by the glass.

Studies here and elsewhere have been made[34,72,94,107] with cadmium, boron and lithium added to the ferrous solutions. The $G(Fe^{3+})$ for the particles from neutron absorption in boron and lithium have been measured in this manner. These additional solutes somewhat change the effect of gamma radiation on the ferrous sulfate. The cadmium ion may be a catalyst[73] for the destruction of hydrogen peroxide. Since these systems had been studied extensively, it was decided to look for a

system that had not been given as much attention.

These initial studies proved to be valuable in that they indicated some prerequisites for a chemical system suitable for a study of the effects of pile radiations. The initial studies had shown that the chemical effect of the neutrons from the Ford Reactor would be very small because the available flux consisted almost entirely of thermal neutrons. In order to increase the energy release due to the thermal neutrons, atoms with high absorption cross-sections must be added to the reactants. If possible, these additives should not affect the radiation reaction.

The reaction also should yield a specific major product that can be accurately and rapidly analyzed. The number of variables affecting the radiation yield should be minimized so that the derived results can be clearly interpreted. The reaction rate should not be too sensitive to temperature because of the difficulty of controlling temperatures in the cobalt source room and the pool. Because the temperature of the reactor pool governed the reactant temperature, the reaction must proceed at the pool temperature ($\sim$90°F). The reactant atoms should not become highly active when exposed to a thermal neutron flux or they should have a short half life.

The reaction should not need elaborate equipment that would become radioactive. This requirement ruled out high pressure reactions needing heavy vessels. With the master-slave manipulators, it was possible, but extremely difficult to perform many ordinary operations that would be required with a pressure vessel.

Water solutions saturated with benzene fulfilled most of these requirements.

IV. FINAL EXPERIMENTAL PROGRAM

A. Reactions Studies

The reaction of aqueous benzene to form phenol was studied in some detail. The variables that were studied are:

1. Total gamma dose
2. Gamma dose rate
3. Benzene concentration
4. Oxygen concentration
5. Temperature
6. Total neutron dose
7. Neutron flux
8. Product concentration

To increase the effect of the thermal neutrons, solutes with high neutron absorption cross-sections were dissolved in the aqueous benzene. The solutes used were:

1. Cadmium sulphate
2. Boric acid
3. Lithium metaborate

The effect of each dissolved salt on the reaction was studied in the cobalt-60 source. The effects of various neutron doses and fluxes were then studied in the Ford Reactor. The phenol yield from the reactor irradiations was compared to the yield from the cobalt-60 irradiations. The Fricke dosimeter was used as the basis of comparison for the two radiations. The yield of ferric ions was a direct measure of the gamma dose only.

B. Apparatus

1. Bridge

A movable bridge was constructed to span the reactor pool. Samples to be irradiated could be suspended anywhere in the pool by means

of this bridge. The bridge (Figure 20) consisted of two 2-inch steel pipes 20 feet long securely clamped to two supports on either side of the pool. The bridge supports were welded from 1-1/2 inch steel angle. The supports were mounted on casters so that the bridge could be moved to any north-south position over the pool.

A trolley (Figure 21) traveled along the pipes on four casters. The trolley could be moved along the pipes by means of a continuous "trolley guide cable" attached to the trolley and running through pulleys on each support. The trolley position was secured by clamping the guide cables together.

The sample to be irradiated hung on a stainless steel cable running through a pulley on the bottom of the trolley. The cable ran back to a reel on the east bridge support so that the sample could be raised or lowered to the desired location. A lead brick on the end of the long cable hanging in the water added stability. To prevent rotation of the irradiated samples, two lines were fastened to the samples and run through two pulleys hung on either side of the pool. One ounce lead weights were tied to the other end to keep tension on the lines.

The bridge was so designed that it could be disassembled and removed easily if required by other experiments in the pool.

2. Sample Bottles

The benzene-water and ferrous dosimetry irradiations were carried out in one ounce polyethylene or soft glass bottles. The polyethylene bottles were used for the majority of the runs. The glass bottles became highly active due to the 14.8 hour sodium-24 activity and had to be handled quickly or stored for several days. The polyethylene never showed

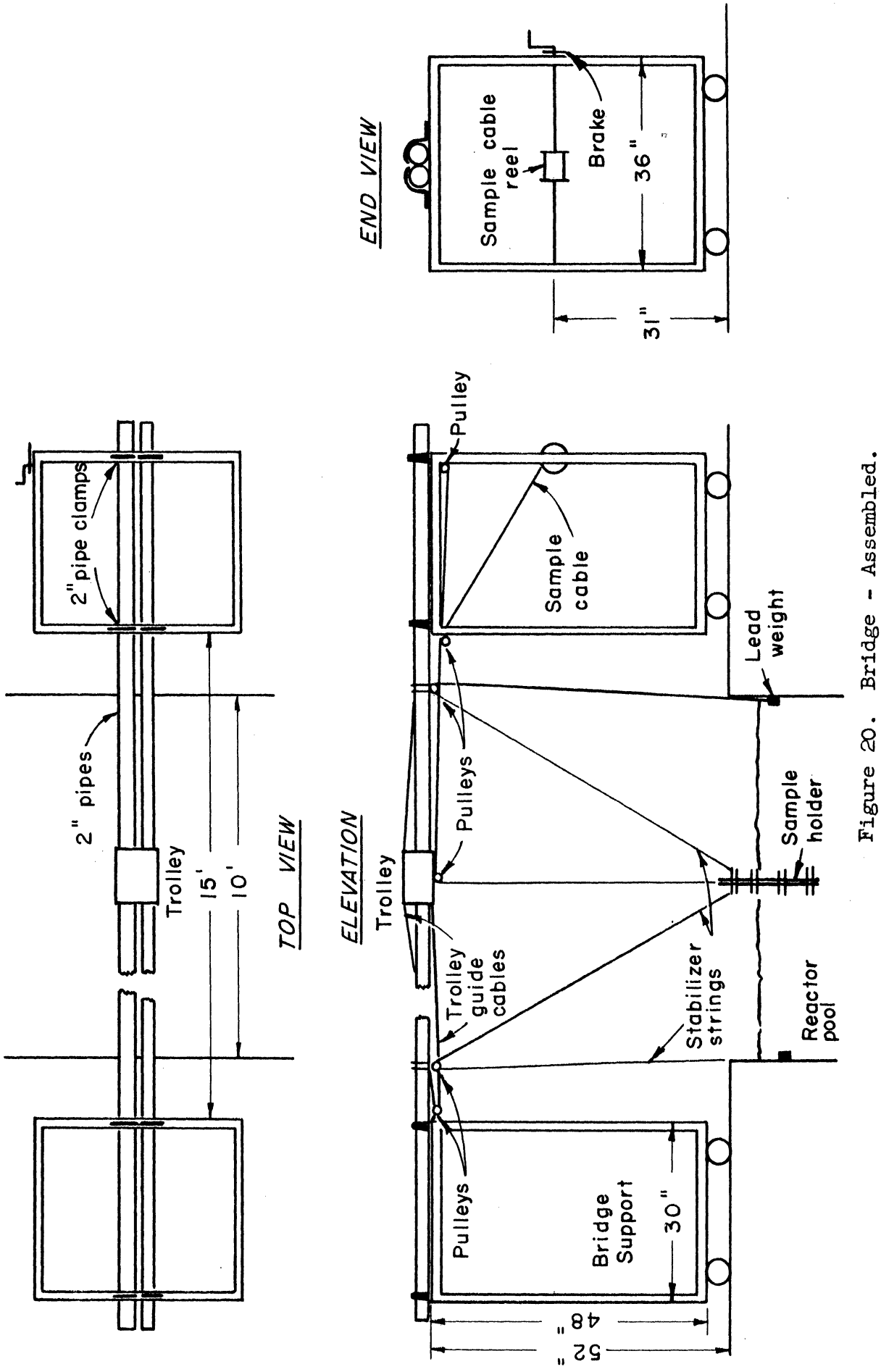

Figure 20. Bridge - Assembled.

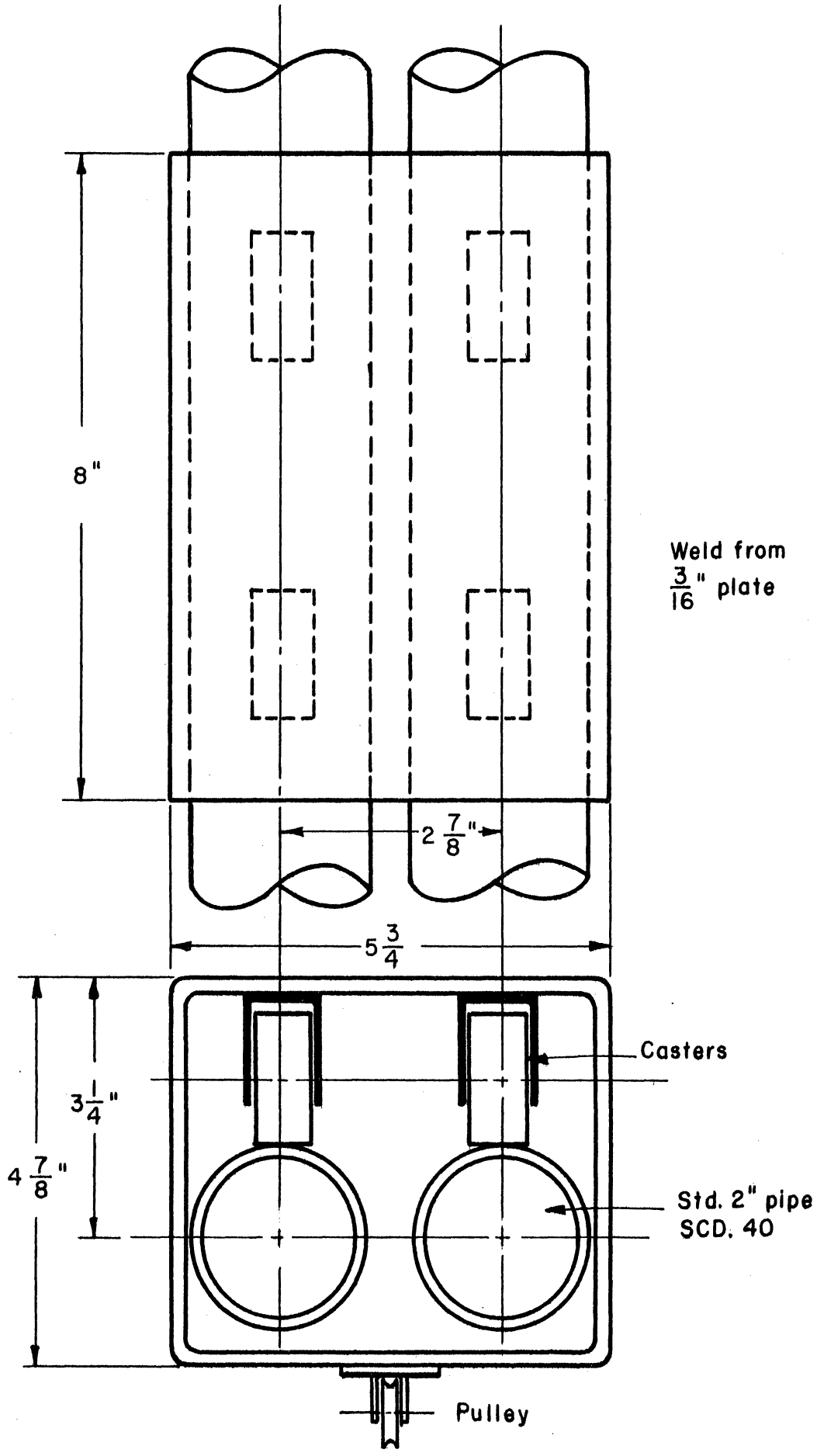

Figure 21. Trolley

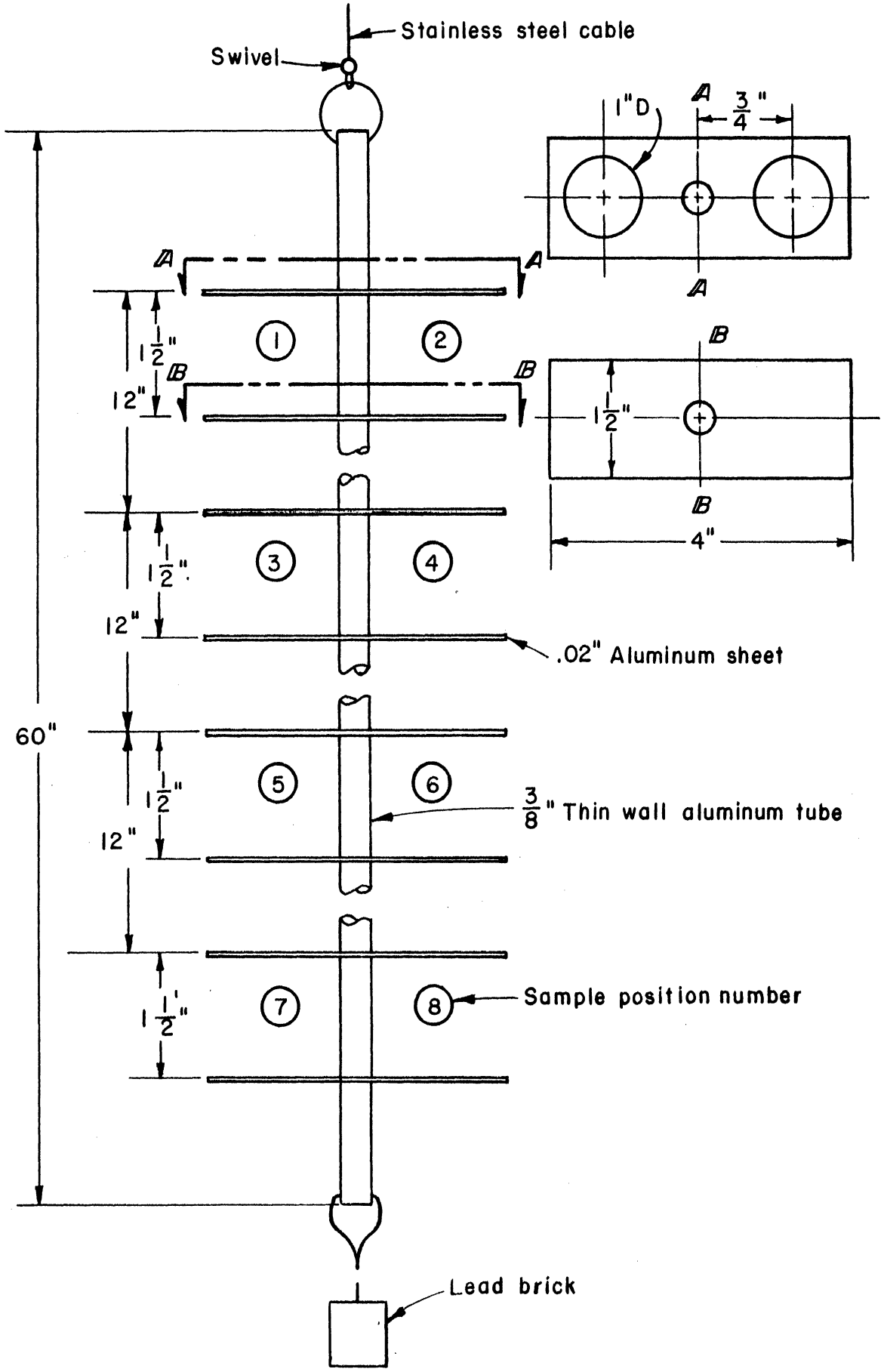

Figure 22. Sample Holder.

any detectable activity. The polyethylene had no effect on the ferrous dosimeter as reported by some workers. Several measurements in glass and polyethylene bottles in the cobalt-60 source showed no significant differences. The polyethylene bottles were cleaned before every run with dichromate cleaning solution and rinsed several times with tap water, distilled water and the experimental solution.

3. Sample Holder

A sample holder (Figure 22) was fabricated from 2-S aluminum. Very thin aluminum was used to minimize the mass of metal, thus decreasing the radiation emitted. The glass bottles had to be tied in place so that if they came out of the rack they would not fall to the bottom of the pool. The polyethylene bottles were held securely by the holder. Since they would float in the pool, they were not tied to the rack.

C. Experimental Procedures

1. Irradiation Procedures

Samples to be irradiated in the cobalt-60 source were placed at predetermined locations in the source room. The gamma dose rates at these points had been determined by ferrous dosimetry. Bottles used in all benzene-water and chlorinated hydrocarbon runs were placed on the floor at various distances from the source to obtain different dose rates. Polysulfone reactions were carried out in the aluminum pressure vessel clamped in the center of the source. The length of irradiation time was kept by a stop watch or electric timer, started and stopped when the source danger light came on and went off. A correction was made for the coming up and going down dosage only for samples in the center of the source.

Samples to be irradiated in the reactor pool were loaded into the eight positions in the sample holder. The contemplated runs first had to be approved by the Reactor Supervisor. The Reactor Operator was kept informed of any movement of the samples in the pool. The activity of the holder was checked whenever it was withdrawn from the pool. When the samples were in the holder, the bridge supports were placed at a fixed position on the floor. This determined the north-sourth position. Next the trolley was run out to the center of the pool. The exact east-west position was reproduced by matching two marks on the trolley guide cables and clamping the cables together. At this point the samples were directly above the intended position for the irradiation. Then the samples were rapidly lowered. A stop watch was started when a mark on the sample cable appeared indicating that the samples were within a few inches of the desired location. The desired level was reproduced by stopping the cable reel at the same position each time.

The samples were removed from the core, after notification of the reactor operator, by reversing the above procedure. The rack was allowed to remain in the pool (away from the core) for about 30 minutes to allow the aluminum-28 activity to decay (half life 2.4 min.). This waiting time reduced the initial activity by a factor of a 1000.

The sample rack was monitored continuously with a GM survey meter while the rack was being brought out of the pool, unloaded, and re-loaded for another run. The maximum level allowed for this operation was 50 milliroentgens/hour at the surface of the rack. The complete operation of unloading and reloading the holder with eight polyethylene bottles took less than a minute and was done at arms length from the operator.

The accuracy of the measurement of the irradiation times was considered adequate. The sample holder could be lowered from the surface of the pool to the desired depth in 5-10 seconds, and raised in the same time. It was estimated that a sample was at a "wrong" flux for less than two seconds. This would be an error of less than 1% for a three minute irradiation.

A blank sample was run for all irradiations. Except for the radiation step, it was treated like the irradiated samples. After analysis, the samples were carefully disposed of in "hot drains" provided in the laboratory.

2. Benzene-Water

Triple distilled water was saturated with benzene by shaking together one liter of water and a few milliliters of benzene. The benzene saturated water was stored in glass stoppered amber-glass bottles. A solution was kept for several months with no detectable phenol formation. A layer of benzene was kept over the water to keep it saturated. About 25 ml of the water layer was withdrawn from the storage bottle and pipetted into a one ounce polyethylene bottle for irradiation. The bottle was tightly capped to prevent undue evaporation of the benzene and to prevent the pool water from leaking in.

Solutions prepared by this technique were saturated with air. Several runs were made with deaerated solutions. These were prepared by boiling distilled water for about an hour. Helium or nitrogen was slowly bubbled through the solution during the boiling and cooling periods. When the water had cooled, boiling benzene was poured into the water and mixed.

The polyethylene bottles were flushed with the inert gas just before the solution was forced into the bottles by gas pressure.

Several methods were considered for the analysis of phenol in the irradiated solution. Because of the small amounts of solution and the low concentrations of phenol, photometric analysis was considered to be the most accurate and convenient. Phenol has an absorption peak at 2700-2735 Å. The molar extinction coefficient has been reported as 2170 liter/mol/cm at 2735 Å[8] and as 1470 at 2700 Å.[79] Values of 1320 and 1460 respectively were found in this study. Benzene has a very low extinction coefficient at 2700 Å (~4.3).[79] It interfered significantly with the phenol absorption because the benzene concentration was about 100 times that of phenol in the irradiated solution. Diphenyl, a by-product in the reaction, interfered to an even greater extent. Baxendale and Magee[8] have suggested extraction of the benzene into hexane and then correcting for the remaining benzene in the aqueous phase by measuring the optical density at 2550 Å.

Folin[38] developed a standard photometric analysis for phenol. The addition of a special reagent develops a color with a peak at 2500 Å. It has a very favorable extinction coefficient (~10,000 liter/mol/cm). Folin's reagent is very difficult to prepare but it is unstable. Although it has been used with success, several investigators have reported occasional unsatisfactory results attributed to spoiled reagent. In this study, a fresh bottle of the reagent gave erratic results during the standardization runs and was not used again.

The method for phenol analysis used in this study was suggested by Sworski.[108] The phenol peak at 2730 Å in neutral solutions shifted

to 2880 Å in basic solutions (pH > 12). A wave length of 2900 Å and slit width of 0.5 millimeter were used for the phenol analysis. Silica cells were used since corex glass cells were unsuitable at this wave length. Other organics present in the irradiated solutions had a significant absorption in this range. A correction was made for their absorbance by subtracting the optical density of the neutral solution from that of the basic solution. The molar extinction coefficient of phenol in neutral solutions was zero at this wave length.

The analytical procedure used was the following:

1. Two 5 ml samples of the irradiated solution were pipetted into two 30 ml beakers.
2. Into one beaker 5 ml of distilled water was pipetted. This was the unbuffered sample.
3. 5 ml of 0.06 N NaOH were pipetted into the second beaker. This was the alkaline sample.
4. The optical density of both samples were read at 2900 Å. The optical density of the alkaline sample was read as a function of time after the solution was prepared.
5. The concentration of phenol was calculated by:

$$[P] = F \kappa [(D_{AS} - D_{US}) - (D_{AB} - D_{UB})] \qquad (32)$$

where:

[P] = concentration of phenol in micromols/liter.

F = dilution factor = 2.

D_{AS} = optical density of the alkaline sample.

D_{US} = optical density of the unbuffered sample.

D_{AB} = optical density of the alkaline blank.

D_{UB} = optical density of the unbuffered blank.

κ = phenol calibration constant.

The constant K was determined by analyzing standard phenol solutions. These solutions were prepared by diluting a purchased standard phenol solution. Direct weighing of reagent grade phenol crystals was difficult but calibrations conducted in this manner gave a value for K of 398. Figure 23 is the calibration line obtained with the phenol standards. The constant K is related to the molar extinction coefficient by:

$$K = \frac{10^6}{\epsilon p} = 393 \pm 2 \qquad (33)$$

ϵ = molar extinction coefficient of phenol = 2520 ± 10 (liter/mol/cm)

p = path length = 1.009 cm for the silica cells used.

Sworski[108] reported a value of 397 for K. However, he did not report the path length of his photometer cells. Assuming that it was 1.000 centimeters, his value agrees with the value found in this study. Figure 23a shows the variation of extinction coefficient for phenol with the amount of NaOH added and the pH of the solution. The analysis is not sensitive to the amount of excess base added to the solution. The molar extinction coefficient as a function of wave length is shown in Figure 24.

The irradiated alkaline sample increased in optical density with time after addition of hydroxide. The optical density of the neutral sample did not change. This was attributed to a reaction by-product decomposing in the basic solution. The radiation phenol yield was determined by extrapolating the concentration to zero time.

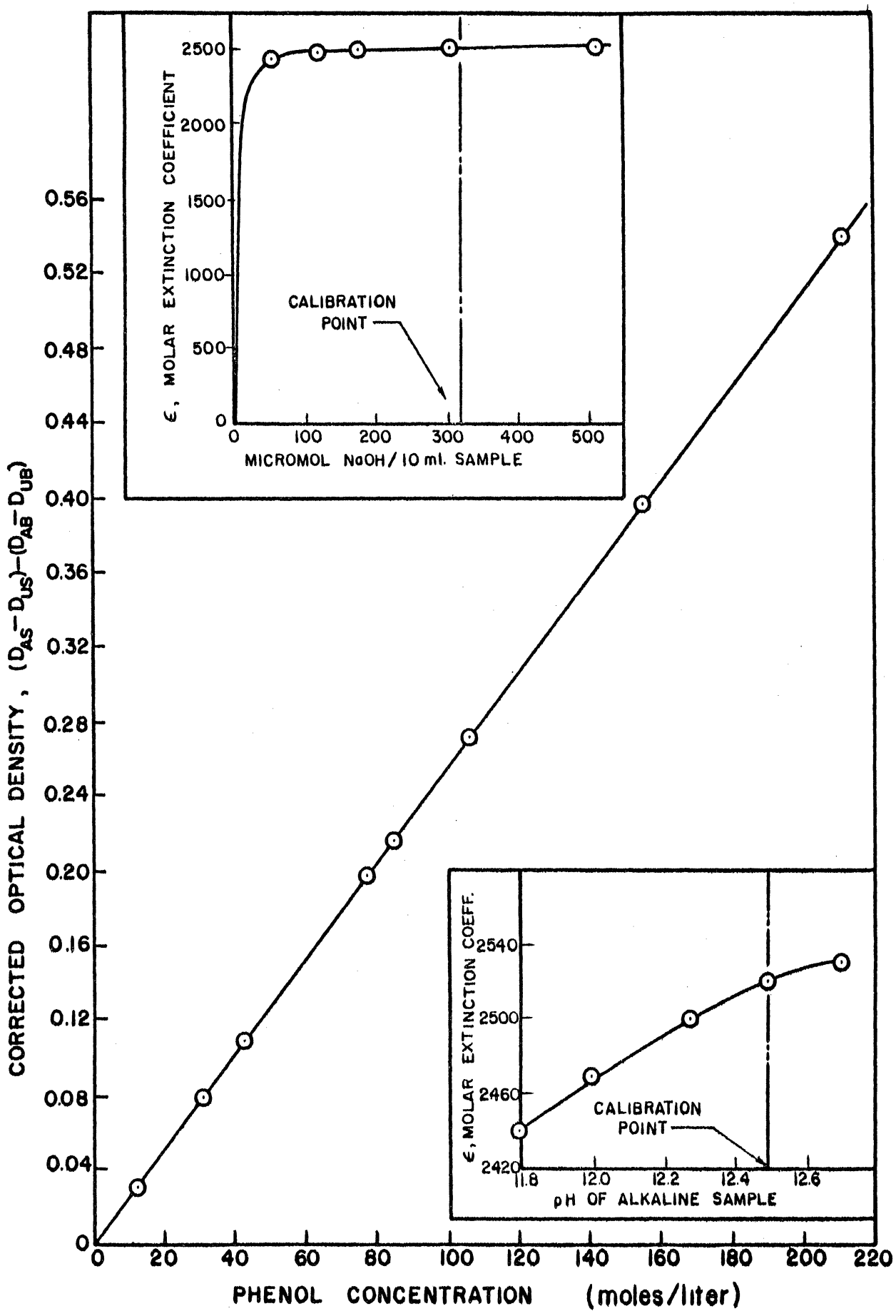

Figure 23. Calibration of Phenol Analysis

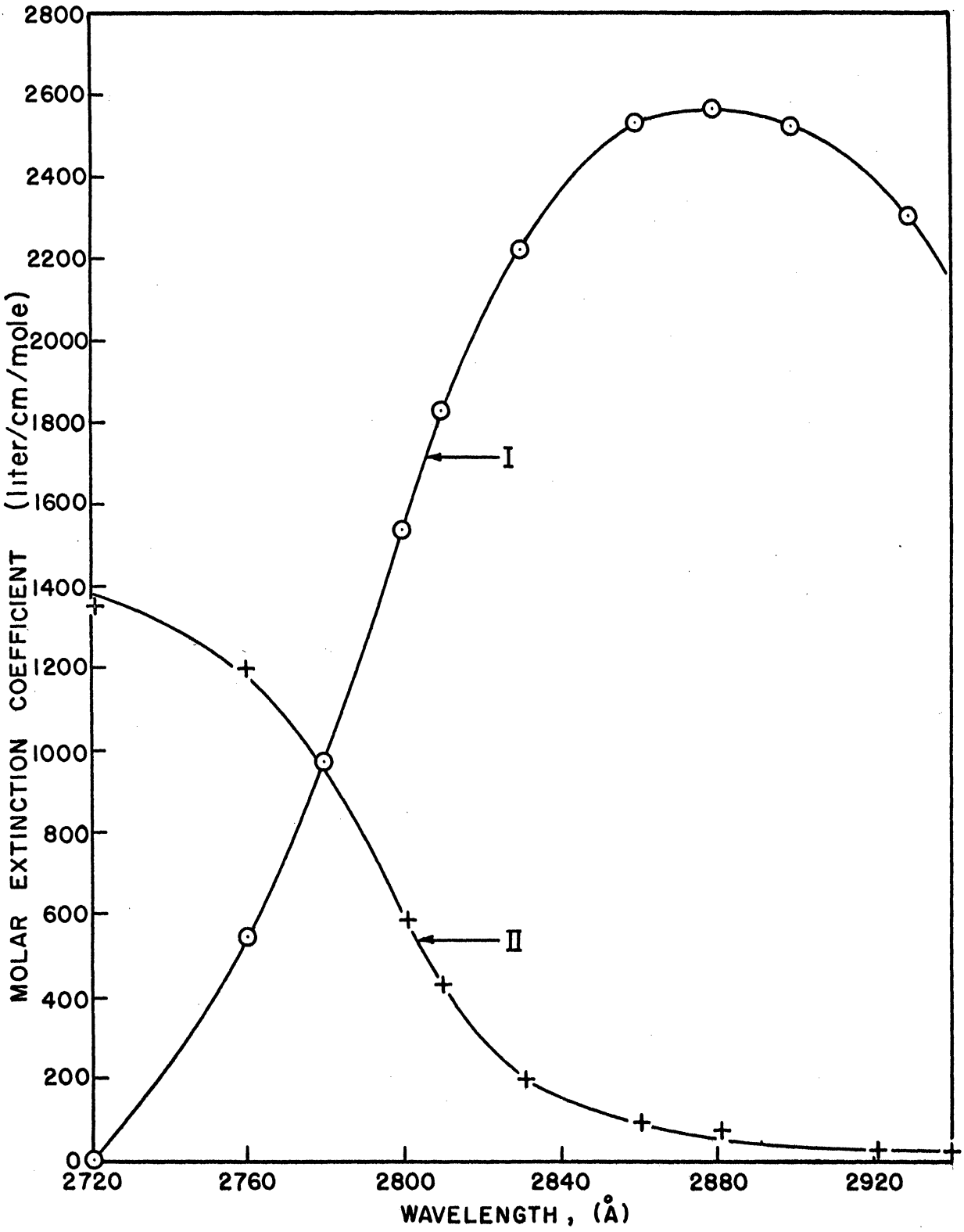

Figure 24. Molar Extinction Coefficient of Phenol Solutions as a Function of Wave Length.
I. Alkaline Sample Compared to Unbuffered Sample
II. Unbuffered Sample Compared to Pure Water.

3. Benzene-Water-Cadmium Sulfate

Solutions of known cadmium concentration were prepared by dissolving weighted amounts of cadmium sulfate in triple distilled water. The salt was dried for 24 hours at 120°C before weighing. The solution was then saturated with benzene and irradiated by the usual procedures. The saturated solution was stable to light for long periods of time.

The steps of the analysis were:

1. One 5 ml sample was pipetted into a 30 ml beaker and diluted with 5 ml of distilled water (unbuffered sample).
2. A second 5 ml sample was pipetted into a 15 ml centrifuge tube (alkaline sample).
3. The required amount of standardized NaOH ($\sim$0.5M) was accurately measured into the tube from a burette. The required amount was that needed to precipitate all the cadmium as $Cd(OH)_2$ plus 500 micromols of NaOH excess per 10 ml sample needed to make the solution pH > 12.
4. The alkaline solution was centrifuged for not less than 5 minutes.
5. The supernatant liquid was decanted into a 10 ml volumetric flask, the tube was washed with a small amount of distilled water, and recentrifuged. Again the supernatant liquid was decanted into the flask. The volume in the flask at this point had to be less than 10 ml.
6. The solution was diluted with water to a total volume of 10 ml.
7. The optical density of the alkaline and unbuffered sample was measured at 2900 Å.

8. The concentration of phenol was calculated by Equation (32) except that K was a function of the concentration of cadmium in the original solution.

The analysis was calibrated with solutions of known phenol and cadmium concentrations. The parameters K and ϵ are plotted in Figure 25 as functions of cadmium concentration in the original solution. The decrease in the molar extinction coefficient was attributed to a portion of the phenol occluded in the cadmium hydroxide precipitate. An empirical equation for K was fitted to the points.

$$K = 615\ [Cd] + 393 \qquad (34)$$

[Cd] = cadmium concentration (moles/liter).

4. Benzene-Water-Boric Acid

Solutions of known boric acid concentration were prepared by weighing reagent grade boric acid directly from the bottle. Boric acid is relatively volatile and unstable[75] above 80°C so it could not be oven dried. A sample kept in a vacuum dessicator for several days lost negligible weight. The solution was saturated with benzene in the usual manner. The solutions were stable to light and stable with time.

Analytical methods were similar to those used for benzene-pure water solutions. To form the alkaline sample, enough sodium hydroxide was added to neutralize one equivalent of the boric acid plus an excess of 500 micromols of hydroxide per 10 ml sample. The sample was diluted to 10 ml. The boric acid-sodium hydroxide solution formed an effective buffer. The analysis was very insensitive to the amount of excess NaOH added. No increase with time in the optical density of the irradiated

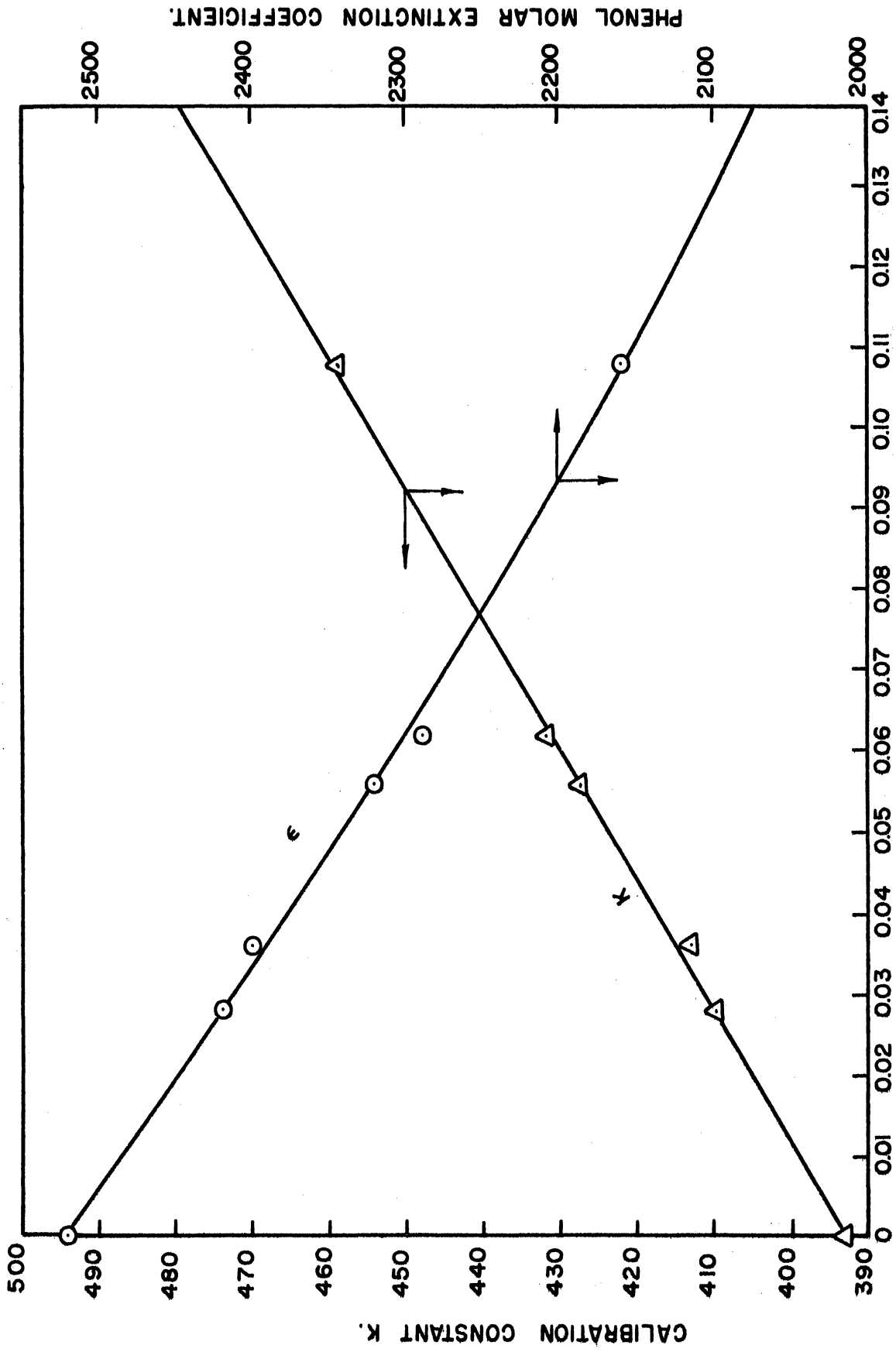

Figure 25. Molar Extinction Coefficient and Calibration Constant of Phenol in Cadmium Solutions as a Function of Cadmium Concentration.

alkaline sample was noted. Figures 26 and 27 show the molar extinction coefficient of phenol as a function of boric acid concentration, pH and excess NaOH. The pH of the solutions was measured on a Beckman pH-meter.

The phenol molar extinction coefficient for boric acid solutions was 2510 ± 20, independent of the boric acid concentration.

5. Benzene-Water-Lithium Metaborate

The lithium metaborate was dried by heating in a crucible over a bunsen flame. The crystals swelled to several times their original volume and yielded an extremely light powder. Known concentrations were prepared by weighing this powder as $LiBO_2$. The solutions at first were very turbid but cleared completely within 24 hours. The pH of the borate solutions was between 10-11. The solution was saturated and irradiated in the usual manner.

Analysis was similar to that of pure water solutions. An excess of 300-500 micromols of sodium hydroxide per 10 ml sample was added to form the alkaline sample. The unbuffered or neutral samples were made by adding a number of equivalents of sulfuric acid greater than the number of mols of lithium metaborate. A large excess of sulfuric acid (5 ml of 0.1M) was usually added since the optical density was insensitive to pH's below 7.

Figure 28 shows the molar extinction coefficient of lithium borate solutions as a function of the sum of the micromols of NaOH and $LiBO_2$ per 10 ml sample. The negative abscissa was calculated as micromols of $LiBO_2$ minus twice the micromols of H_2SO_4 per 10 ml sample. A phenol molar extinction coefficient of 2510 ± 20 was determined. It was independent of the lithium metaborate concentration.

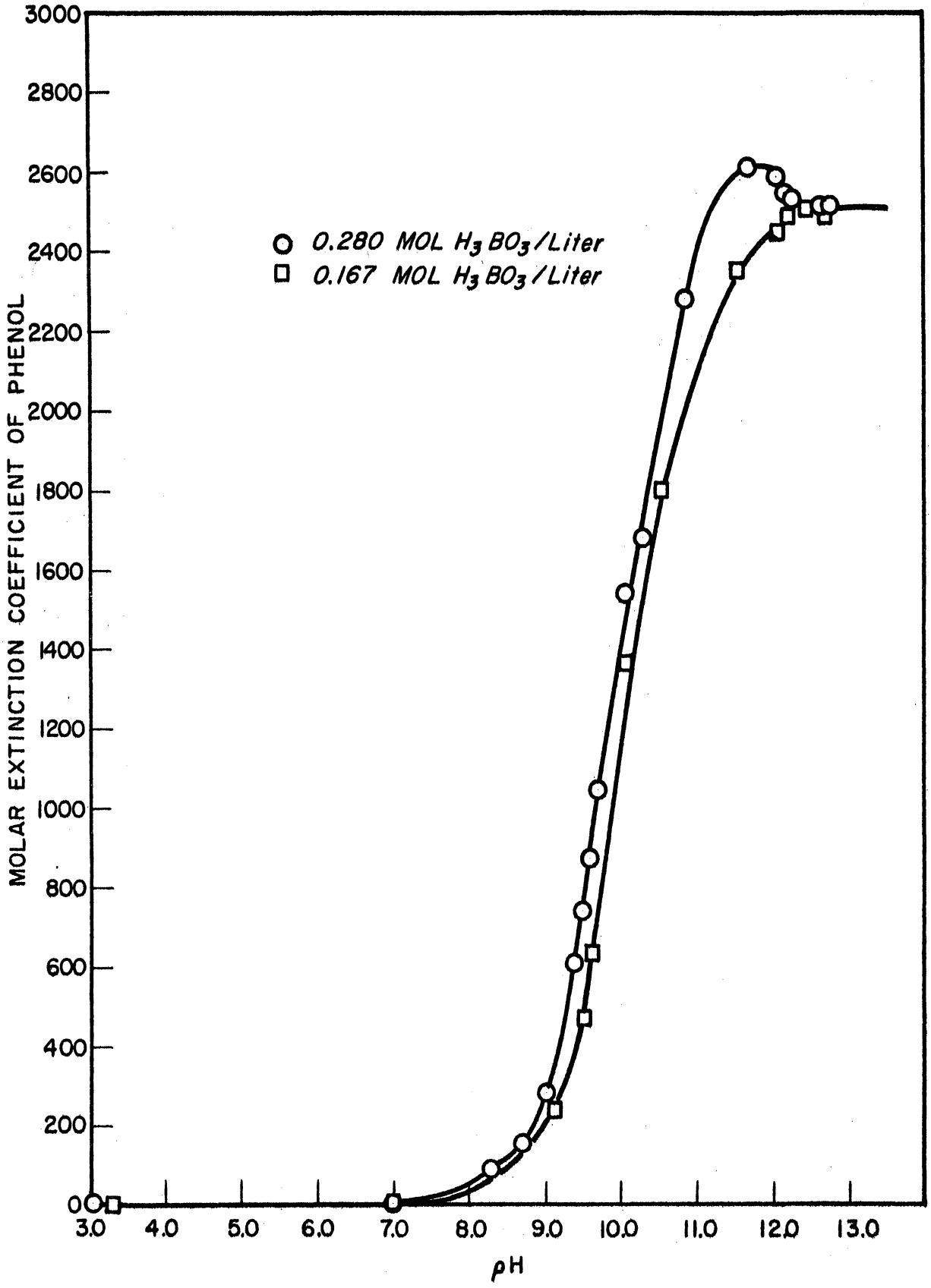

Figure 26. Phenol Molar Extinction Coefficient as a Function of pH of the Boric Acid Solution.

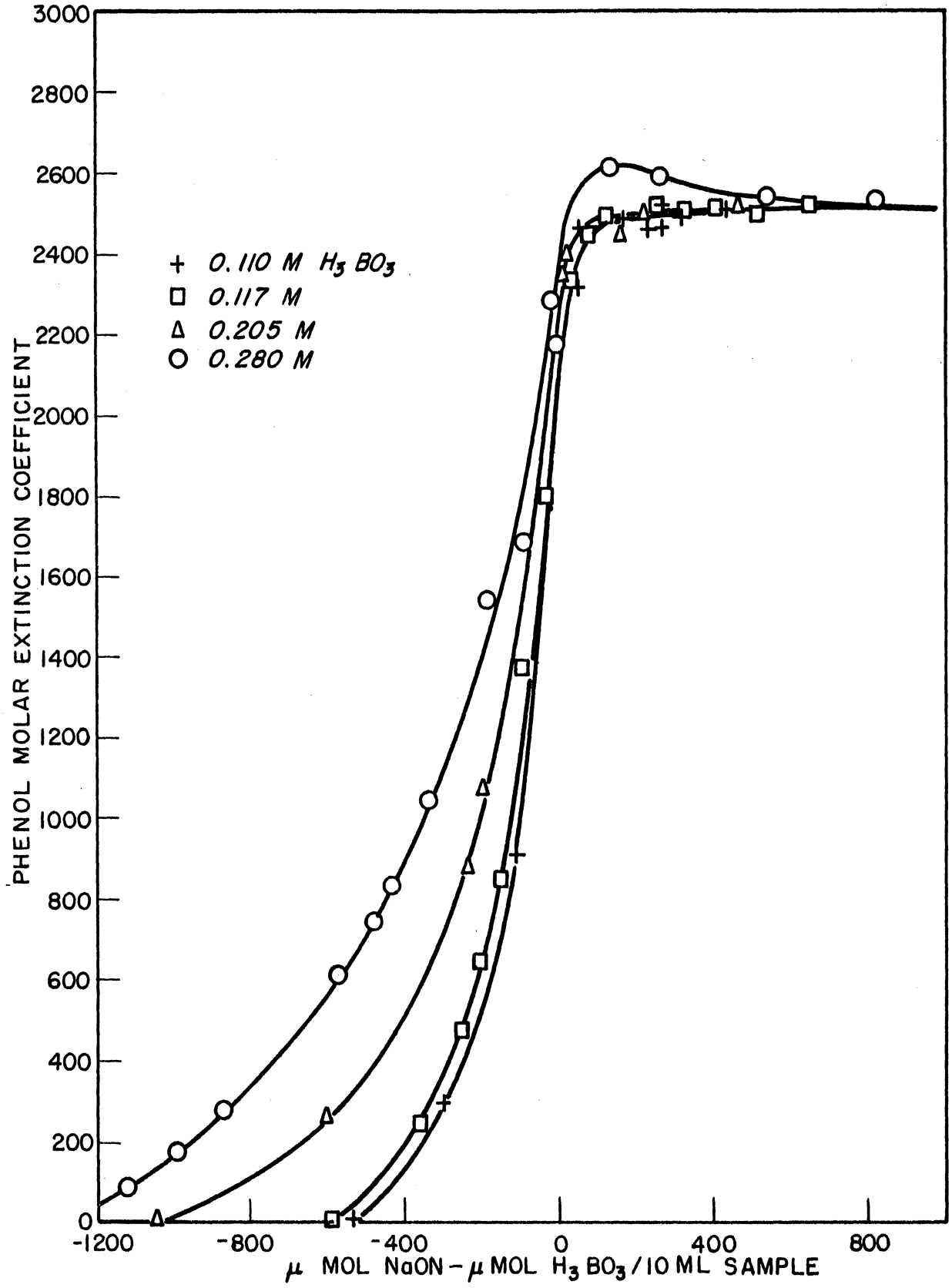

Figure 27. Molar Extinction Coefficient of Phenol in Boric Acid Solutions as a Function of the Micromols of Excess Sodium Hydroxide Added per 10 ml Alkaline Sample.

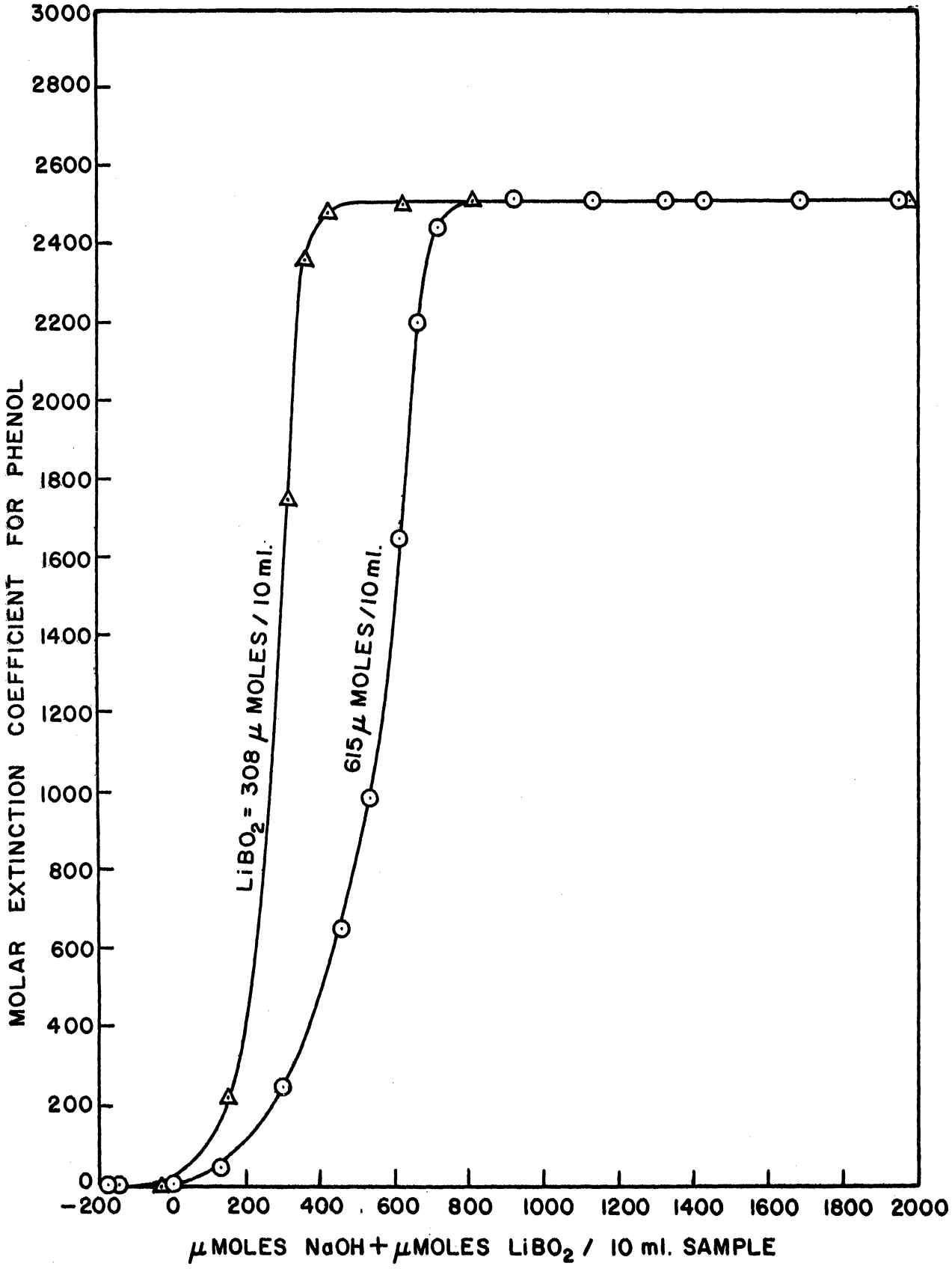

Figure 28. Phenol Molar Extinction Coefficient in Lithium Metaborate Solutions as a Function of the Micromols of NaOH and $LiBO_2$ per 10 ml Alkaline Sample.

6. Benzene Analysis

Figure 29 is the molar extinction coefficient of benzene in water as a function of wave length in the ultraviolet region. The two peaks at 2540 and 2600 Å were both used for analysis. Extinction coefficients of 153 ± 1 and 105 ± 1 respectively were determined from solutions of known benzene concentration. A 0.1 ml pipette was carefully calibrated with benzene by weighing the liquid delivered. The delivered amount was dissolved completely in one liter of distilled water to form a known concentration of benzene. The photometric analysis for benzene had to be performed rapidly since the benzene evaporated rapidly from the solution.

The saturation benzene concentration in the various solutions was determined as a function of solute concentration (Figure 30). The saturated solutions had to be diluted by 1/3 before the analysis could be performed. The inorganic solutes had negligible absorption at these wave lengths. The saturation concentration of benzene in pure water was .0212 mols per liter at 20°C.

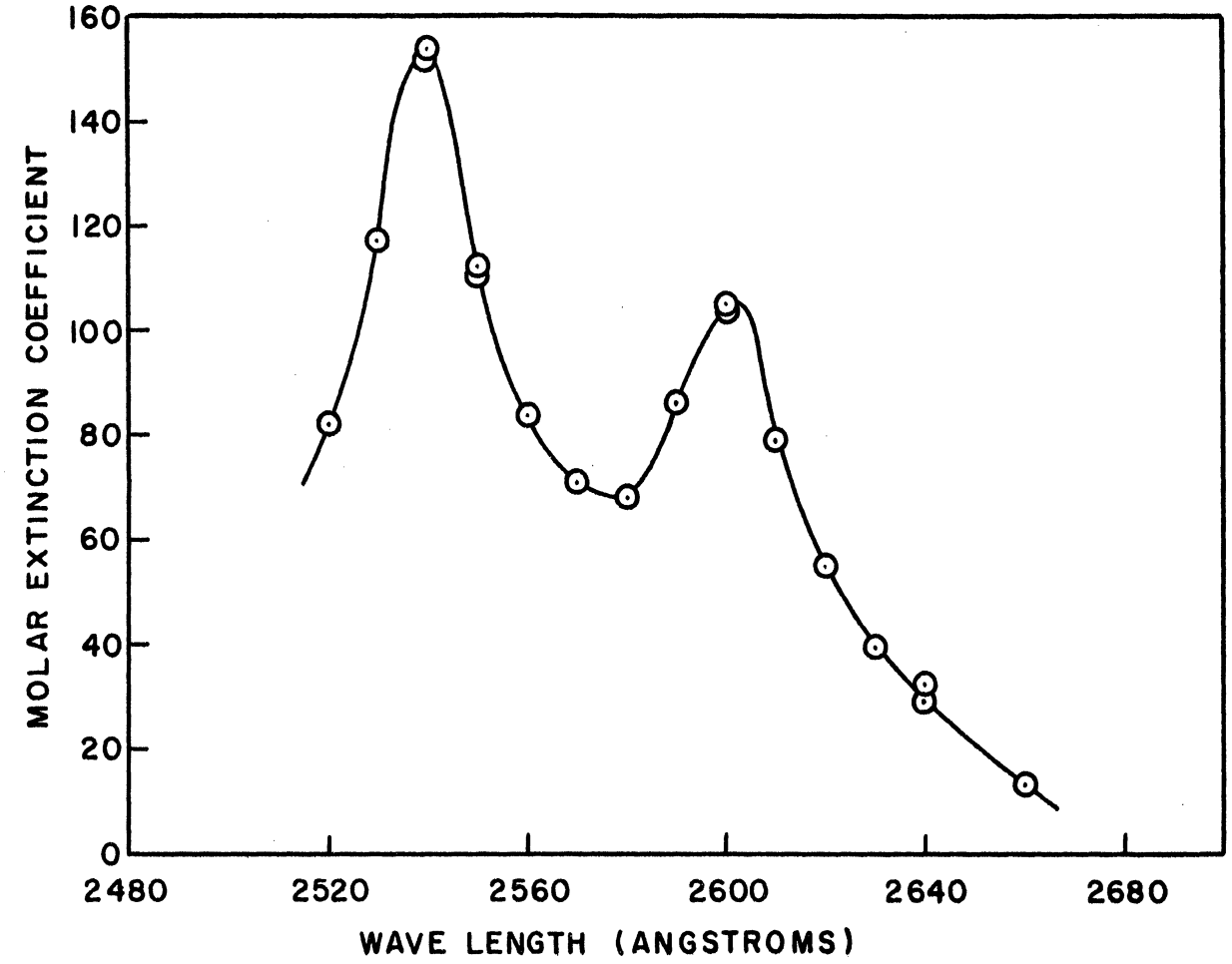

Figure 29. Molar Extinction Coefficient of Benzene as a Function of Wave Length.

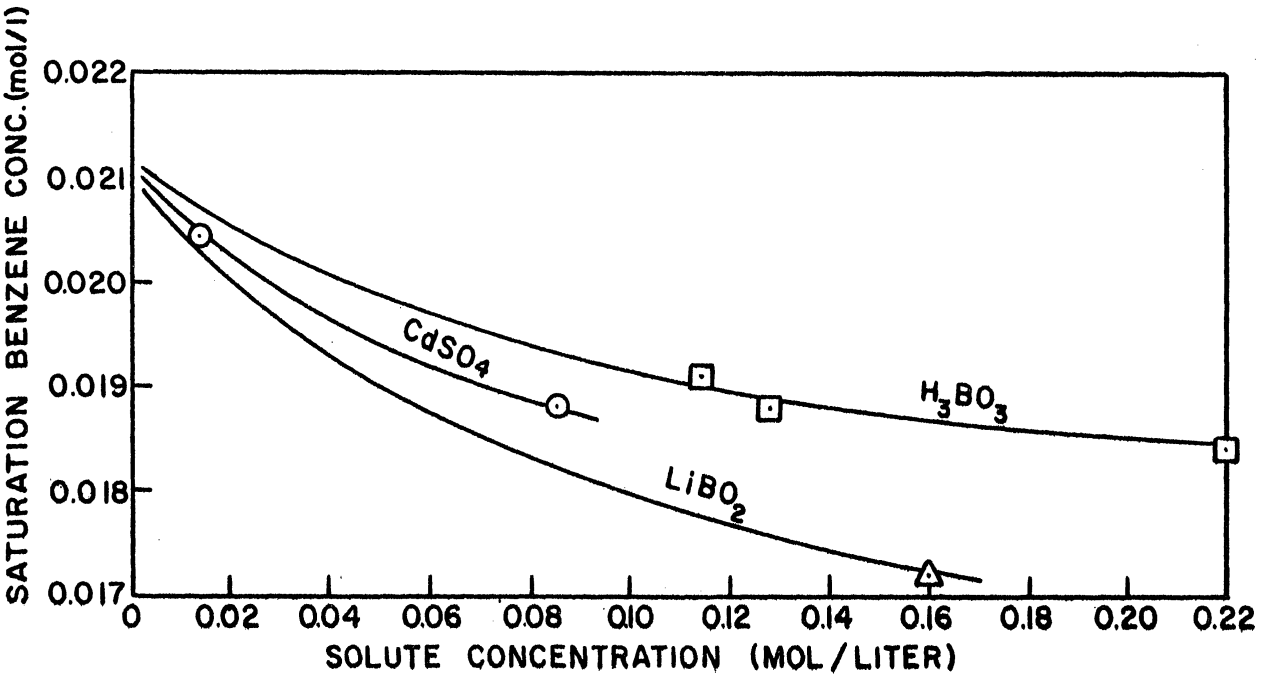

Figure 30. Saturation Benzene Concentration as a Function of Solute Concentration.

V. EXPERIMENTAL RESULTS

A. Benzene-Water

1. Cobalt-60 Radiation - Gammas

In air-saturated, benzene-water solutions the phenol concentration in the irradiated samples was proportional to the total gamma dose to about 80,000 reps. The yield was independent of dose rate between 100 to 7000 reps/min. The data obtained in this study are plotted in Figure 31 and compared to other data reported in the literature. The average slope of the experimental points yielded an A value for phenol, (micromols phenol formed)/(liter)(kilorep), of 2.06 $\pm$ .02. The A value is related to the more commonly used G value.

$$G = 1.038\ A/\rho \qquad (35)$$

The G value was 2.14 $\pm$ .02 molecules of phenol formed per 100 ev absorbed. The abscissae, labeled "Total Gamma Dose" of all yield curves, were determined by the Fricke dosimeter using a G value of 15.6 for the yield of ferric ions. The G value was not corrected for temperature.

The effect of benzene concentration on the yield was studied. Benzene concentrations below saturation (.021M at 20°C) were prepared by diluting the saturated solution with distilled water. The phenol yield remained independent of the benzene concentration above .007M. Below this concentration the yield decreased. The phenol yield in solutions of low benzene concentration was slightly affected by the dose rate.

The yield curve (Figure 31) shows a relatively sharp break at a total dose of about 80,000 reps. Above this dose the rate of phenol production becomes lower. This was due to the depletion of dissolved

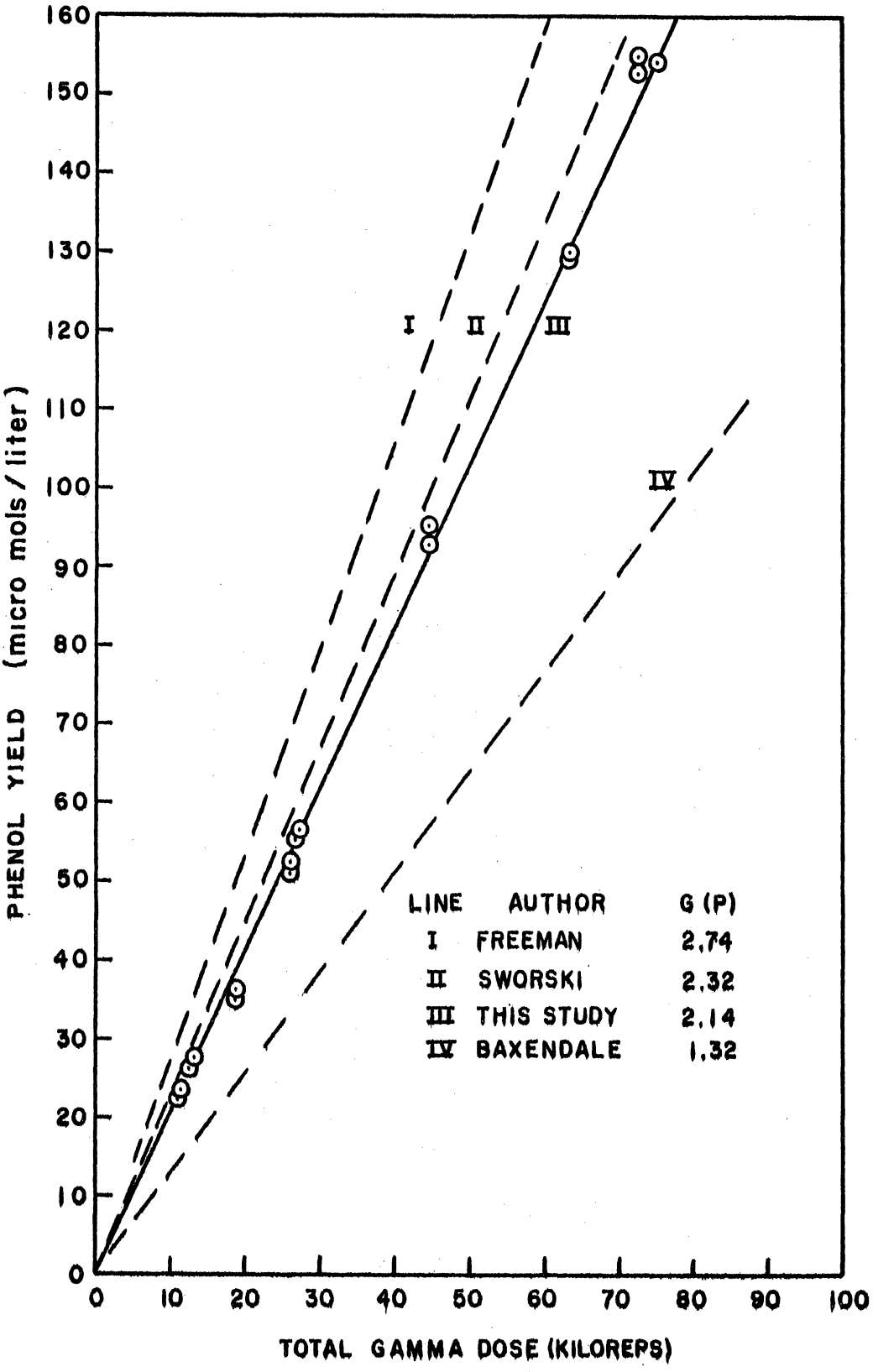

Figure 31. Phenol Yield in Water as a Function of Total Gamma Dose - Cobalt 60 Radiation.

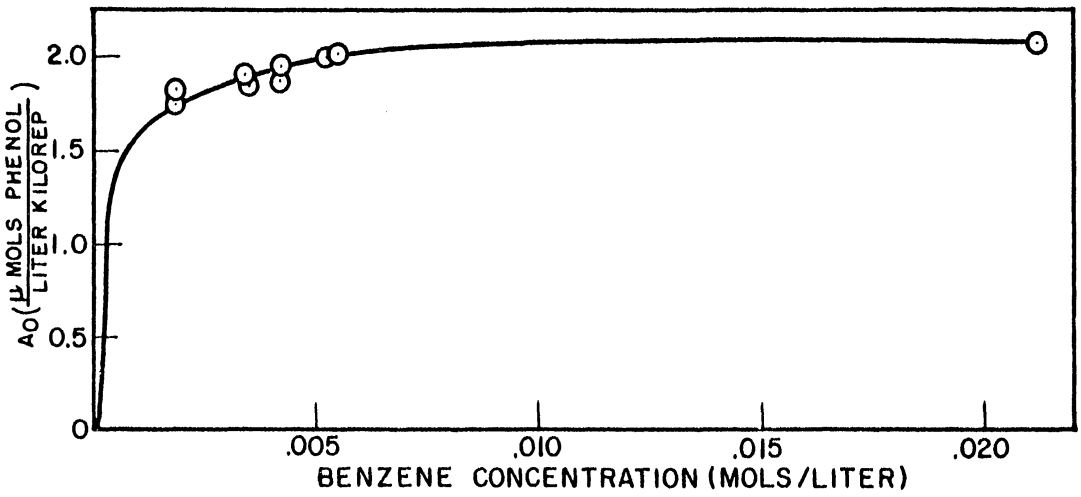

Figure 32. Phenol Yield as a Function of Benzene Concentration.

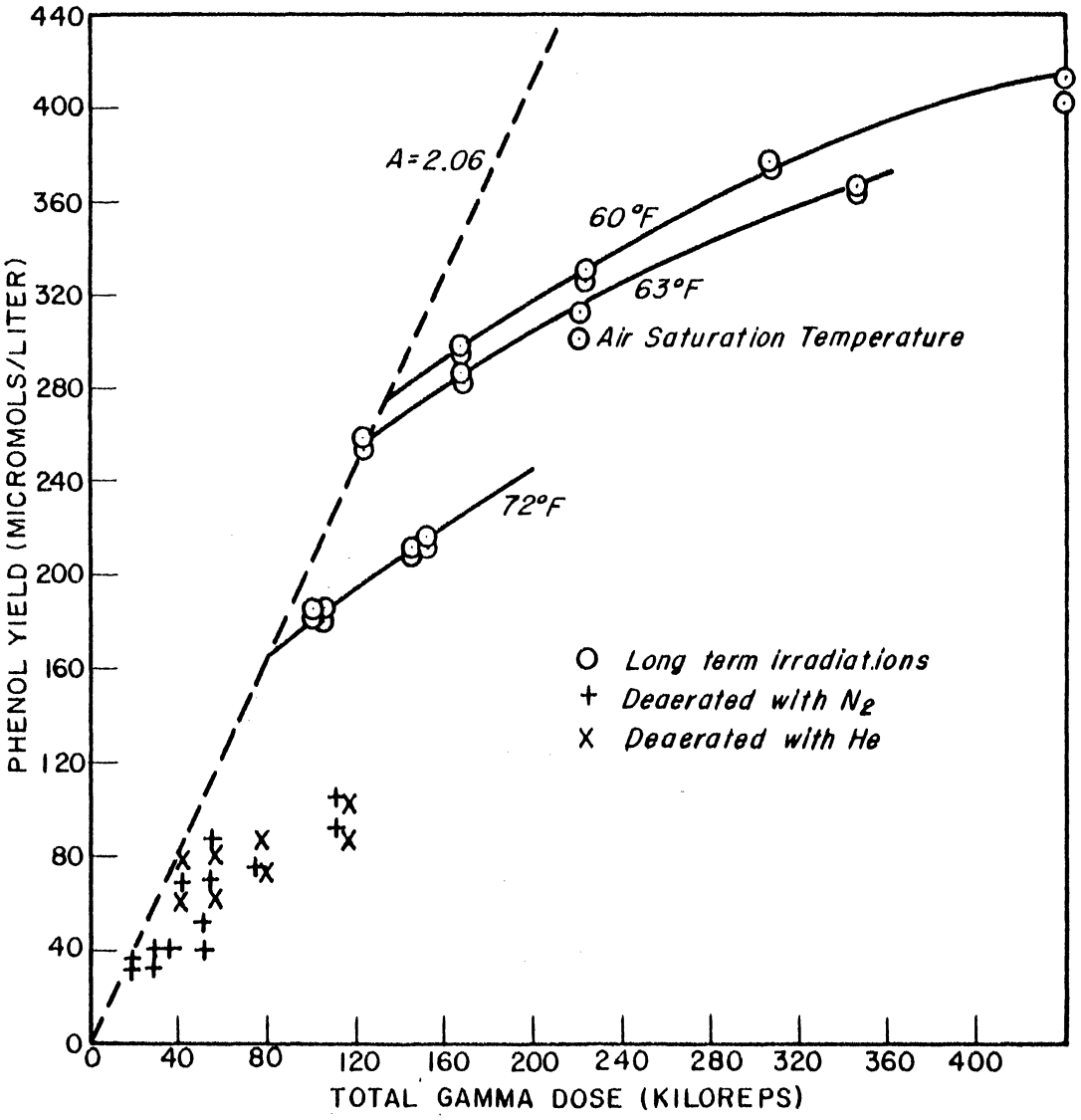

Figure 33. Effect of Oxygen on the Radiation Yield of Phenol.

oxygen in the solutions similar to the effect of oxygen in ferrous solutions. Several runs were made with deaerated solutions. The yield of phenol in these runs was greatly depressed. However, the method of deaeration did not seem to be effective. The deaerated samples gave erratic data due to small quantities of oxygen remaining. The deaeration procedure was described in Section IV C2. Helium or nitrogen was used as the deaerating gas. Both gave approximately the same results which was surprising since the nitrogen contained approximately 3% oxygen. However, the qualitative results showed that the oxygen concentration was important to the reaction mechanism.

Aerated samples receiving high total doses were used to study the effect of oxygen and the "oxygen break" further. The break occured at a point depending on the oxygen concentration which depended on the temperature at which the solution was saturated with air. As an irradiation progressed, oxygen diffused into the solution from the air space in the sample bottle adding to the oxygen already in solution. Over the irradiation times used, the amount of oxygen diffusing into the solution was estimated to be small. The data for high total doses are correlated in Figure 33 with the air saturation temperature as a parameter. The oxygen break was a relatively sharp break indicating that even very low oxygen concentrations were effective in accelerating the production of phenol. Above the break the yield curves were not straight lines. The rate of phenol production decreased as the total dose increased above the break point.

The prior addition of phenol or hydrogen peroxide to samples to be irradiated did not affect the radiation yield of phenol.

No effect of temperature on the yield of phenol was found over the limited range employed (60-95°F). The solutions were not heated or cooled but were at the temperature of their surroundings plus whatever increase resulted from gamma heating. The rise in temperature due to gamma heating was less than 5°F. Miley[77] irradiated aqueous benzene solutions in a high pressure flow apparatus at temperatures up to 212°F and found no detectable effect of temperature. The reaction probably had zero activation energy which is usual for free radical reactions.

2. Pile Radiation - Gammas and Neutrons

No effect of fast or thermal neutrons in the radiation from the nuclear reactor could be detected. The yield of phenol from pile radiation was the same, within the experimental uncertainties, as the yield of phenol in cobalt-60 gammas based on the energy absorbed as measured by the Fricke dosimeter. The neutrons had negligible effect on the dosimeter. The data from the reactor runs are plotted in Figure 34. The line shown is that derived from the cobalt-60 runs. The average of the pile irradiations yielded an A value of $2.05 \pm .05$.

The oxygen break for in-pool irradiations occurred at a total dose of about 70 kiloreps, which is slightly lower than the 80 kiloreps observed in the cobalt-60 experiments. This could be attributed to the higher solution temperatures in the pool reducing the oxygen concentration. The higher dose rates in the pool would make the break less sharp due to local depletion of oxygen. The shorter irradiation times would decrease the amount of oxygen diffusing into the solutions from the air space in the sample bottle.

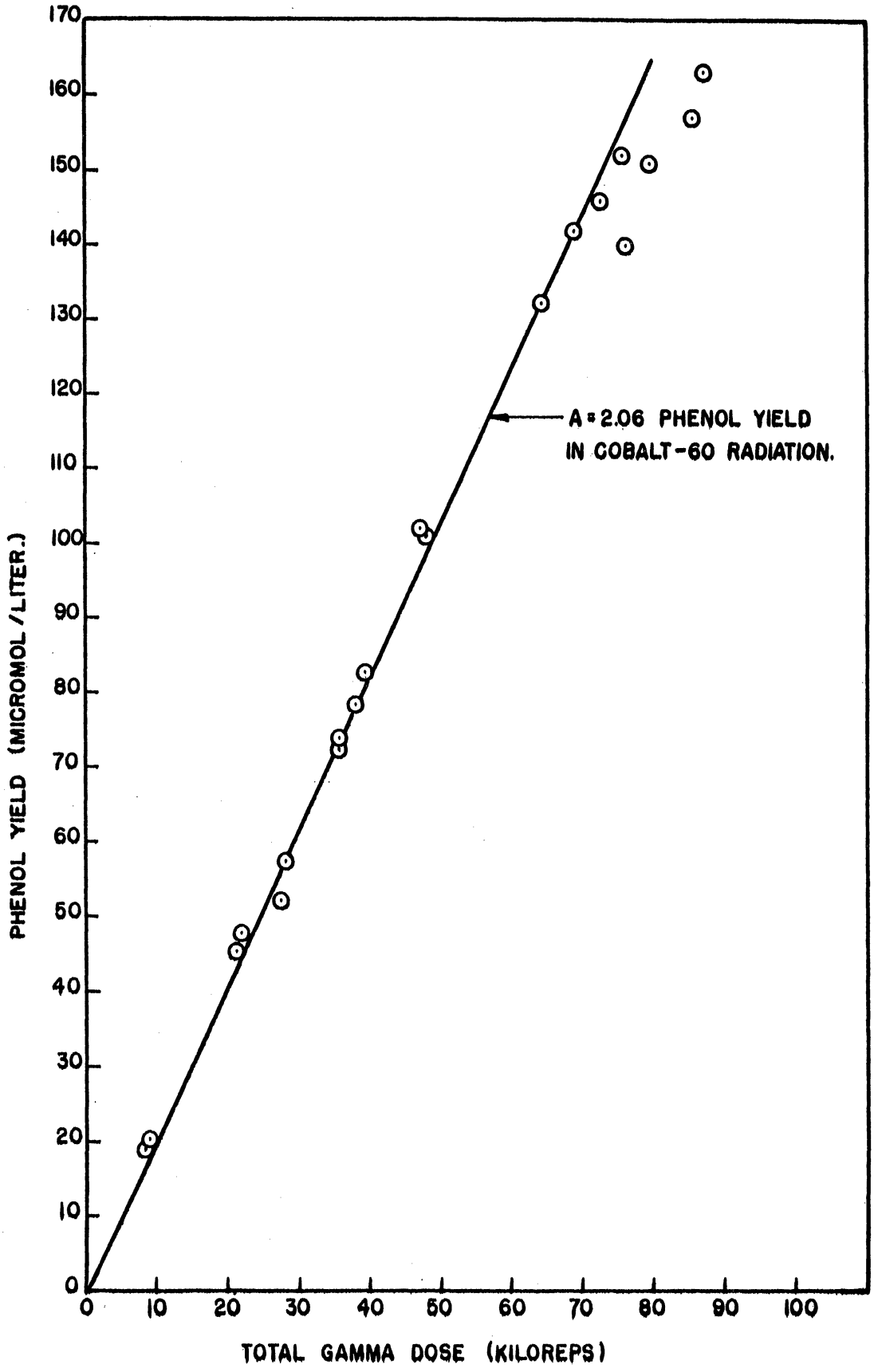

Figure 34. Phenol Yield as a Function of Total Gamma Dose - Reactor Radiation.

During the analysis of the irradiated solutions, the optical density of the alkaline sample for all runs showed an increase with time after the addition of the sodium hydroxide. The first reading of the optical density was taken within two minutes after the solution was prepared. The maximum value was usually attained within 8-10 minutes. The phenol concentration was calculated at both zero time, A_o, and at the maximum concentration, A_∞. This increase in phenol formed was not large and no appreciable error was introduced by extrapolating the phenol concentration to zero time on a simple graph of phenol concentration (or optical density) versus time on Cartesian coordinates. It is shown in Section VI C3 that a semilogarithmic plot of the data produces a straight line. The increase was observed to be a constant percentage of the phenol concentration. The ratio A_o/A_∞ had an average value of $.91 \pm .04$ (Figure 40). The increase of the phenol concentration was observed only in the irradiated samples. The standard phenol solutions did not show the phenomenon. It was attributed to phenyl peroxide, a side product of the benzene-water reaction. This compound might be stable for a limited time in neutral solutions but would be hydrolyzed rapidly in strongly basic or acid solutions forming phenol.

B. Benzene-Water-Cadmium Sulfate

The results of the cobalt-60 and reactor irradiations are shown in Figure 35. The line shown is the average yield of phenol in cadmium solutions for pure gamma radiation. The A value is $2.08 \pm .10$, independent of cadmium concentration and gamma dose rate. The data for the cadmium solutions were not as reproducible as that for the other systems.

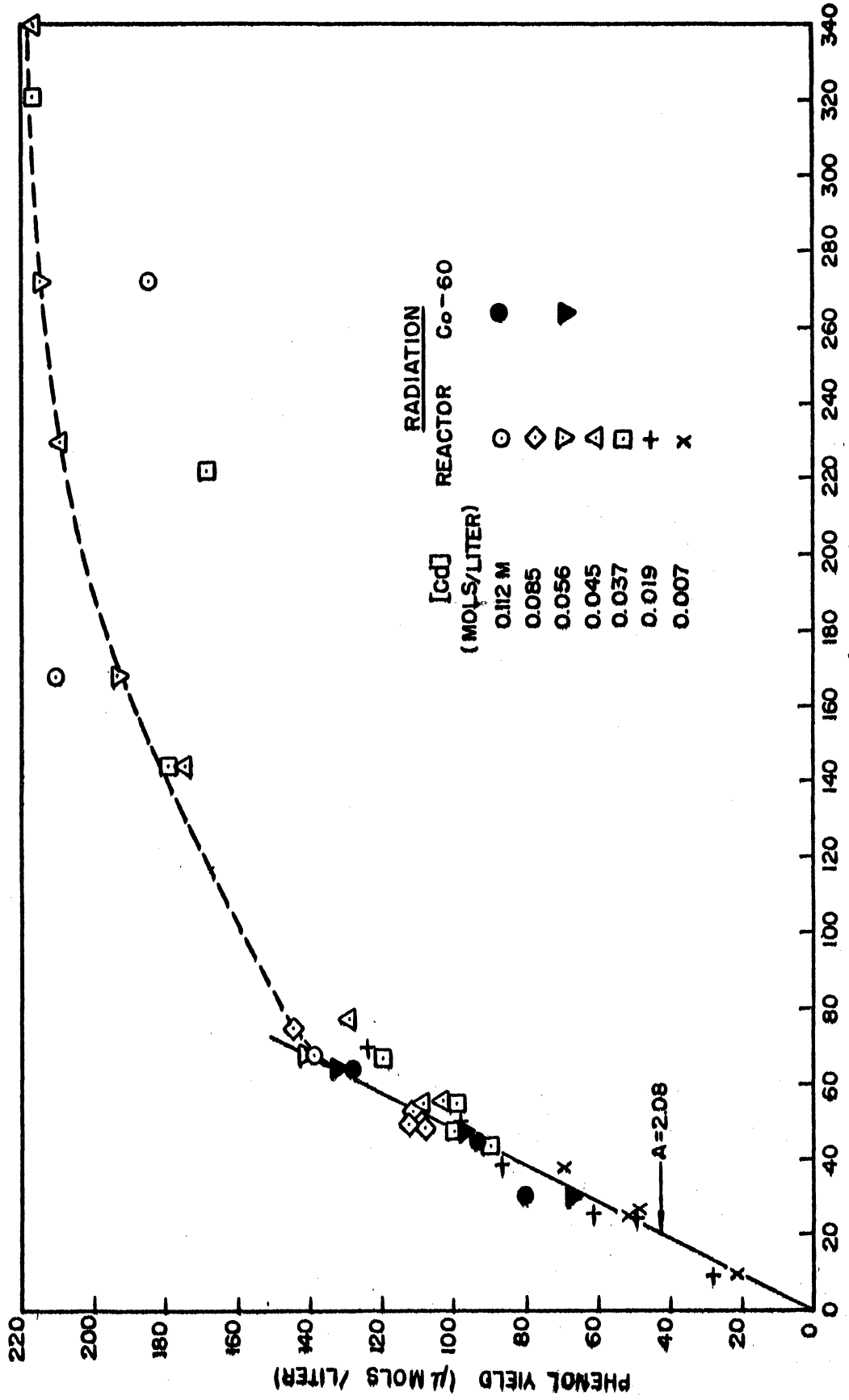

Figure 35. Phenol Yield in Cadmium Sulfate Solutions as a Function of Total Gamma Dose - Cobalt 60 and Reactor Radiation.

This was attributed to the analytical technique employed. If the alkaline sample was centrifuged for less than five minutes, the solution would be cloudy and the analysis would be poor.

The oxygen break occurred at a lower dose ($\sim$60 kiloreps) than the break in pure water. The shape and slope of the curve above the oxygen break were similar to the curve for pure water. The data scattered badly at the high doses.

The data for the reactor irradiations scattered about the line corresponding to A = 2.06. The average yield of phenol was approximately the same for cobalt-60 and reactor radiations. There was no measurable effect of the neutrons captured by the cadmium. No effect of cadmium concentration was noted for the reactor irradiation as would be expected if the neutron capture energy was important. The number of neutrons captured was roughly proportional to the cadmium concentration. The amount of neutron capture gamma energy absorbed by the solution was less than 5% of the incident gamma energy for all runs. This was less than the estimated accuracy of the phenol analysis ($\pm$ 10%). A large amount of neutron capture energy was released, but only about 4.7% of the radiated energy was absorbed in the solution.

No increase of the optical density of the alkaline sample was noted for cadmium solutions during the analysis of irradiated samples. Several analyses were rapidly performed specifically to observe the rise. The lack of increase of phenol concentration was caused by the decomposition of the phenyl peroxide to oxygen and benzene catalyzed[73] by the cadmium ion.

C. Benzene-Water-Boric Acid

The yield of phenol in boric acid solutions is shown in Figure 36 for cobalt-60 and pile irradiations. The yield was independent of total gamma dose rate (100-7000 rep/min) and boric acid concentration (0.1-0.25M). The average A(P) value observed was 2.30 ± .05 in cobalt-60 gammas. The measured yields in the reactor radiation were slightly lower (A = 2.28). The difference was not significant. This value was, as usual, based on the yield of ferric ions in the Fricke dosimeter. The energy absorbed in the solution due to neutron capture by boron added significantly to the total energy, but no chemical effect of the neutron capture energy was noted. About 85% of the neutron energy released was absorbed in the solution. The maximum amount of absorbed neutron energy was approximately 30% of the total gamma dose.

There was no apparent rise in the optical density of the alkaline sample during analysis of the irradiated samples containing boric acid. The boric acid hydrolyzed the phenyl peroxide continuously during the irradiation period, which explained the higher yield of phenol.

D. Benzene-Water-Lithium Metaborate

The phenol yields in solutions of lithium metaborate were lower than in the other systems investigated. The A(P) value in pure gamma radiation was 1.67 ± .03. The lithium solutions were made acid for a few runs by the addition of sulfuric or boric acid. The yield of phenol did not change. The molarity of the lithium was not varied significantly so no effect of concentration was observed. The yield of phenol was linear to 50 kiloreps and then gradually decreased. The reaction was studied only to a total gamma dose of 77 kiloreps. It was not determined if this

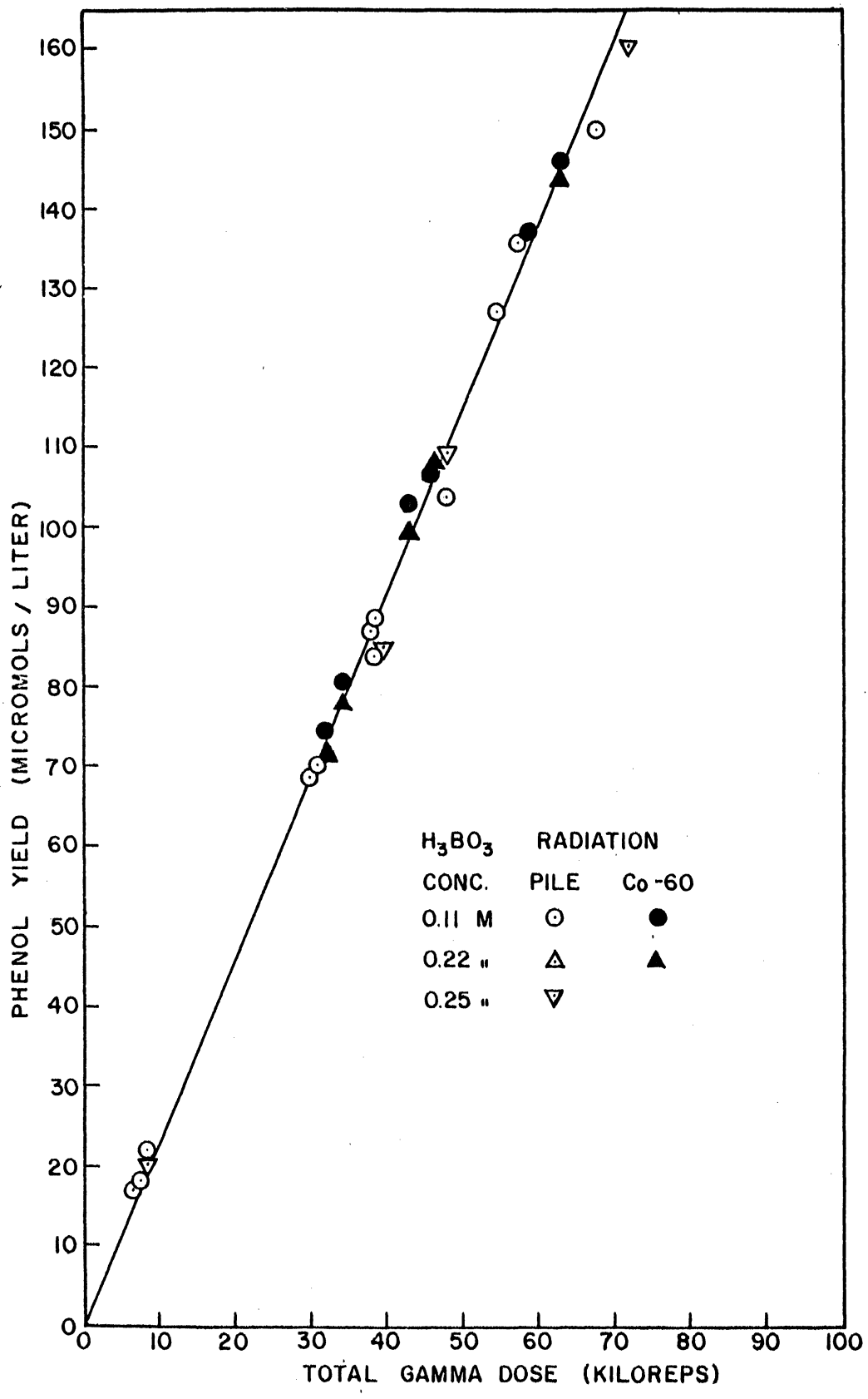

Figure 36. Phenol Yield in Boric Acid Solutions as a Function of Total Gamma Dose - Cobalt 60 and Reactor Radiation.

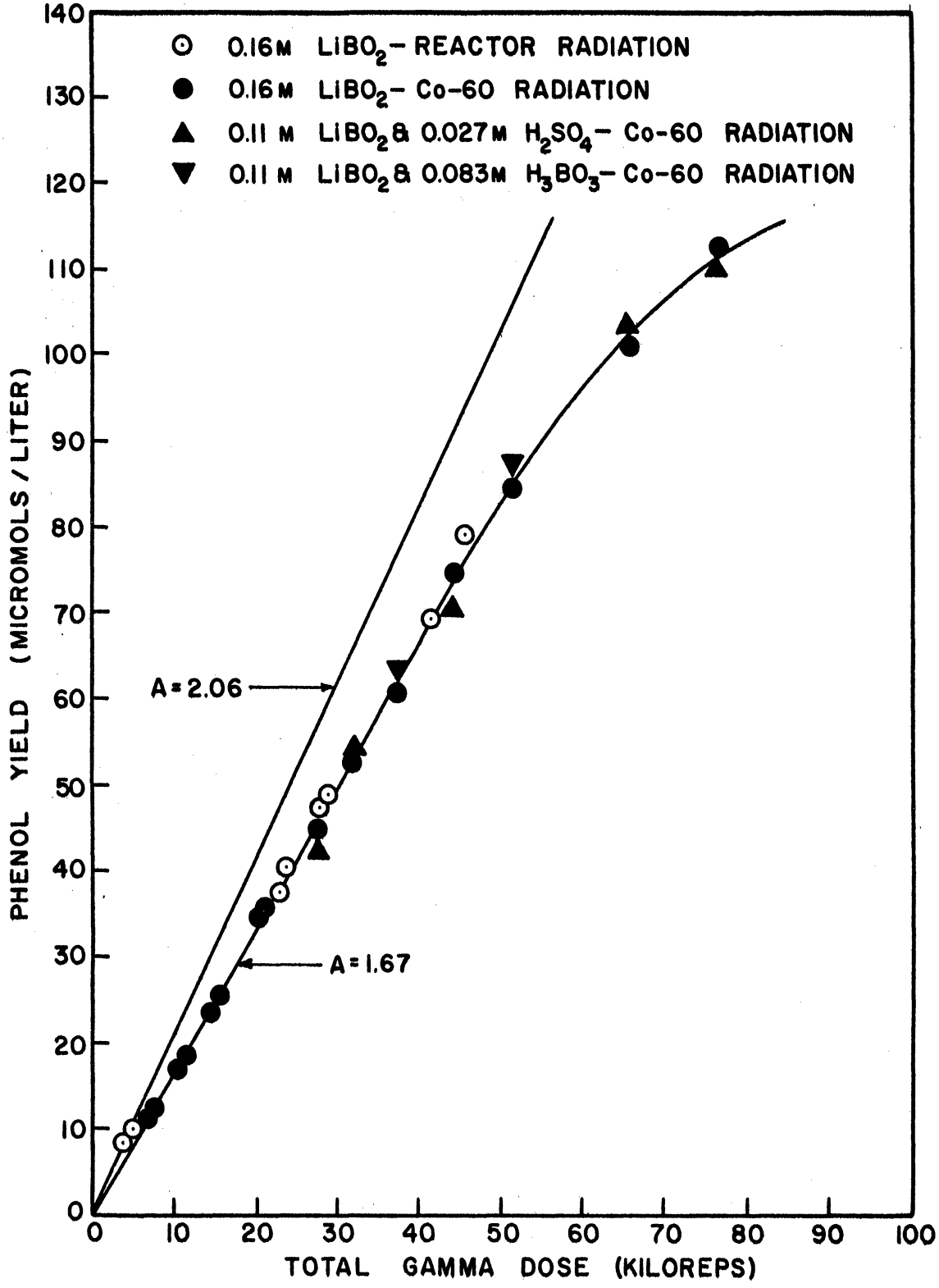

Figure 37. Phenol Yield in Lithium Metaborate Solutions as a Function of Total Gamma Dose - Cobalt 60 and Reactor Radiation.

decline was due to the depletion of oxygen as in the other systems, however, it seems probable that it was.

The results are shown in Figure 37 for both cobalt-60 and reactor runs. The average yield (below 50 kiloreps) is 1.67 $\pm$ .03 micromols phenol/(liter)(kilorep) for pure gammas and 1.71 $\pm$ .03 for pile radiation. The energy absorbed in the solution due to neutron capture by lithium and boron contributed a large fraction of the total energy absorbed. The neutron energy was a maximum of 45% of the total gamma energy. However, no significant effect of the neutron capture energy was measured.

No satisfactory explanation could be presented for the lower phenol yield in metaborate solutions. The lower yield was not caused by the high pH since the yield in acidified solutions was the same. It is probable that the metaborate ions captured hydroxyl radicals, thus reducing the phenol yield. The yield was independent of dose rate over the range studied (100-7000 reps/min.).

VI. DISCUSSION OF RESULTS

A. Survey of Literature on Benzene

There are several reports in the literature of radiation studies of benzene and benzene solutions. Burton and co-workers[70,83] have studied the effect of gammas and electrons on pure benzene and the protective effect of benzene when mixed with other hydrocarbons. Pure benzene is quite stable under radiation. Some hydrogen is produced and a polymer is formed. There is an average of six benzene rings per polymer molecule. No ring scission was detected. Benzene exhibits a protective effect on other hydrocarbons. Excitation in the other hydrocarbon is transferred preferentially to the benzene because the benzene has a lower excitation energy. Selke et al,[98] reported no phenol formation in gamma irradiated benzene saturated with water.

Aqueous benzene solutions have been studied by several authors.[9,40,108,109] Phenol and diphenyl have been reported as the principal products. Day and Stein[28] proposed the system as a convenient dosimeter and studied sodium benzoate solutions for use as a dosimeter. The solutions have not received wide acceptance as dosimeters. Weiss and co-workers[104,105,106] have made a study of the products other than phenol and diphenyl formed. They reported a dialdehyde, probably muconidialdehyde, formed by ring scission in irradiations with fast neutrons. Other products of doubtful identity have been found[27], but all are produced with a yield of less than 0.1 molecules per 100 ev.

Weiss et al,[105] found that oxygen had a pronounced effect on the reaction of benzene in irradiated water. Aerated solutions produce

mostly phenol and very little diphenyl. Deaerated solutions produce less phenol but diphenyl is an important product. In aerated solutions there is an increase of phenol production in 0.8N sulfuric acid.

Loeble et al,(66) found that the usual aromatic ring addition rules held for the hydroxylation of substituted benzene compounds by irradiated water. The nitro group is meta directing, and the hydroxyl and carboxyl groups are ortho-para directing. The ratios of the amounts of each isomer formed are identical with that formed by the usual hydroxylation methods.

Baxendale and Magee(8) have studied the kinetics of the reaction between the OH radical and benzene in Fenton's reagent (H_2O_2 and ferrous ions in water). The action of Fenton's reagent on benzene is similar to the action of radiation. Diphenyl and phenol are the only products, but the reaction mechanism is somewhat obscure. Because the ferrous and ferric ions take part in the reaction, the results cannot be applied to irradiated benzene-water solutions. Baxendale and Smithies(9) studied the radiation yields of diphenyl, phenol, and hydrogen peroxide in solutions of other solutes at various pH's.

Phung and Burton(84) have investigated solutions of benzene and deuterated benzene in water. Contrary to the results of several other workers, they found no H_2O_2 production in neutral air free solutions and no diphenyl in aerated solutions.

Reported radiation yields of phenol, diphenyl, and hydrogen peroxide are summarized in Table VIII.

TABLE VIII

PUBLISHED RESULTS ON RADIOLYSIS OF
AQUEOUS BENZENE (GAMMAS OR FAST ELECTRONS)

	Solution Conditions	G Diphenyl	G Phenol	G H_2O_2	Lit. Ref.
d	0.8N H_2SO_4	0.44	0.30	0.51	A
d	0.1M NH_2SO_4	0.47	0.29	0.64	A
d	Neutral	0.50	0.27	0.25	A
d	0.1 M NaOH	0.38	0.29	0.34	A
d	Benzene Conc. = 4×10^{-3} M	0.49	0.27	0.18	A
d	5×10^{-4} M Fe^{++} in 0.8N H_2SO_4	0.79	0.80	--	A
d	5×10^{-4} M Fe^{++} & 2×10^{-3} M Cu^{++} in 0.8N H_2SO_4	0.09	2.79	--	A
	Neutral	None	1.32	2.14	A
	Neutral	>0.0	2.32	(~2)*	B
d	Neutral	--	0.29	>0.0	C
d	H_2O_2, acidic	--	0.29	-2.1	C
	Acidic	--	2.6	2.8	C
	Neutral, γ radiation	--	3.05	--	D
	Neutral, β radiation	--	2.74	--	D
	Neutral	>0.0	2.1	--	E
	Neutral	>0.0	2.2	--	F
d	Neutral	1.22	0.36	None	G
	Neutral	None	2.64	2.88	G
d	0.8N H_2SO_4	0.96	0.35	0.57	G
o	Neutral	None	2.64	3.27	G
o	0.8N H_2SO_4	None	2.64	3.30	G
	0.8N H_2SO_4	None	2.64	2.84	G

TABLE VIII (CONT'D)

Notes:

d indicates deaerated solution

o indicates oxygenated solution

no superscript indicates air saturated solution

Neutral means water saturated with benzene

None indicates that within the accuracy of the measurement zero yield was found

>0.0 indicates that the yield was greater than zero but no value was reported

-- indicates that no value was reported

G is the 100 ev yield

*(~2) approximate initial yield

Lit. Ref.		Bibliography
A	Baxendale, and Smithies	9
B	Sworski	108
C	Sworski	109
D	Freeman et al	40
E	Stein and Weiss	105
F	Daniels, Scholes, and Weiss	27
G	Phung and Burton	84

B. General Discussion and Comparison of Results

There is considerable disagreement in the literature on the radiation yields in benzene-water solutions. The phenol yield obtained in this study (G(P) = 2.14) agrees with those reported by Weiss and co-workers[27,105] (2.1 - 2.2) and that of Sworski[108] (2.32). (See Table VIII.) It is higher than the value of 1.32 reported by Baxendale.[9] It is lower than the values reported by Freeman[40] and by Phung.[84] Freeman et al, reported different phenol yields for cobalt-60 gammas (G = 3.05) and fast electrons (2.74). However, he found a $G(Fe^{3+})$ of 17.4 for the Fricke dosimeter in gamma radiation. If Freeman's yield of phenol in gammas is corrected for his high value of $G(Fe^{3+})$ by the ratio 15.6/17.4, the phenol yields in electrons and gammas are the same ($\sim$2.74). The corrected value agrees with the work of Phung and Burton. Phung reported no change in phenol production at low pH as other workers have found.[105]

Phung's[84] values for the diphenyl yield in deaerated solution are somewhat higher than those of Baxendale[9], but analysis for diphenyl is difficult and uncertain. In this study attempts to find a reliable diphenyl analysis failed. Phenol and benzene interfere with the diphenyl absorption at wave lengths below 2800 Å.

Sworski[109] reported that added hydrogen peroxide had no effect on the production of phenol in aerated acid solutions but that the benzene increased the yield of hydrogen peroxide. After the oxygen was consumed the hydrogen peroxide in solution was rapidly destroyed by the radicals.

The position of the oxygen break in the phenol yield curve for air-saturated water was slightly higher than that reported by several

authors. Day[28] has reported it to occur about 70 kilorep. Stein[105] reported a value between 60-70 kiloreps. In this study it occurred at approximately 80 kiloreps. This value would depend on the degree of oxygen saturation, the atmospheric pressure, and the air saturation temperature. These are not generally reported in radiation studies. The break point is probably a function of dose rate. The break might be sharper for lower dose rates. The position of the oxygen break found in this study is in fair agreement with reported values.

No effect of neutrons on the phenol yield was measured even though a significant amount of energy was released by the neutrons in solutions of lithium and boron. The radiations resulting from neutron capture in boron or lithium have very high linear energy transfers. These ionizing radiations favor the formation in water of molecular hydrogen and hydrogen peroxide and depress the yield of radicals. The experimental observations from this and reported studies support a reaction mechanism in which only the radicals react with benzene. The yield of phenol equaled the yield of hydroxyl radicals. Therefore, the yield of phenol from the action of heavy charged particles was low. The radiation yields in neutral water of reactions F, E, and R for densely ionizing radiations are not known with any certainty.

C. Reaction Mechanisms

1. Aerated Solutions

The radiolysis reactions of water have been discussed in Section II D of this paper. The 100 ev yields in pure water for each reaction are listed below.

(F) $2H_2O \rightarrow H_2O_2 + H_2$ G(F) = 0.43

(E) $2H_2O \rightarrow H_2O_2 + 2H$ G(E) = 0.3

(R) $H_2O \rightarrow H + OH$ G(R) = 2.15

These yield values have been determined by several different radical scavengers that apparently cannot compete with radical combination reactions in the initial spur. As a result, these yields are independent[54] of the scavenger concentration (above some low concentration) and the particular scavenger employed. Benzene in aqueous solutions reacted like this type of radical trap. As mentioned earlier, other radical scavengers are able to compete[23,97] with radical reactions in the spur and can influence the measured yields of reactions F, E, and R.

For the purpose of this discussion, the above reactions can be considered primary events. The benzene cannot compete with the combination of two hydroxyl radicals in the spur to form hydrogen peroxide and thus increase G(R) and decrease G(F). The values of G(F), G(E), and G(R) depend only on the type of radiation. Benzene can react with the radicals only when they have escaped from the spur into the solution. In the solution the radical concentration is very low. For a scavenger concentration above some minimum the probability of radical-radical reactions in the homogeneous solution is negligibly small. Therefore, these reactions are not considered important.

(34) $H + H \rightarrow H_2$ radical combinations

(35) $OH + OH \rightarrow H_2O_2$ radical combinations

(36) $H + OH \rightarrow H_2O$ radical recombination

In aerated benzene solutions the following reactions are considered to be important for the production of phenol and diphenyl.

		Rate Constant
(37)	$H + O_2 \rightarrow HO_2$	k_7
(38)	$C_6H_6 + HO_2 \rightarrow C_6H_5^\circ + H_2O_2$	k_8
(39)	$C_6H_5^\circ + OH \rightarrow C_6H_5OH$	k_9
(40)	$C_6H_5^\circ + HO_2 \rightarrow C_6H_5OOH$	k_0
(41)	$C_6H_5^\circ + C_6H_5^\circ \rightarrow (C_6H_5)_2$	k_1

Reaction 37 is well established and is important[23] in the explanation of the radiation reactions of many dilute aqueous solutions. The hydroperoxy radical attacks the benzene ring to form the phenyl radicals (Reaction 38). Reactions 39, 40 and 41 are radical reactions forming the observed final products; phenol, diphenyl and phenyl peroxide.

If it is assumed that all hydroxyl radicals react by Reaction 39 then the yield of phenol, G(P), equals G(OH) or G(R) which was observed experimentally. Reaction 42 does not occur because all the available hydrogen radicals

(42) $C_6H_5^\circ + H \rightarrow C_6H_6$

have reacted with the dissolved oxygen, i.e. Reaction 37 is very fast compared to Reaction 42. By the same reasoning Reaction 43 is not important.

(43) $C_6H_6 + H \rightarrow C_6H_5^\circ + H_2$

There are other reasons to doubt that Reaction 43 occurs.[60] However, 43 is assumed to be a slow reaction compared to Reaction 38 and not important in aerated solutions. By analogy Reaction 44 may be slow.

If it occurs G(P) will be less than G(R) which was not observed experimentally.

(44) $C_6H_6 + OH \rightarrow C_6H_5 + H_2O$

The hydrogen peroxide and hydrogen molecules formed by Reactions F and E may take part in the reaction mechanisms. In Section II D of this paper it was mentioned that the molecular products are destroyed by the radicals in a chain reaction.

(24) $H + H_2O_2 \rightarrow H_2O + OH$

(25) $OH + H_2 \rightarrow H_2O + H$

In water irradiated with radiation of low LET, the radicals completely destroy the molecular products so that no net reaction is observed. Oxygen in the solution effectively prevents the destruction of the molecules by capturing H atoms. It is assumed that these chain reactions are slow compared to Reactions 37, 38, and 39, and they cannot compete in the phenol reactions. The presence of benzene, increases the radiation yield of hydrogen peroxide by Reaction 38. Sworski[108,109] has shown that the hydrogen peroxide does not effect the reactions producing phenol. Hydrogen peroxide added to solutions in this study did not affect the yield of phenol. According to the above mechanisms the yield of hydrogen peroxide will be:

$$G(H_2O_2) = G(F) + 3G(E) + R - G(PX) \qquad (36)$$

where G(PX) is the yield of Reaction 40. It was observed experimentally that the $G(PX) \sim G(P)/10$. Therefore:

$$G(H_2O_2) = 0.43 + 0.9 + 2.15 - 0.22 = 3.26$$

It is difficult to compare this value to values reported in the literature. The phenyl peroxide was observed to be unstable in most solutions. If it is hydrolyzed one of the products is hydrogen peroxide.

(45) $$C_6H_5OOH + H_2O \rightarrow C_6H_5OH + H_2O_2$$

If this species is destroyed in the analytical procedure the observed yield of hydrogen peroxide will be 3.48. Phung and Burton[84] reported 2.88 for $G(H_2O_2)$. Other reported values are lower (2 - 2.2).[108]

The proposed reaction mechanism predicts that the yield of diphenyl is low in aerated solutions.

$$G(DP) = 2G(E) - 0.1\ G(P) = 0.38 \qquad (37)$$

Phung and Burton[84] reported that G(DP) is zero. Other writers[105] have reported that G(DP) was not zero but gave no numerical values. The value 0.38 for the yield of diphenyl is probably too high.

The above reaction scheme yields an expression for the rate of formation of phenol that depends only on the dose rate. Steady state conditions are assumed. Rate of change of the radical concentration = 0.

$$\frac{d[H]}{dt} = \left(\frac{dE_\gamma}{dt}\right)_a k'_R - k_7[H][O_2] = 0 \quad ; \quad [H] = \frac{k'_R}{k_7[O_2]}\left(\frac{dE_\gamma}{dt}\right)_a \qquad (38)$$

$$\frac{d[OH]}{dt} = \left(\frac{dE_\gamma}{dt}\right)_a k_R - k_9[C_6H_5\cdot][OH] = 0 \quad ; \quad [OH] = \frac{k_R}{k_9[C_6H_5\cdot]}\left(\frac{dE_\gamma}{dt}\right)_a \qquad (39)$$

where the k's are the rate constants for the reactions as shown earlier;

$\left(\frac{dE_\gamma}{dt}\right)_a$ = gamma dose rate; $k'_R = 2k_E + k_R$

$$\frac{d[HO_2]}{dt} = k_7[H][O_2] - k_8[C_6H_6][HO_2] - k_0[C_6H_5\cdot][HO_2] = 0 \tag{40}$$

$$[HO_2] = \frac{k'_R}{k_8[C_6H_6] + k_0[C_6H_5\cdot]}\left(\frac{dE_\gamma}{dt}\right)_a \tag{41}$$

$$\frac{d[C_6H_5\cdot]}{dt} = k_8[C_6H_6][HO_2] - k_9[C_6H_5\cdot][OH] - k_0[C_6H_5\cdot][HO_2] - k_1[C_6H_5\cdot]^2 \tag{42}$$

Neglect the term for the formation of diphenyl and substitute the value for $[HO_2]$;

$$\frac{k'_R k_8 [C_6H_6]}{k_8[C_6H_6] + k_0[C_6H_5\cdot]} - \frac{k_R k_9 [C_6H_5\cdot]}{k_9[C_6H_5\cdot]} - \frac{k'_R k_0 [C_6H_5]}{k_8[C_6H_6] + k_0[C_6H_5]} = 0 \tag{43}$$

$$[C_6H_5\cdot] = \frac{k_8(k'_R - k_R)}{k_0(k'_R + k_R)}[C_6H_6] = C_1[C_6H_6] \tag{44}$$

The rate of phenol formation:

$$\frac{d[P]}{dt} = \frac{d[C_6H_5OH]}{dt} = k_6[C_6H_5\cdot][OH] = k_R\left(\frac{dE_\gamma}{dt}\right)_a \tag{45}$$

Therefore, the concentration of phenyl radicals is proportional to the benzene concentration. The rate of formation of phenol equals the rate of formation of hydroxyl radicals by Reaction R with is proportional to

the dose rate. The rate of formation of phenyl peroxide is given by:

$$\frac{d[PX]}{dt} = \frac{d[C_6H_5OOH]}{dt} = k_0 [HO_2][C_6H_5\cdot] \tag{46}$$

$$= \frac{k_0 k_2' K_1 [C_6H_6]}{k_3[C_6H_6] + k_0 K_1 [C_6H_6]} \left(\frac{dE_\gamma}{dt}\right)_a = C_2 \left(\frac{dE_\gamma}{dt}\right)_a$$

The rate of phenyl peroxide formation is also proportional to the dose rate. The ratio of the phenyl peroxide to the phenol formed is a constant.

This derivation neglects the reaction of the radicals with species other than benzene and phenyl radicals. At lower benzene concentrations, the radicals H and OH can be lost through other reactions.

2. Effect of Benzene Concentration

The reaction in water saturated with air and benzene agrees qualitatively with a reaction mechanism in which all the radicals formed ultimately react with benzene. It was observed experimentally that the yield of phenol decreased for benzene concentrations below 0.007 M. According to the theory of radiation effects in water, the yield of primary radicals would not decrease with low benzene concentrations. Therefore some of the water radicals would escape capture by the benzene. In the experiments performed, the solutions were saturated with air so that all of the hydrogen atoms reacted with the dissolved oxygen. The hydroperoxy and hydroxyl radicals must have reacted with other species in solution.

It is assumed for following treatment that the hydroperoxy and hydroxyl radicals are lost in reactions with themselves. Both reactions

have been postulated[2,3] by several writers to explain effects in aqueous solutions.

		Rate Constant
(46)	$2HO_2 \rightarrow H_2O_2 + O_2$	k_A
(47)	$2OH \rightarrow H_2O_2$	k_B

Side Reactions 40 and 41 of the phenyl radical are neglected for this derivation to make the result less involved. Steady state concentration of the radicals is assumed.

$$\frac{d[H]}{dt} = k_R'\left(\frac{dE_\gamma}{dt}\right)_a - k_7[H][O_2] = 0 \; ; \; [H] = \frac{k_R}{k_7[O_2]}\left(\frac{dE_\gamma}{dt}\right)_a \tag{47}$$

$$-\frac{d[HO_2]}{dt} = -k_7[H][O_2] + k_7[C_6H_6][HO_2] + k_A[HO_2]^2 = 0 \tag{48}$$

$$[HO_2] = \frac{-k_7[C_6H_6] + \sqrt{k_7^2[C_6H_6]^2 + 4k_A k_R'\left(\frac{dE_\gamma}{dt}\right)_a}}{2k_A} \tag{49}$$

Only the positive square root is used since only positive concentrations are realistic.

$$\frac{d[C_6H_5]}{dt} = k_8[C_6H_6][HO_2] - k_9[C_6H_5\cdot][OH] = 0 \tag{50}$$

$$[C_6H_5\cdot] = \frac{k_8[C_6H_6][HO_2]}{k_9[OH]}$$

The rate of phenol production is:

$$\frac{d[P]}{dt} = \frac{d[C_6H_5OH]}{dt} = k_9[C_6H_5\cdot][OH] = k_8[C_6H_6][HO_2] \qquad (51)$$

Substituting the expression for $[HO_2]$ and rearranging:

$$\frac{d[P]}{dt} = \frac{k_7^2[C_6H_6]^2}{2k_A}\left\{\sqrt{1 + \frac{4k_A k_R}{k_7^2[C_6H_6]^2}\left(\frac{dE_\gamma}{dt}\right)_a} - 1\right\} \qquad (52)$$

$$\frac{d[P]}{dt} = C_3[C_6H_6]^2\left\{\sqrt{1 + \frac{C_4}{[C_6H_6]^2}\left(\frac{dE_\gamma}{dt}\right)_a} - 1\right\} \qquad (53)$$

Expanding the square root by the binomial expansion and neglecting all terms beyond the first three:

$$\sqrt{1+a} = 1 + \frac{1}{2}a - \frac{1}{8}a^2 + \cdots\cdots$$

$$\frac{d[P]}{dt} = \frac{C_3C_4}{2}\left(\frac{dE_\gamma}{dt}\right)_a - \frac{C_3C_4^2}{8[C_6H_6]^2}\left(\frac{dE_\gamma}{dt}\right)_a^2 = C_5\left(\frac{dE_\gamma}{dt}\right)_a - \frac{C_6}{[C_6H_6]^2}\left(\frac{dE_\gamma}{dt}\right)_a^2 \qquad (54)$$

$$A(P) = \left(\frac{d[P]}{dt}\right)\left(\frac{1}{(dE_\gamma/dt)_a}\right) = C_5 - \frac{C_6}{[C_6H_6]^2}\left(\frac{dE_\gamma}{dt}\right)_a \qquad (55)$$

The experimental data is plotted in Figure 38 in accordance with this simplified model. (See Figure 32.) The dose rate range used (100-560 reps/min) is not large enough and the data too scattered to decide if the results follow this model. The model does not apply at higher benzene concentrations since the assumptions made in the derivation become poor.

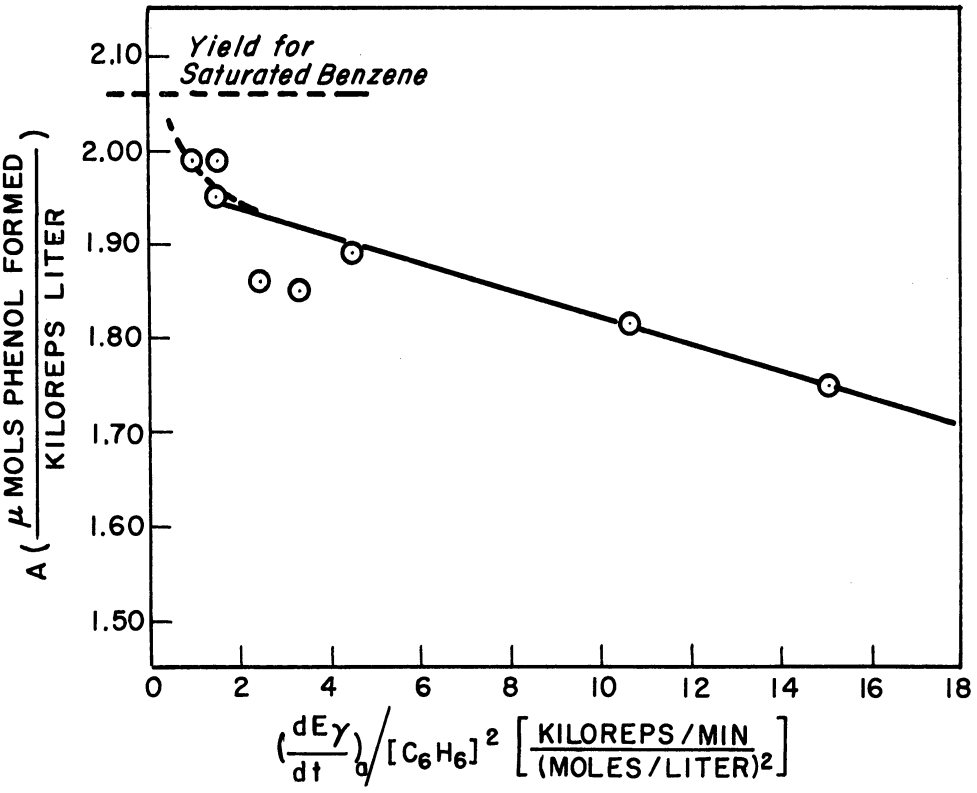

Figure 38. Phenol Yield in Dilute Benzene Solutions.

TABLE IX

CALCULATED DATA FOR DILUTE BENZENE SOLUTIONS

Irradiation Time: 120 minutes			
Benzene Conc. $[C_6H_6]$ (mols/liter)	Dose Rate $(dE\gamma/dt)_a$ (kilorep/min)	Phenol Yield A(P) $\frac{\mu \text{ mols/liter})}{\text{kilorep}}$	$\frac{\left(\frac{dE_\gamma}{dt}\right)_a}{[C_6H_6]^2}$
0.00193	0.563	1.75	15.1×10^4
0.00193	0.397	1.81	10.7×10^4
0.00354	0.397	1.85	3.16×10^4
0.00354	0.563	1.89	4.50×10^4
0.00424	0.273	1.95	1.54×10^4
0.00424	0.430	1.86	2.41×10^4
0.00530	0.430	1.99	1.54×10^4
0.00530	0.273	1.98	0.96×10^4

3. Phenyl Peroxide

Some authors[40] have suggested that the phenyl radical reacted with the dissolved oxygen to yield the observed unstable product.

(48) $$C_6H_5\circ + O_2 \rightarrow C_6H_5OO\circ$$

This new radical would react with atomic hydrogen to form phenyl peroxide.

(49) $$C_6H_5OO + H \_ C_6H_5OOH$$

The net result is the same as that of Reactions 38 and 40.

In the "alkaline sample" prepared for the phenol analysis, the phenyl peroxide was decomposed, (Reaction 50). The increase in the phenol concentration of the alkaline sample was caused by the destruction of phenyl peroxide.

(50) $$C_6H_5OOH + OH^- \rightarrow C_6H_5O^- + H_2O_2$$

This unstable species also decomposed continuously during the irradiation in the water-inorganic solute solutions. The cadmium ion has been reported[73] to be a catalyst for the destruction of hydrogen peroxide.

(51) $$H_2O_2 \xrightarrow{Cd^{++}} H_2 + O_2$$

It is logical that cadmium would decompose the phenyl peroxide in an analogous way. This explains why no increase in the optical density of the "alkaline sample" of irradiated cadmium solutions was observed.

(52) $$C_6H_5OOH \xrightarrow{Cd^{++}} C_6H_6 + O_2$$

In boric acid solutions the peroxide was hydrolyzed to phenol and hydrogen

peroxide. Since $G(PX) \sim G(P)/10$, the phenol yield in boric acid solutions would be:

$$G(P) \cong 2.14 + 0.1 \times 2.14 = 2.35 \tag{56}$$

The experimentally determined value was 2.34. The pH of the boric acid solutions was 2 or higher. A pH of 2 was not low enough to increase the yield of OH radicals above 2.15 as observed in more acid solutions. The higher G(P) value was attributed solely to the continuous destruction of the phenyl peroxide during the irradiation rather than to a higher yield of hydroxyl radicals.

The destruction of phenyl peroxide may be described by a simple kinetic model. Let k_c be the rate constant for Reaction 50.

$$-\left(\frac{d[PX]}{dt}\right)_t = \left(\frac{d[P]}{dt}\right)_t = k_c [PX]_t [OH]_t \tag{57}$$

$[P\ ]$ = phenol concentration

$[PX]_t$ = phenyl peroxide concentration at time t after adding base

$$\int_{[PX]_o}^{[PX]_t} \frac{d[PX]}{[PX]} = \ln \frac{[PX]_t}{[PX]_o} = -\int_o^t k_c [OH^-]\, dt = -k_c [OH^-] t \tag{58}$$

Since $[OH^-]$ is large and remains constant, let $K_4 = k[OH^-]$

$$[PX]_t = [PX]_o e^{-K_4 t} \tag{59}$$

By a material balance:

$$[P]_o = [P]_t - ([PX]_o - [PX]_t)$$
$$= [P]_t - [PX]_o(1 - e^{-K_4 t}) \qquad (60)$$

$$\text{At: } t = \infty \; ; \; [PX]_\infty = 0 \; ; \; [P]_t = [P]_\infty$$
$$[P]_o = [P]_\infty - [PX]_o \qquad (61)$$

Subtracting: $$[P]_\infty - [P]_t = [PX]_o e^{-K_4 t} \qquad (62)$$

Assuming that a constant fraction of phenyl radicals react by Reactions 39 and 40 as shown by the reaction mechanisms.

$$\frac{[PX]_o}{[P]_\infty} = C \qquad (63)$$

then:

$$\frac{[P]_\infty - [P]_t}{[P]_\infty} = C e^{-K_4 t} \qquad (64)$$

A plot of the logarithm of the left hand side of the equation versus time should give a straight line. The intercept should be independent of the phenol concentration. Figure 39 shows typical data plotted on rectangular and semilogarithmic coordinates.

The phenyl peroxide was probably metastable in neutral water. This possibly explains the fact that irradiated benzene-water samples usually could be kept safely for several days before analysis and would give accurate results. Occasionally a sample stored for a day or more

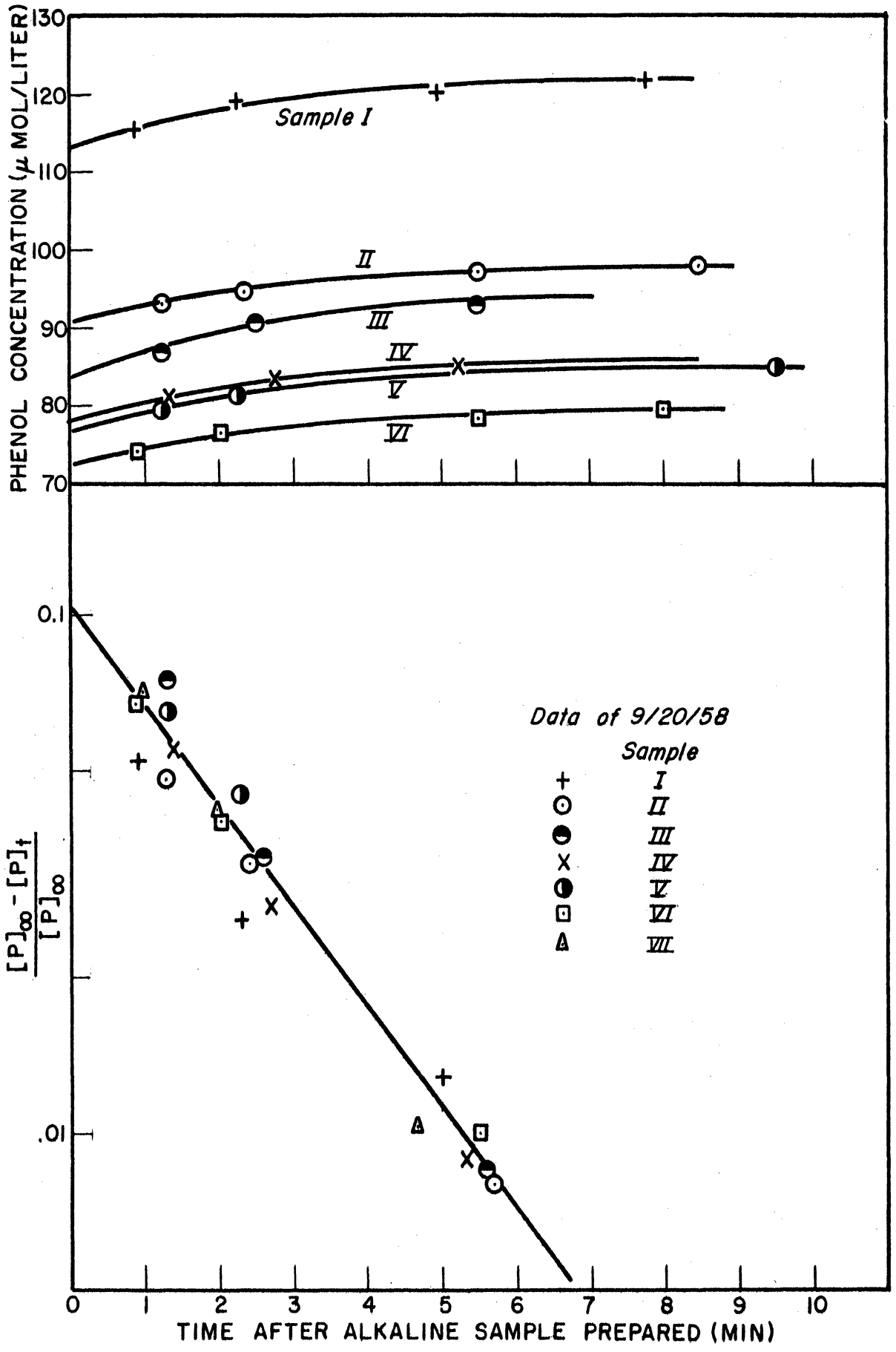

Figure 39. Increase in Phenol Concentration of Alkaline Samples with Time - Typical Data

would show little or no increase of the optical density of the alkaline sample. The peroxide was probably sensitive to temperature and traces of dissolved metal ions, and decomposed during the storage period.

4. Deaerated Solutions

The reaction mechanisms in deaerated solutions are more complicated than in aerated solutions. Many of the reactions neglected as too slow in aerated solutions cannot be neglected in the oxygen free solutions. Oxygen acts as a catalyst (not a true catalyst since it is consumed in the reaction) for the production of phenyl radicals. In the absence of oxygen, the phenyl radical may be produced by hydrogen abstraction reactions. However, some authors have doubted the abstraction by hydrogen atoms.(60)

(43) $C_6H_6 + H \rightarrow C_6H_5^\circ + H_2$

(44) $C_6H_6 + OH \rightarrow C_6H_5^\circ + H_2O$

The amount of hydrogen peroxide and hydrogen gas produced by the action of low LET readiation on pure water is very small. Phung and Burton(84) reported no hydrogen peroxide in deaerated aqueous solutions. Others have reported low yields. The molecular products are destroyed by the radicals in a chain process.

(24) $OH + H_2 \rightarrow H_2O + H$

(25) $H + H_2O_2 \rightarrow H_2O + OH$

The chain reactions do not result in any net loss of radicals. The radicals are lost by the competing reaction of hydrogen peroxide and hydroxyl

radicals and by radical recombination and

(26) $OH + H_2O_2 \rightarrow H_2O + HO_2$

(27) $HO_2 + HO_2 \rightarrow H_2O_2 + O_2$

(28) $H + O_2 \rightarrow HO_2$

combination reactions. The yield of hydroperoxy radicals is greatly reduced in oxygen free systems. It is formed by the action of hydroxyl radicals with hydrogen peroxide which is present in only small amounts. Reaction 26 must be slow. In aerated solutions, hydrogen peroxide concentrations one hundred times greater had no effect on the phenol yield. For every hydroxyl radical reacting with hydrogen peroxide the phenol yield will be reduced below the value of G(R). Therefore, Reaction 26 cannot compete with phenyl radicals for hydroxyl radicals. In deaerated solutions, hydroperoxy radicals are not an important source of phenyl radicals.

Phenyl peroxide was observed in deaerated samples. It was formed principally while the small amount of unremoved oxygen was consumed. During the initial period before the oxygen in the samples was exhausted, some hydrogen peroxide was formed. The high hydrogen peroxide concentration may make Reaction 26 important until the hydrogen peroxide is consumed by the radicals.

Whatever the source of phenyl radicals, the probability of two phenyl radicals combining to form diphenyl is high in deaerated solutions. Because the concentrations of the H and OH radicals is low, they cannot compete as effectively with the phenyl combination reaction as in aerated solutions.

The reactions felt to be important in deaerated aqueous benzene solutions are Reactions F, E and R and the following three sets of reactions:

I. Production of phenyl radicals.

(43) $C_6H_6 + H \rightarrow C_6H_5\circ + H_2$

(44) $C_6H_6 + OH \rightarrow C_6H_5 + H_2O$

II. Reactions of phenyl radicals.

(42) $C_6H_5\circ + H \rightarrow C_6H_6$

(39) $C_6H_5\circ + OH \rightarrow C_6H_5OH$

(41) $2C_6H_5\circ \rightarrow (C_6H_5)_2$

III. Reactions reducing the radical concentrations.

(34) $2H \rightarrow H_2$

(35) $2OH \rightarrow H_2O_2$

(36) $H + OH \rightarrow H_2O$

A fourth class of reactions involving the hydroperoxy radical would be important in heavy particle irradiations where the concentration of hydrogen peroxide is larger and oxygen is produced.

The reaction scheme is too complex to derive any useful results with which to test the experimental data. The reaction rate after the oxygen break was not a constant but decreased with dose. Figure 40 is a plot of the experimental phenol yield, A(P), versus gamma dose after the oxygen break. The yield decreases rapidly to a short plateau as the last trace of oxygen is consumed. This plateau is probably caused by Reaction 26 being important in the mechanism because of the hydrogen peroxide remaining in the solution. As the hydrogen peroxide is consumed by the

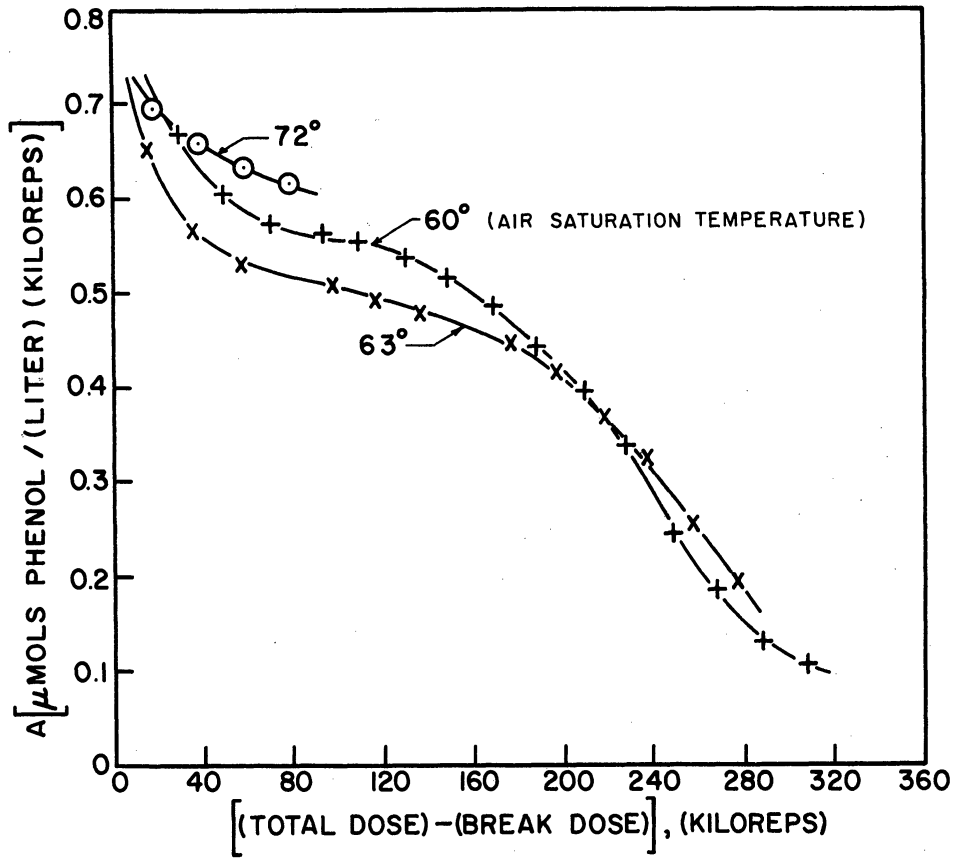

Figure 40. Phenol Yield in Water as a Function of Gamma Dose after Oxygen Break.

TABLE X

PHENOL YIELD ABOVE OXYGEN BREAK POINT

Air Sat. Temp. 72°F		63°F		60°F	
Total Dose	Instant. A	Total Dose	Instant. A	Total Dose	Instant. A
kilorep	μ mol/l/kr	kilorep	μ mol/l/kr	kilorep	μ mol/l/kr
100	0.69	140	0.66	160	.66
120	0.65	160	0.57	180	.60
140	0.63	180	0.53	200	.57
160	0.61	200	0.52	220	.56
		220	0.50	240	.55
		240	0.49	260	.54
		260	0.47	280	.52
		300	0.44	300	.48
		320	0.41	320	.44
		340	0.37	340	.39
		360	0.32	360	.34
		380	0.25	380	.24
		400	0.20	400	.19
				420	.13
				440	.11

radicals the phenol yield decreases rapidly to a low value ($A \sim 0.1$). Selke et al,[98] reported that the phenol yield does not fall to zero for doses higher than 400 kiloreps. The data for Figure 40 was obtained by drawing tangents to the curves in Figure 33. The three yield curves calculated for the three different air saturation temperatures are not felt to be significantly different. The general trends shown by all the curves are important.

The rate of oxygen consumption in air saturated solutions was calculated from the initial concentration in the solution. The initial oxygen concentration was estimated from literature data[120] for an atmospheric pressure of 740 mm Hg. From the estimated air saturation temperature of the irradiated solution and the apparent break point of the yield curves in Figure 33, the rate of oxygen consumption was calculated. The experimental data is shown in Table XI.

TABLE XI

Rate of Oxygen Consumption

Air Sat. Temp. °F	Conc. O_2 $\frac{\mu mol}{liter}$	Dose at Break Kiloreps	$A(-O_2)$	$\frac{A(-O_2)}{A(P)}$
60	310	132	2.35	1.14
63	300	124	2.41	1.17
72	272	80	3.40	1.65

The theoretical value of $G(-O_2)$ from the proposed reaction mechanism is:

$$G(-O_2) = G(P) + 2G(PX) + 2G(DP) = 2.14 + 2(.21) + 2(.2) = 2.97 \quad (65)$$

An estimate for G(DP) was made in lieu of experimental data. The data are not accurate enough to compare with the theoretically predicted value. Stein and Weiss have reported detecting several low yield products from irradiated water-benzene. These minor products have a maximum yield of 0.1 molecules per 100 ev but are reported to be oxidation products containing one or more oxygen atoms per molecule. If the formation of these molecules involved the dissolved oxygen, the theoretical value of 2.9 could be low by as much as 0.6.

D. Effect of Thermal Neutrons

The neutron capture energy absorbed in solutions of boron and lithium was a significant fraction of the total energy, but there was no increase in the phenol concentration measured due to the added energy.

There are several reports in the literature of studies in which cadmium, lithium or boron were added to the ferrous dosimeter. These metals have high thermal neutron absorption cross-sections and release large amounts of prompt energy as gammas and heavy particles after capturing a neutron. The important parameters for these neutron reactions are listed in Table XII.

Thermal neutron capture in cadmium results in a spectrum of high energy photons being emitted. The most intense gammas in the spectrum have energies around 0.56 - 0.8 Mev.[36] The gammas around 1.32 Mev and 2.53 Mev have intensities[15] of about one-tenth of the low energy photons. Photons with energies up to the 9.20 Mev maximum are present[87] but their relative intensities have not been determined. Because of the low absorption coefficient of water for these high energy photons, very little of the energy released will be absorbed in a chemical system. The

fraction of the energy absorbed depends on the geometry and size of the reacting system. An energy of 2 Mev was assumed for the average energy of the prompt cadmium photons in order to calculate the absorption coefficient of the gammas.

Neutron capture by boron 10 yields 2.79 Mev[94] appearing mainly as kinetic energy of a helium and a lithium-7 nucleus. An 0.48 Mev gamma photon is emitted in 93% of the neutron captures. Capture by lithium-6 yields 4.78 Mev[94] per neutron capture which appeares entirely as kinetic energy of the alpha and triton.

Sutton, Draganic and Hering[107] added lithium sulfate to the ferrous dosimeter and exposed the solution to the radiation in a graphite pile. They measured the increased yield of ferric ions in the lithium solutions. Other authors[72] have used boric acid as well as lithium sulfate. If the neutron flux in the solution is known, the number of neutron captures can be calculated for a given solute concentration. Then the energy released and absorbed can be calculated. From the number of ferric ions formed by the neutron captures alone, the $G(Fe^{3+})$ for the fission fragments of boron and lithium can be calculated. This is one method by which Ehrenberg and Saeland[34] obtained the data shown in Figure 4.

These reported studies were all carried out in 0.8N sulfuric acid. The radiation chemistry of this acid solution is known to be different than the chemistry of pure water. The only studies of pure water reported are decomposition studies of water-boric acid solutions. Such studies do not elucidate the primary events occurring in the water. Solutions of benzene in water would be well adapted for this purpose

since they are quite water-like. The primary events can be inferred more easily by the use of the benzene as a scavenger for the hydroxyl radical.

Since the neutron capture energy was 30 - 45% of the total gamma energy absorbed, a measurable increase in the phenol yield should be expected. The benzene dissolved in the system was a radical scavenger for hydroxyl radicals. It is known that in acidic solutions the yield of radicals decreases for radiations of high LET. For 8 Mev deuterons G(R) is 1.5 and G(E) is 0.1. There is no corresponding data for neutral solutions. The lack of a measurable yield of phenol from the neutron capture energy possibly can set an upper limit on G(R) in pure water for high LET radiation.

The total A(P) value was calculated from the total phenol yield and the gamma energy absorbed.

$$A_t(P) = [P]_t/E_\gamma \tag{66}$$

The total A_t was compared to the A_γ value found for pure gamma radiation.

$$A_\gamma(P) = [P]/E_\gamma \tag{67}$$

The maximum possible average error in A values was thought to be 0.1 micromols/kilorep/liter.

$$A_t(P) - A_\gamma(P) < 0.1 \tag{68}$$

$$[P]_n = [P]_t - [P]_\gamma < 0.1E_\gamma \tag{69}$$

$$\text{Let } \theta = E_n/E_\gamma; \quad [P]_n < \frac{0.1E_n}{\theta} \tag{70}$$

$$A_n(P) = \frac{[P]_n}{E_n} < \frac{0.1}{\theta} \tag{71}$$

Since the yield of phenol equaled the yield of hydroxyl radicals, the yield of Reaction R for high LET radiations is:

$$G(R) < \frac{0.1}{\theta} \tag{72}$$

No significant increase in the phenol yield was measured in the lithium metaborate solutions, where $\theta = 0.4$.

Therefore:

$$G(R) < 0.25 \tag{73}$$

It was quite possible that the phenyl radicals could not effectively compete with the radical combination reactions in the high radical concentrations in the tracks of the heavy particles.

The Ford Nuclear Reactor was not well suited for the study of the chemical effects of neutrons. The gamma flux in the pool was very high and the neutron flux was low by comparison. Other reported neutron studies were carried out in a graphite pile or in a large graphite thermal column. The graphite has a lower absorption cross section than water (.003 barns compared to .3 for hydrogen)[10] so the neutrons are attenuated faster in water than graphite. Gamma photons are attenuated faster in graphite than in water because of the higher density of the carbon. The prompt photons from neutron capture in hydrogen tends to increase the gamma flux. A summary of experimental data from neutron irradiations appears in Tables XIV to XVI with the estimated neutron energy absorbed compared to the total gamma dose.

VII. SUMMARY AND CONCLUSIONS

A. General

In this study, the Ford Nuclear Reactor was investigated as a possible source of ionizing and neutron radiation for use in promoting chemical reactions. In-pool or "fishing" experiments were used exclusively in irradiating small batch samples. Miley[77] has investigated the use of the beam ports for carrying out chemical reactions under radiation. The beam ports were better adapted to the use of semi-permanent chemical reaction vessels.

A survey of the methods and hazards of pile irradiations showed that direct, rather than remote, handling techniques were desirable for a preliminary study of chemical reactions. A few reaction were investigated briefly to determine their suitability for these studies. Benzene-water systems were chosen over polysulfone reactions and chlorinated hydrocarbon systems.

A moveable bridge was constructed which allowed samples to be lowered to any desired location in the pool. The samples could be placed in a satisfactorily reproducible position near the core. The sample holder, sample bottles, and chemical reactants became only very slightly radioactive so that after a short cooling period the samples could be handled and analyzed directly with only moderate precautions.

The effect of the important variables were studied on the reaction induced by radiation in water saturated with benzene. The principal stable organic products were phenol and diphenyl. In aerated solutions, the production rate of phenol was a function only of total gamma dose and benzene concentrations below 0.007 M. Above 0.007M to saturation (.021M),

the yield of phenol was independent of benzene concentration. In deaerated solutions the phenol yield was lower while the diphenyl yield was increased. In aerated solutions, the phenol yield was equal to the yield of hydroxyl radicals that were formed by the action of the ionizing radiation on water. Reaction mechanisms and kinetic expressions have been proposed for the observed reactions. The unstable product has been tentatively identified as phenyl peroxide. Comparison of experiments carried out in cobalt-60 and pile radiation indicate that there was no measurable effect of neutrons on the reaction. The gamma flux originating from neutron capture by hydrogen in the pool water was considered as part of the total gamma flux. The total incident gamma flux was high enough to mask any effects of the neutrons.

Atoms with high thermal neutron absorption cross-sections were dissolved in the benzene water solutions. These were cadmium sulfate, boric acid, and lithium metaborate. The effects of these solutes on the phenol reaction were studied in cobalt-60 gamma photons. The differences noted could be simply explained except in the case of lithium metaborate solutions. The neutrons had no noticeable effect on the phenol yield in any of the solutions irradiated near the reactor. The energy absorbed in the solution due to neutron capture in the solution was a significant fraction of the total energy absorbed by the reacting solution. It was postulated that no effects were measured because the radical yields in neutral water due to densely ionizing radiation were low. A plausible alternate explanation was that the phenyl radicals were not able to compete with the radical reactions in the densely ionized tracks of the heavy particles.

The swimming pool type reactor was not well adapted for studies of the effects of neutrons in chemical systems. The water around the

reactor, in place of the graphite used in nuclear piles, tended to decrease the neutron flux and increase the gamma flux.

B. Benzene-Water Dosimeter

The use of water saturated with benzene as a chemical dosimeter for ionizing radiation was suggested several years ago but has received very little notice or acceptance. The Fricke dosimeter is used almost exclusively and is accepted as a standard.

A chemical dosimeter has several advantages over ion chamber and cavity measurements at least for chemical studies. A dose rate measured with a chemical dosimeter having similar physical and atomic properties to the experimental system is more applicable than a dose rate determined electronically. Most experimental systems are water or water-like, so a water-base dosimeter has the widest application. A chemical dosimeter can frequently be placed directly in the reaction vessel so that geometry and scattering errors for irregular volumes can be reduced. Generally higher dose rates are measurable with chemical systems than with simple electronic apparatus. Chemical dosimeters may be used for high energy photons in the range where the roentgen loses its meaning.

The requirements of an acceptable chemical dosimeter are listed below.

1. The effective atomic number of the solution should be about that of the system to which the results are applied.
2. The dosimeter should work with solutions saturated with air under normal conditions.
3. The dosimeter must be stable under the working conditions before and after irradiation.

4. The reaction should yield only one major product which must be easily, quickly and accurately determined.
5. The product yield should be independent of solute concentration over some convenient range.
6. The yield must be directly and accurately related to the dose received.
7. The yield should be independent of several other parameters including: oxygen concentration, temperature, dose rate, and pH.
8. The chemicals should be commonly available, and the solutions easy to prepare.
9. The dosimeter should be independent of the type and energy of the radiation. No system known satisfies this requirement.

The ferrous dosimeter satisfies most of these requirements. The solution is slightly unstable before and after irradiation. Very pure water is required to prepare the dosimeter solution since the dosimeter is sensitive to trace impurities. The triple distilled water required is not commonly available. Because of the high acid concentration, it is not possible to make measurements with the dosimeter directly in metal reaction vessels. The dosimeter must be contained in very clean glass or plastic vessels.

Aqueous benzene solutions have certain definite advantages as a dosimeter over ferrous solutions. The benzene solutions satisfy all the requirements as well as or better than ferrous solutions. It is as accurate as a carefully run ferrous determination. It is less sensitive to

impurities. The occasional erratic results from ferrous dosimetry are encountered less frequently with benzene-water solutions. Several runs were made with benzene dissolved in tap water and the measured yield agreed with the yield in triple distilled water. Some ions, especially reducible ions, show a strong effect on the phenol yield but these are easily avoided. Organic impurities have no effect. Benzene solutions are more water-like than 0.8N sulfuric acid. The solutions can safely be put in metal reaction vessels or pumped through a continuous flow system to measure the dose rate in an irregular shaped reaction vessel. Miley successfully used the benzene dosimeter for this purpose since the ferrous dosimeter could not be used in his metal apparatus.

The benzene-water solutions are more easily prepared and can be stored for long periods without deterioration. The analysis for phenol is slightly more tedious than the analysis for ferric ions. It involves mixing two solutions and taking readings with time, plotting the results and extrapolating to zero time. The latter difficulty can be easily overcome by calibrating the dosimeter for the maximum phenol yield, i.e. reading the optical density several minutes after adding the base when the phenyl peroxide has completely decomposed. In this study, the maximum yield was as reproducible as the yield at zero time.

VIII. SUGGESTIONS FOR FUTURE WORK

It is felt that aqueous benzene solutions definitely deserve more attention as a dosimeter for ionizing radiation. A calorimetric standardization of the G value for phenol might be undertaken before this system is used for dosimetry.

The production of phenol by this method probably has no commercial importance. Not only would the cost of radiation be prohibitive but also the cost of separating small amounts of phenol from large amounts of water would rule out the process. However, it would be interesting to study the reaction at high temperatures and in the gas phase.

This system holds great promise for the theoretical investigation of the primary products from the radiolysis of water. The measurement of the diphenyl yield should allow the estimation of the yield of hydrogen atoms in irradiated water. The reaction mechanism for benzene in aerated solutions is more straight forward than that of other radical traps commonly used in mechanism studies. Therefore, the results are easier to interprete. Irradiation of the system with heavy particles may allow the measurement of the yields of radicals and molecules for radiations with high linear energy transfers. This information has not been determined for pure water and is needed to extend the theory of dilute aqueous solutions.

IX. APPENDIX

A. Average Path of a Particle in Experimental System

An expression is derived below for the average distance traveled in the experimental system by ionizing particles born in the system. The particles are photons born as a result of neutron captures within the system. A cylindrical system is approximated by a sphere of the same volume.

Assume: 1. The particles are born uniformly throughout the volume of the sphere.

2. The particles leave the site of their birth in a random direction.

3. Every particle leaves the sphere.

The average path in a sphere is the same as the average path of a particle travelling in two dimensions in a circle. A particle born at $P_o(x_o,y_o)$ moves at an angle α with the x axis. Draw the x',y' axis through point P_o parellel to the x, y axis. The particle leaves

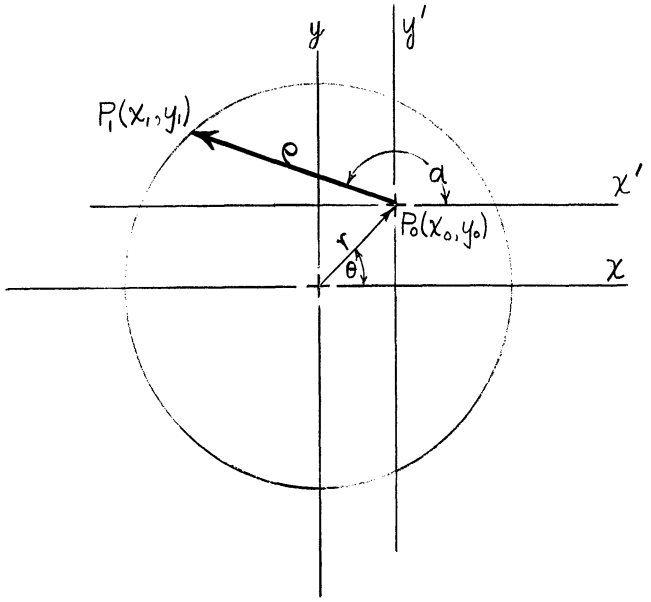

at point P_1. Integrating over all angles around P_o gives the average distance travelled by particles born at x_o, y_o. Then integrating over the area of the circle gives the average desired.

Distance traveled in the circle = $\rho(x_o, y_o, \alpha)$

$$\bar{\rho}(x_o, y_o) = \frac{1}{2\pi}\int_0^{2\pi} \rho(x_o, y_o, \alpha)\, d\alpha \tag{74}$$

$$\bar{R} = \frac{1}{\pi R^2}\int_{-R}^{+R}\int_{-\sqrt{R^2-y^2}}^{+\sqrt{R^2-y^2}} \bar{\rho}(x_o, y_o)\, dx\, dy \tag{75}$$

$$\rho^2 = (x_1 - x_o)^2 + (y_1 - y_o)^2 = (x_1')^2 + (y_1')^2 \tag{76}$$

$$R^2 = x_1^2 + y_1^2 = (\rho\cos\alpha + x_o)^2 + (\rho\sin\alpha + y_o)^2 \tag{77}$$

Solving for ρ

$$\rho = -x_o\cos\alpha - y_o\sin\alpha \pm \sqrt{R^2 - (x_o\sin\alpha - y_o\cos\alpha)^2} \tag{78}$$

$$\bar{\rho}(x_o, y_o) = \frac{1}{2\pi}\int_o^{2\pi} \rho\, d\alpha = \pm\frac{1}{2\pi}\int_o^{2\pi}\sqrt{R^2 - (x_o\sin\alpha - y_o\cos\alpha)^2}\, d\alpha \tag{79}$$

Transforming to polar coordinates

$$\bar{\rho}(r, \theta) = \pm\frac{R}{2\pi}\int_o^{2\pi}\sqrt{1 - \frac{r^2}{R^2}(\sin\alpha\cos\theta - \cos\alpha\sin\theta)^2}\, d\alpha \tag{80}$$

Because of the symmetry of the circle $\bar{\rho}(r,\theta)$ is independent of the choice of θ. Let $\theta = 0$, and $\frac{r}{R} = \omega$

$$\bar{\rho}(r) = \frac{R}{2\pi}\int_0^{2\pi}\pm\sqrt{1 - \omega^2\sin^2\alpha}\, d\alpha = \frac{R}{2\pi}\int_o^{\pi}\sqrt{1 - \omega^2\sin^2\alpha}\, d\alpha \tag{81}$$

This is a complete elliptical integral[121].

Let $$E(\omega) = \int_0^{\pi/2} \sqrt{1 - \omega^2 \sin^2\alpha}\, d\alpha$$

$$\bar{\rho}(r) = \bar{\rho}(\omega) = \frac{R}{\pi} E(\omega) \tag{82}$$

$$\bar{R} = \frac{1}{2R} \int_{-R}^{+R} \bar{\rho}(r)\, dr = \int_0^1 \bar{\rho}(\omega)\, d\omega = \frac{R}{\pi} \int_0^1 E(\omega)\, d\omega \tag{83}$$

Integrating graphically:

$$\int_0^1 E(\omega)\, d\omega \cong 1.415$$

$$\bar{R} = 0.405 R \tag{84}$$

B. Number of Thermal Neutron Captures

In order to calculate the total number of neutron captures occurring per second in an experimental system, it is necessary to know the neutron flux as a function of position in the system. The total number of captures is then expressed by:

$$V\left(\frac{dn}{dt}\right) = \int_V \Sigma_{ac} \phi(V)\, dV \tag{85}$$

Assume the experimental system (a sample bottle) is an infinite cylinder of radius R and that it is in water in a uniform infinite thermal neutron flux equal to 1.

In the cylinder (the experimental system):

$$-D_c\left[\frac{d^2\phi_c}{dr^2} + \frac{d\phi_c}{r dr}\right] + \Sigma_{ac}\phi_c = Q \tag{86}$$

In the water:

$$-D_w\left[\frac{d^2\phi_w}{dr^2} + \frac{d\phi_w}{rdr}\right] + \Sigma_{aw}\phi_w = Q \qquad (87)$$

Q = slowing down density (assumed to be the same in both the water and cylinder) (neutrons/cm^3/sec)

D = diffusion coefficient of thermal neutrons (cm^{+1})

Σ_a = macroscopic absorption cross-section (cm^{-1})

The subscripts c and w refer to the cylinder and water respectively.

Boundary conditions:

$$\phi_w(\infty) = 1 \qquad \phi_c(0) \text{ is defined}$$

$$\frac{d\phi_w(\infty)}{dr} = 0 \qquad \frac{d\phi_c(0)}{dr} = 0$$

$$\phi_c(R) = \phi_w(R) \qquad D_c\frac{d\phi_c(R)}{dr} = D_w\frac{d\phi_w(R)}{dr}$$

The solution of the differential equations:

$$\phi_w(r) = \frac{C_1}{\Sigma_{aw}} I_o(\gamma_w r) + \frac{C_2}{\Sigma_{aw}} K_o(\gamma_w r) + \frac{Q}{\Sigma_{aw}} \qquad (88)$$

$$\phi_c(r) = \frac{C_3}{\Sigma_{ac}} I_o(\gamma_c r) + \frac{C_4}{\Sigma_{ac}} K_o(\gamma_c r) + \frac{Q}{\Sigma_{ac}} \qquad (89)$$

Where: $\gamma = \sqrt{\Sigma_a/D}$ Applying the boundary conditions:

Since: $\phi_w(\infty) = 1 \quad \therefore \quad C_1 = 0 \quad ; \quad Q = \Sigma_{aw}$

Since: $\phi_c(0)$ is defined, $C_4 = 0$

Since $\phi_w(R) = \phi_c(R)$; $\frac{C_2}{\Sigma_{aw}} K_o(\gamma_w R) + 1 = \frac{\Sigma_{aw}}{\Sigma_{ac}} + \frac{C_3}{\Sigma_{ac}} I_o(\gamma_c R)$ (90)

$$C_3 = \frac{C_2 \Sigma_{ac} K_o(\gamma_w R)}{\Sigma_{aw} I_o(\gamma_c R)} + \frac{\Sigma_{ac} - \Sigma_{aw}}{I_o(\gamma_c R)} \tag{91}$$

Since:

$$D_c \frac{d\phi_c(R)}{dr} = D_w \frac{d\phi_w(R)}{dr}$$

$$\frac{D_c C_3 \gamma_c}{\Sigma_{ac}} I_1(\gamma_c R) = -\frac{D_w C_2 \gamma_w}{\Sigma_{aw}} K_1(\gamma_w R) \tag{92}$$

$$C_3 = -\frac{C_2 \gamma_c K_1(\gamma_w R)}{\gamma_w I_1(\gamma_c R)} \tag{93}$$

$$C_2 = \frac{\Sigma_{aw} - \Sigma_{ac}}{I_o(\gamma_c R)\left[\frac{\Sigma_{ac} K_o(\gamma_w R)}{\Sigma_{aw} I_o(\gamma_c R)} + \frac{\gamma_c K_1(\gamma_w R)}{\gamma_w I_1(\gamma_c R)}\right]} \tag{94}$$

For pure water:[44]

$$D_w = 0.142 = \frac{1}{3\Sigma_{tw}(1-\bar{\mu})} \tag{95}$$

$\bar{\mu}$ = average cosine of the scattering angle = 2/3A

= 0.037 (for low energy neutrons - energy less than the bonding energy of the water molecule)

Σ_t = total cross-section = $\Sigma_a + \Sigma_s$

Σ_{tw} = 2.44 cm^{-1}

$$\Sigma_{aw} = \frac{2\sigma_{aH} a}{(MW)} = \frac{2 \times .33 \times 10^{-24} \times .602 \times 10^{24}}{18} = 0.022 \text{ cm}^{-1}$$

$$\gamma_w = \sqrt{\Sigma_{aw}/D_w} = 0.394 \text{ cm}^{-1}$$

The experimental systems used in this study that had the largest flux depression were solutions of 0.112M $CdSO_4$.

For natural cadmium: σ_a = 2200 barns

$$\Sigma_a = \frac{\quad}{1000} = \frac{.602 \times 10^{24} \times .112 \times 2200 \times 10^{-24}}{1000} = 0.149 \text{ cm}^{-1}$$

$$\Sigma_{ac} = 0.149 + .022 = 0.171 \text{ cm}^{-1}$$

$$\Sigma_{tc} = 2.44 + .15 = 2.59 \text{ cm}^{-1}$$

$$D_c = \frac{1}{3\Sigma_{tc}(1-\bar{\mu})\left[1 - \frac{4\Sigma_{ac}}{5\Sigma_{tc}} + \frac{\Sigma_{ac}\bar{\mu}}{\Sigma_{tc}(1-\bar{\mu})}\right]} \quad * \qquad (96)$$

$$D_c = 0.141 \quad ie \quad D_c = D_w$$

$$\gamma_c = \sqrt{\Sigma_{ac}/D_c} = 1.07\ cm^{-1}$$

$$C_2 = \frac{-0.149}{I_0(1.07R)\left[7.77\frac{K_0(.394R)}{I_0(1.07R)} + 2.72\frac{K_1(.394R)}{I_1(1.07R)}\right]}$$

$$C_3 = -\frac{2.72\,K_1(.394R)}{I_0(1.07R)} \cdot C_2$$

The sample bottles were 2.8 cm. in diameter.

$I_0\ (1.50) = 1.647$ $\qquad$ $I_1\ (1.50) = 0.982$

$K_0\ (0.55) = 0.846$ $\qquad$ $K_1\ (0.55) = 1.47$

$C_2 = -0.0112$ $\qquad$ $C_3 = 0.0456$

$\Phi_w(r) = 1 - 0.509\ K_0(.394r)$

$\Phi_c(r) = .129 + .267\ I_0(1.07r)$

$\Phi_c(0) = 0.396$ $\qquad$ $\Phi_c(R) = 0.569 = \Phi_w(R)$

The average number of neutron captures per centimeter of height:

$$\left(\frac{\overline{dn}}{dt}\right)_c = \frac{\int_v \Sigma_{ac}\phi_c(V)dV}{V} = \frac{2\Sigma_{ac}\int_0^R \phi_c(r)r\,dr}{R^2} \qquad (97)$$

$$\left(\frac{\overline{dn}}{dt}\right)_c = \frac{2\Sigma_{ac}}{R^2}\left\{\frac{\Sigma_{aw}}{\Sigma_{ac}}\int_0^R r\,dr + \frac{C_3}{\Sigma_{ac}}\int_0^R r\,I_0(\gamma_c r)dr\right\} \qquad (98)$$

$$= \Sigma_{aw} + \frac{2C_3}{\gamma_c R}I_1(\gamma_c R)$$

For 0.112M $CdSO_4$ and R = 1.4 cm.:

$$\left(\frac{\overline{dn}}{dt}\right)_c = .022 + \frac{2 \times .0456}{1.07 \times 1.4}(.982) = .082$$

If there is no flux depression the number of captures is a maximum.

---

* See Reference 44.

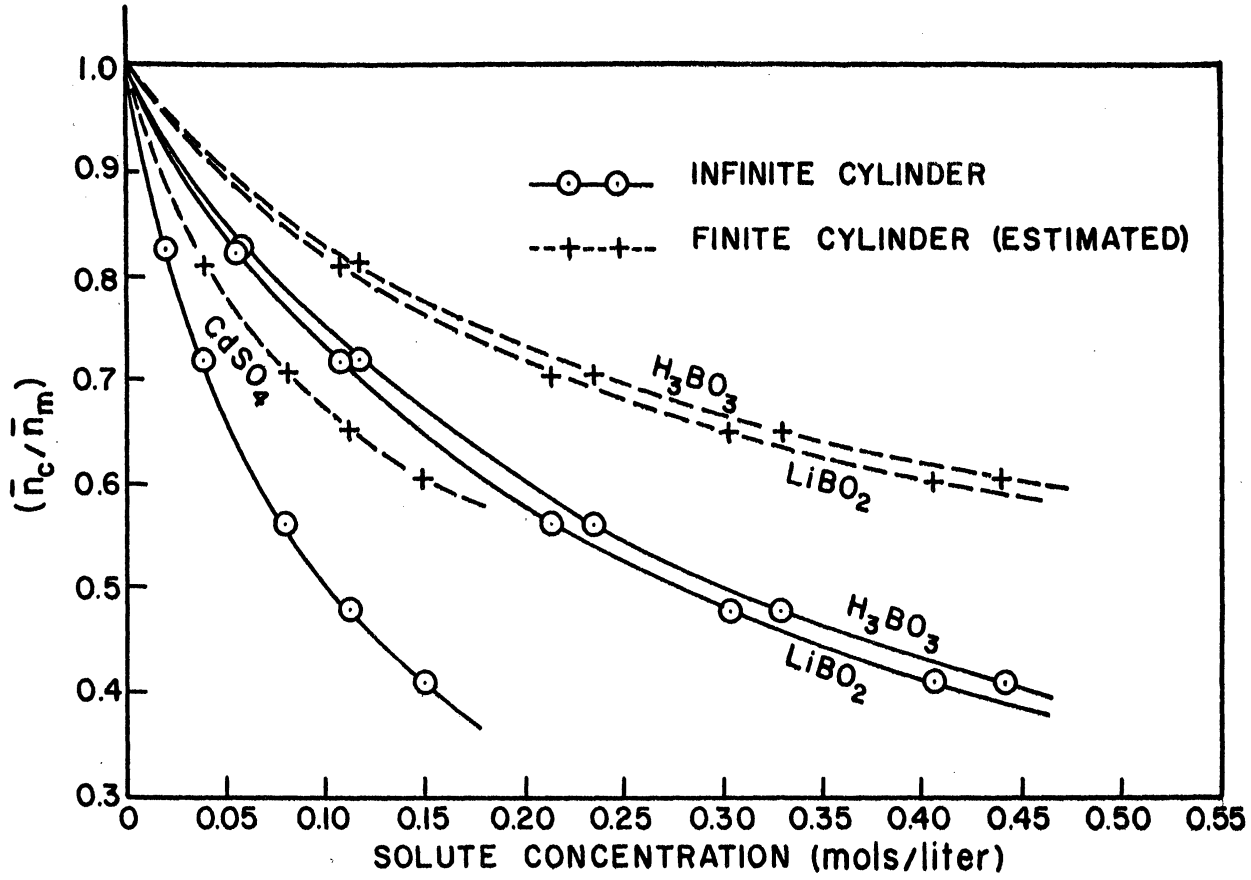

Figure 41. Relative Number of Neutron Captures in a Cylinder as a Function of Solute Concentration.

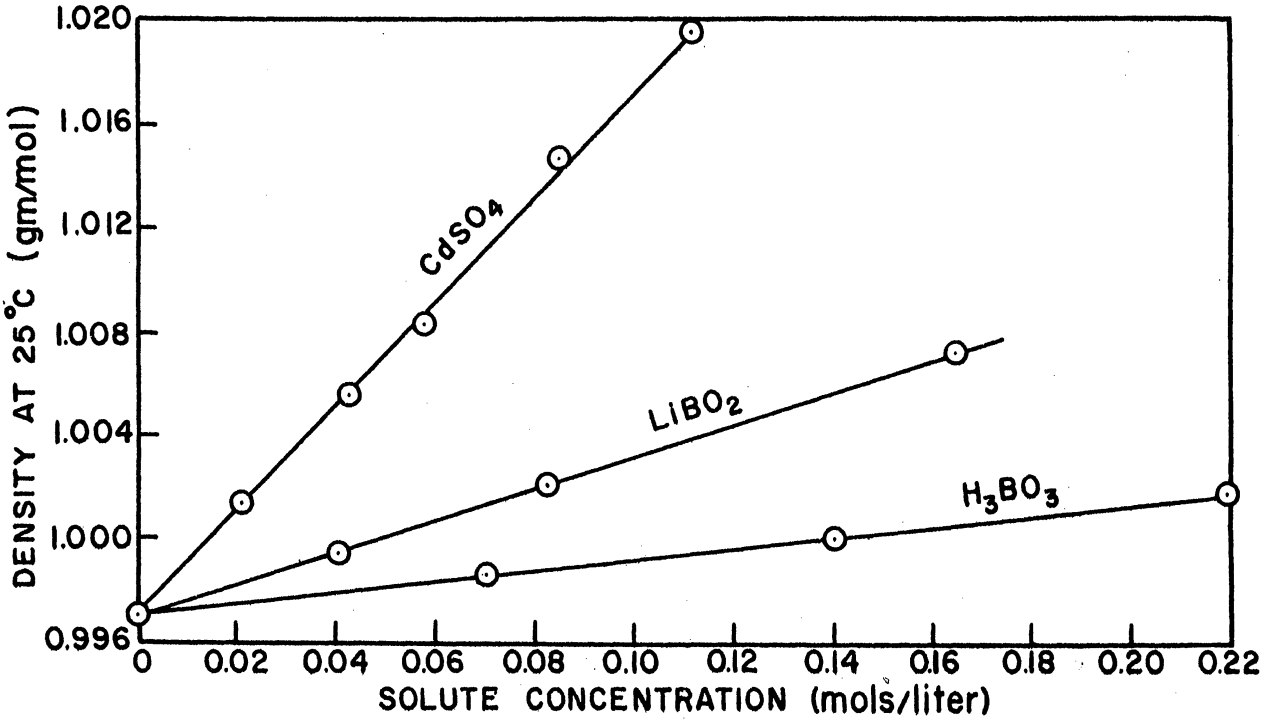

Figure 42. Density of Aqueous Solutions as a Function of Solute Concentration.

$$\left(\frac{dn}{dt}\right)_{max} = \Sigma_{ac}\phi_w(\infty) = 0.171$$

$$\left(\frac{dn}{dt}\right)_c \Big/ \left(\frac{dn}{dt}\right)_{max} \equiv \left(\frac{\bar{n}_c}{\bar{n}_m}\right)_\infty = 0.48$$

The quantity $(n_c/n_m)_\infty$ is shown in Figure 41 as a function of solute concentration for the three solutes used. Because an infinite cylinder was assumed in the above derivation, the actual flux depression would be smaller than that calculated. Therefore:

$$1 > \left(\frac{\bar{n}_c}{\bar{n}_m}\right)_{actual} > \left(\frac{\bar{n}_c}{\bar{n}_\infty}\right)_\infty \tag{99}$$

For the purpose of estimating of the actual number of neutron captures, it was estimated that for the sample bottles used that:

$$1 - \left(\frac{\bar{n}_c}{\bar{n}_m}\right)_{act} = 2\left[\left(\frac{\bar{n}_c}{\bar{n}_m}\right)_{act} - \left(\frac{\bar{n}_c}{\bar{n}_m}\right)_\infty\right] \tag{100}$$

The estimated relative number of neutron captures is shown in Figure 41 as a broken line.

C. List of Chemicals and Equipment Used

Chemical	Brand	Grade
Benzene	Mallinckrodt	Reagent - thiophene free
Boric Acid	J.T. Baker	Reagent - crystal
Cadmium sulfate	J.T. Baker	Reagent
Ferrous Ammonium Sulfate	Baker and Adamson	Reagent

Chemical	Brand	Grade
Helium	Airco	
n-Hexene-1	Phillips Petroleum Co.	Pure
Hydrogen Peroxide	Mallinckrodt	Reagent - 30%
Lithium Metaborate	Anderson Chemical Co.	#130
Phenol	Mallinckrodt	Reagent
Phenol Reagent Folin-Ciocalteu	Hartman-Leddon	
Phenol-Standard	Hartman-Leddon	
Sodium Chloride	Baker and Adamson	Reagent
Sodium Hydroxide	Mallinckrodt	Reagent - pellets
Sulfur Dioxide	Matheson	Anhydrous
Sulfuric Acid	du Pont	95 - 98%
Trichloroethylene	Fisher Scientific	Boiling Range - 86 - 87°C

Spectrophotometer: Beckman Model DU Quartz Spectrometer - Hydrogen Lamp

pH Meter: Beckman - glass electrode

Counting Equipment: Baird Associates - Atomic Instruments Co.

- Bench Type Scintillation Detector Model 810

- Super-Stable High Voltage Power Supply #312

TABLE XII

PERTINENT NUCLEAR DATA

Nucleus	Absorption Cross-Section (barns) (10)	Reaction	Prompt Energy Released (Mev)	Half Life of Product	Energy Appears as	Ref.
H-1	.33	$H^1(n,\gamma)H^2$	2.23	∞	Single photon 2.23 Mev	10
Li-6	71	$Li^6(n,\alpha)H^3$	4.78	12.5 yr.	Kinetic energy of charged particles	94
B-10	755	$B^{10}(n,\alpha)Li^7$	2.79	∞	Kinetic energy of charged particles except 93% of captures emit 0.48 Mev gamma	94
Mg-26	0.055	$Mg^{26}(n,\alpha)Mg^{27}$	?	9.5 min.	?	10
Al-27	0.23	$Al^{27}(n,\gamma)Al^{28}$	?	2.27 min.	?	10
Cl-37	0.14	$Cl^{37}(n,\gamma)Cl^{38}$	?	37.2 min.	?	10
S-34	0.011	$S^{34}(n,\gamma)S^{35}$	?	87.1 d.	Equal intensities at 0.84 and 2.34 Mev	10 15
Cd-113	2200	$Cd^{113}(n,\gamma)Cd^{114}$	9.20	∞	Spectrum of photons up to 9.20 Mev maximum. Highest intensity photons grouped about 0.56, 1.32 and 2.53 Mev	15 36 87

D. Sample Calculations

Reaction Yield of Phenol - Cobalt-60

Experimental Data: (Data of 6/21)

Dose rate: 0.101 kiloreps/min.

Irradiation time: 259 min.

$D_{AB} = .006$, $D_{UB} = .002$, $= D_{US} = .016$

D_{AS}	.088	.090	.092
Time	2.0	4.0	7.0 min.

Extrapolating to $t = 0$; $[D_{AS} - D_{US} - (D_{AB} - D_{UB})] = .066$

Extrapolating to $t \rightarrow \infty$; $[D_{AS} - D_{US} - (D_{AB} - D_{UB})] = .072$

$[P]_o = 393 \times 2 \times .066 = 51.8$ micromols/liter

$A_o(P) = 51.8/(259 \times .101) = 1.98$ micromols/liter/kilorep

$A_\infty(P) = 393 \times 2 \times .072/(259 \times .101) = 2.14$

$G_o(P) = 1.038A_o/\rho = 1.98 \times 1.038/.997 = 2.06 \frac{\text{molecules}}{100 \text{ ev}}$

Radiation Yield of Phenol - Pile Radiation

Experimental Data (Data of 9/19)

Lithium Metaborate Concentration: 0.162 M

Gamma Dose Rate: 6.84 kiloreps/min

Irradiation time: 6.0 min.

$[D_{AS} - D_{US} - (D_{AB} - D_{UB})] = 0.088$

$[P] = 395 \times 2 \times .088 = 69.5$ micromols/liter

$A(P) = 69.5/(6.84 \times 6.0) = 1.69$ micromols/liter/kilorep

$G(P) = 1.69 \times 1.038/1.006 = 1.75$ molecules/100 ev

$(\Phi_T)_{avg} = 1.9 \times 10^{10}$ neutrons/cm^2/sec (Figure 15)

For lithium metaborate, the neutron capture energy absorbed in the solution/cm. is:

$$E_n = \left[\Sigma_a \phi_T \left(\frac{\bar{n}_c}{\bar{n}_m}\right)_{act} t \beta y\right]_{Li} + \left[\Sigma_a \phi_T \left(\frac{\bar{n}_c}{\bar{n}_m}\right)_{act} t \beta y\right]_B \qquad (101)$$

$$= a \frac{m \phi_T}{1000} \left(\frac{\bar{n}_c}{\bar{n}_m}\right)_{act} t \left\{(\sigma_a \beta y)_{Li} + (\sigma_a \beta y)_B\right\} \qquad (102)$$

$\left(\bar{n}_c/\bar{n}_m\right)_{act} = 0.75$ (Figure 41)

$$E_n = \frac{(.602)(.162)(1.9\times10^{10})(.75)(360)\left[71(\beta y)_{Li} + 755(\beta y)_B\right]}{1000}$$

$$E_n = 5.0\times10^{8}\left\{(71\,\beta y)_{Li} + (755\,\beta y)_B\right\}$$

For Lithium: β = 4.78 Mev/capture; y = 1.0 (Table XII)

For Boron: The energy must be divided into two parts - the energy of the photon and the energy of the heavy particles. For the heavy particles: y = 1.0

$$\beta = 2.79 - (0.48)(.93) = 2.34 \text{ Mev/capture}$$

For the photon: β = 0.45 Mev/capture

y is estimated from the average path traveled in a sphere having the same volume. (See Appendix A)

$$R = \frac{\sqrt[3]{3V}}{4} \quad \sqrt[3]{\frac{(3)(25)}{4}} = 1.82 \text{ cm.}$$

$$\bar{R} = 0.45R = 0.82 \text{ cm.}$$

μ for 0.48 Mev gammas$^{(121)}$ = 0.104 cm^{-1}

$$y = 1 - \exp(-.104 \times .82) = 0.082$$

Thus for boron, the energy absorbed per neutron capture is:

$$(\beta y)_B = 2.34 + (0.45)(.082) = 2.38 \text{ Mev/capture.}$$

The total neutron energy absorbed then is

$$En = 5.0 \times 10^8 [(71)(4.78) + (755)(2.38)]$$

$$= 1.07 \times 10^{12} \text{ Mev/cm}^3 = 18 \text{ kiloreps}$$

E. Tabulated Data

TABLE XIII

BENZENE - PURE WATER
CO-60 IRRADIATIONS

Date	Run No.	Gamma Dose Rate Kilorep/Min.	Total Dose Krep	$[P]_o$ μmols/Liter	$[P]_\infty$ μmols/Liter	A_o μmols/(Liter)(Krep)	A_∞ μmols/(Liter)(Krep)	Notes
6-12-58	16-II	.563	26.8	55.0	60.5	2.06	2.26	
	A	.563	26.8	55.0	61.4	2.06	2.29	
		.397	18.8	36.2	40.1	1.93	2.14	
		.397	18.8	34.6	38.6	1.84	2.05	
		.273	13.0	26.8	29.9	2.06	2.30	
		.273	13.0	26.8	31.5	2.06	2.42	
6-12	16-II	.563	63.1	129.8	141	2.05	2.23	
	B	.563	63.1	129.0	140	2.04	2.22	
		.397	44.5	92.7	101.4	2.08	2.28	
		.397	44.5	95.2	102	2.14	2.29	
		.273	30.6	65.2	72.4	2.13	2.36	
		.273	30.6	64.4	71.5	2.10	2.34	
		.101	11.3	22.8	26.0	2.02	2.30	
		.101	11.3	22.8	25.2	2.02	2.23	
6-12	16-II	.563	67.5	118	128	1.75	1.90	[Benzene] = .00193 m/ℓ
	C	.397	47.6	86.2	93.4	1.81	1.96	.00193
		.397	47.6	88.0	93.6	1.85	1.93	.00354
		.563	67.5	128.0	137	1.89	2.03	.00354
		.273	32.7	63.6	69.2	1.95	2.12	.00424

TABLE XIII (CONT'D)

BENZENE - PURE WATER
CO-60 IRRADIATIONS

Date	Run No.	Gamma Dose Rate Kilorep/Min.	Total Dose Krep	$[P]_o$ μmols/Liter	$[P]_\infty$ μmols/Liter	A_o μmols/(Liter)(Krep)	A_∞ μmols/(Liter)(Krep)	Notes
		.430	51.6	96.0	105	1.86	2.02	.00424
		.430	51.6	103.0	111	1.99	2.14	.00530
		.273	32.7	64.4	70.7	1.98	2.16	.00530
6-19	25-II	.396	106.6	180	182	1.69	1.71	Solution Temp. = 72°F
		.396	106.6	186	187	1.74	1.75	
		.563	151.5	217	222	1.43	1.47	
		.563	151.5	216	222	1.43	1.47	
		.279	75.2	(171)	173	2.27	2.36	
6-21	27-II	.397	102.5	183	190	1.78	1.85	Solution Temp. = 72°F
		.397	102.5	183	200	1.78	1.95	
		.563	146.0	209	232	1.43	1.59	
		.563	146.0	214	234	1.47	1.60	
		.279	72.4	153	170	2.11	2.40	
		.279	72.4	155	170	2.14	2.36	
		.101	26.2	52	56	1.98	2.14	
		.101	26.2	52	56	1.98	2.14	

TABLE XIII (CONT'D)

BENZENE - PURE WATER
CO-60 IRRADIATIONS

Date	Run No.	Gamma Dose Rate Krep/Min.	Total Dose Krep	$[P]_o$ μmols/Liter	$[P]_\infty$ μmols/Liter	A_o μmols/(Liter)(Krep)	A_∞ μmols/(Liter)(Krep)	
8/21	46-II	.384	308	376	411	1.22	1.34	Solution Temp.
		.384	308	380	415	1.23	1.35	60°F
		.575	461	404	441	0.875	0.958	
		.575	461	414	456	0.898	0.990	
		.279	224	328	357	1.464	1.60	
		.279	224	332	357	1.483	1.60	
		.208	167	298	318	1.784	1.91	
		.208	167	298	318	1.784	1.90	
8/26	53-II	.384	231	303	326	1.31	1.41	Solution Temp.
		.384	231	314	338	1.36	1.46	68°F
		.575	346	369	404	1.066	1.16	
		.575	346	366	401	1.057	1.17	
		.279	168	284	310	1.69	1.85	
		.279	168	286	307	1.70	1.83	
		.208	125	258	277	2.06	2.21	
		.208	125	261	282	2.08	2.25	
8/21	48-II	.384	75.0	76.2	88.0	1.02	1.17	Deaerated
	I	.384	75.0	73.9	85.8	.985	1.14	with Nitrogen
		.575	112.4	92.0	103	.818	0.915	
		.575	112.4	105	120	.934	1.07	

TABLE XIII (CONT'D)

BENZENE - PURE WATER
CO-60 IRRADIATIONS

Date	Run No.	Gamma Dose Rate Krep/Min.	Total Dose Krep	$[P]_o$ μmols/Liter	$[P]_\infty$ μmols/Liter	A_o μmols/(Liter)(Krep)	A_∞ μmols/(Liter)(Krep)	
		.279	54.5	70.7	80.2	1.30	1.47	
		.279	54.5	86.5	97.5	1.59	1.79	
		.208	40.6	73.0	85.7	1.80	2.11	
8/21	48-II	.384	34.6	39.3	44.8	1.136	1.30	Deaerated
	II	.384	34.6	40.1	44.8	1.159	1.30	with Nitrogen
		.575	51.5	51.8	56.6	1.007	1.10	
		.575	51.5	39.3	45.6	0.763	0.886	
		.279	25.0	36.2	40.1	1.45	1.61	
		.279	25.0	38.5	41.6	1.54	1.67	
		.208	18.6	33.0	36.2	1.78	1.95	
		.208	18.6	37.0	40.1	1.99	2.16	
8/26	53-II	.384	77.4	86.5	94.4	1.12	1.22	Deaerated
		.384	77.4	74.6	81.8	0.965	1.06	with He
		.575	116	85.7	95.9	0.740	0.827	
		.575	116	103.7	112.5	0.893	0.972	
		.279	56.3	62.9	70.0	1.12	1.24	
		.279	56.3	80.2	89.6	1.42	1.59	
		.208	41.9	77.0	83.4	1.84	1.99	
		.208	41.9	60.5	65.2	1.45	1.54	

TABLE XIV

BENZENE-PURE WATER
PILE IRRADIATIONS

Date	Run No.	Gamma Dose Rate Kilorep/Min.	Total Dose Kilorep	$[P]_0$ μmols/Liter	$[P]_\infty$ μmols/Liter	A_0 μmols/(Liter)(Kilorep)	A_∞ μmols/(Liter)(Kilorep)	$\Phi_T \times 10^{-9}$	Notes
4/14/58	45-I	.655	40.9	74.6	82.5	1.83	2.02	.053	
		.635	34.4	73.8	82.5	1.87	2.09	.048	
		2.08	130	172	179	1.32	1.38	1.64	
		2.01	125	146	156	1.12	1.20	1.50	
		2.34	146	173	186	1.18	1.27	2.3	
		1.79	110	174	184	1.58	1.67	1.04	
4/16/58	49-I	.466	21.3	45.5	50.3	2.14	2.36	.0188	
		.477	21.8	48.0	53.5	2.20	2.45	.0201	
		1.65	75.4	152	156	2.02	2.07	.82	
		1.40	64.0	132	139	2.06	2.17	.50	
		1.90	86.9	163	171	1.88	1.97	1.25	
		1.87	85.5	157	167	1.84	1.95	1.18	
		1.67	76.1	140	153	1.84	2.01	.85	
		1.74	79.5	151	158	1.90	1.99	.96	
4/24	59-I	.63	19.2	33.8	40.1	1.76	2.09	.047	Core configuration
		.63	18.6	31.5	40.1	1.69	2.16	.047	changed to slab for this
		1.60	48.5	115	125	2.37	2.58	.84	run only.
		1.70	50.0	145	157	2.90	3.14	.90	
		1.43	42.1	74	81	1.76	1.93	.53	
5/5	63-I	.600	28.1	51.8	58.2	1.84	2.07	.041	Rod dropped
		.600	28.1	57.4	62.9	2.04	2.24	.041	
5/12	66-I	.590	35.4	72.3	77.8	2.04	2.20	.039	Rod dropped
		.590	35.4	73.9	81.0	2.08	2.29	.039	Corrected Time
9/17	80-II	0.83	8.3	19.0	20.4	2.29	2.46	.105	
		0.83	8.3	19.0	20.4	2.29	2.46	.105	
		3.87	38.7	82.5	89.6	2.13	2.32	9.6	
		3.80	38.0	78.6	86.5	2.07	2.28	9.5	
		7.35	73.5	146	154	1.99	2.10	20	
		6.86	68.6	142	149	2.06	2.17	19	
		4.78	47.8	101	108.5	2.11	2.27	14	
		4.71	47.1	102	110	2.16	2.33	14	

TABLE XV

BENZENE - WATER - CADMIUM SULFATE

Date	$[C_d]$ mol/Liter	κ	Gamma Dose Rate Krep/Min.	Total Gamma Dose Krep	$\phi_T \times 10^{-9}$ Neut/cm² sec	$[P]_o$ μmols/Liter	A_o μmols/(Lit)(Krep)	Σ_a cm⁻¹	Neutron E_r Krep	Energy E_a Krep	
4/14/58	.0728	438	2.36	147.	2.4	115	0.78	.0965	47	2.2	Cadmium Acetate
	.0728	438	1.79	110.	1.05	109	0.99	.0965	21	.98	(not enough
4/25/58	.0728	438	1.62	48.8	0.77	30.7	0.63	.0965	15	.72	NaOH added)
	.0728	438	1.72	51.8	0.92	70.1	1.35	.0965	18	.86	
	.0728	438	1.45	43.6	0.55	84.1	1.92	.0965	10.9	.51	
5/5	.112	462	1.61	75.4	0.76	62	0.82	.149	32	1.53	Centrifuged
	"	"	1.61	75.4	0.76	59	0.78	.149	32	1.53	poorly
	"	"	2.23	104	2.0	165	1.59	.149	85	4.0	
	"	"	2.23	104	2.0	139	1.34	.149	85	4.0	
	"	"	1.41	66.0	0.51	127	1.93	.149	22	1.02	
5/12	.112	462	1.60	96.3	0.75	140	1.46	.149	41	1.9	Rod Dropped
	"	"	1.63	98.1	0.79	141	1.44	.149	43	2.0	
	"	"	2.36	142	2.4	187	1.32	.149	130	6.2	
	"	"	2.26	136	2.1	183	1.35	.149	115	5.4	
	"	"	1.43	86	0.53	130	1.51	.149	29	1.37	
	"	"	1.43	86	0.53	147	1.71	.149	29	1.37	
6/13	.112	462	.630	68.0	.047	139	2.04	.149	4.6	.22	
	.056	428	.630	68.0	.047	141	2.07	.074	2.7	.129	
	.056	428	1.55	168	0.68	193	1.15	.074	40	1.87	
	.112	462	1.55	168	0.68	210	1.25	.149	67	3.2	
	.112	462	3.90	421	10.0	245	0.58	.149	980	46	
	.056	428	3.64	393	8.4	247	0.63	.074	490	23	
	.056	428	2.52	272	2.9	214	0.79	.074	170	8.0	
	.112	462	2.62	283	2.9	184	0.65	.149	290	13.5	
6/16	.0448	420	.610	55.0	.043	104	1.89	.0595	1.7	.082	
	.0373	416	.610	55.0	.043	99	1.79	.0495	1.5	.070	
	.0373	416	1.60	144	.74	179	1.24	.0495	25	1.20	
	.0448	420	1.60	144	.74	175	1.22	.0595	30	1.40	
	.0448	420	3.80	342	9.4	217	0.64	.0595	380	17.8	
	.0373	416	3.57	321	7.9	216	0.67	.0495	280	12.8	
	.0373	416	2.46	222	0.57	168	0.76	.0495	19.6	.93	
	.0448	420	2.56	230	0.69	209	0.90	.0595	28	1.31	

TABLE XV (CONT'D)

BENZENE - WATER - CADMIUM SULFATE

Date	[Cd] mol/Liter	κ	Gamma Dose Rate Krep/Min.	Total Gamma Dose Krep	$\phi_T \times 10^{-9}$ Neut/cm² sec	$[P]_o$ μmols/Liter	A_o μmols/(Lit)(Krep)	Σ_a cm-1	Neutron Er Krep	Energy Ea Krep
6/18	.019	405	.68	10.2	.059	28.4	2.78	.025	.019	.0089
	.0070	397	.65	9.74	.051	22.2	2.28	.0093	.064	.0030
	.0070	397	1.77	26.6	1.00	48.4	1.82	.0093	1.25	.059
	.019	405	1.73	26.0	.95	61.6	2.37	.025	3.0	.143
	.019	405	2.62	39.3	3.2	86.0	2.19	.025	10.2	.48
	.0070	397	2.52	37.8	2.9	69.8	1.84	.0093	3.6	.172
	.0070	397	1.66	24.9	.84	51.6	2.07	.0093	1.06	.050
	.019	405	1.63	24.4	.79	51.2	2.10	.025	2.5	.12
6/19	.112	462	.396	44.9	-	93.2	2.08	Co-60 Irradiation		
	.112	462	.563	63.8	-	127.6	2.00			
	.112	462	.273	31.0	-	79.6	2.57			
	.056	428	.396	44.9	-	93.2	2.08			
	.056	428	.563	63.8	-	132.4	2.08			
	.056	428	.272	31.0	-	66.8	2.15			
7/3	.0851	445	1.51	48.1	.64	108.6	2.26	.113	15.2	.72
	.0426	419	1.54	49.4	.67	113.0	2.29	.0565	9.2	.43
	.0426	419	2.40	76.8	2.5	129.8	1.69	.0565	34	1.61
	.0851	445	2.32	74.4	2.2	144.2	1.96	.113	53	2.5
	.0851	445	1.67	53.3	.84	110.4	2.08	.113	20	.95
	.0426	419	1.71	54.7	.92	109.8	2.01	.0565	12.5	.59
7/3	.0284	411	1.51	43.6	.64	90.4	2.07	.0377	5.6	.27
	.0142	402	1.54	44.8	.67	92.4	2.06	.0188	3.1	.15
	.0142	402	2.40	69.6	2.5	123.0	1.77	.0188	11.6	.55
	.0284	411	2.33	67.4	2.3	119.2	1.77	.0377	20	.96
	.0284	411	1.67	48.3	.84	97.8	2.03	.0377	7.4	.35
	.0142	402	1.71	49.6	.92	97.2	1.96	.0188	4.3	.20

TABLE XVI

BENZENE-WATER-BORIC ACID

Date	$[H_3BO_3]$ mol/Liter	Gamma Dose Rate Krep/Min.	Total Gamma Dose Krep	$\phi_T \times 10^{-9}$ Neut/cm^2 sec	$[P]_o$ μmol/Liter	A_o μmols/(Krep)(Lit)	Σ_a cm^{-1}	Neutron Capture Energy Er (Kiloreps)	Neutron Capture Energy Ea (Kiloreps)	Notes
8/21	.1117	.384	46.1	-	99.5	2.16				Co-60 Irradiation
	"	.279	33.5	-	70.9	2.12				Insufficient NaOH
	"	.208	25.0	-	54.9	2.19				added to assure
	.2013	.384	46.1	-	98.5	2.14				proper pH
	"	.575	69.0	-	143.0	2.08				
	"	.279	33.5	-	71.1	2.12				
	"	.208	25.0	-	50.9	2.04				
8/27	.1137	.384	58.9	-	137	2.32				Co-60 Irradiation
	"	.575	88.2	-	187	2.12				Insufficient NaOH
	"	.279	42.8	-	103	2.40				added to assure
	"	.208	31.9	-	74.8	2.34				proper pH
	.220	.279	42.8	-	99.6	2.32				
	.220	.208	31.9	-	71.6	2.24				
9/2	.1139	.384	63.0	-	146	2.32				Co-60 Irradiation
	.220	.384	63.0	-	144	2.29				
	.1139	.575	94.4	-	180	1.91				
	.220	.575	94.4	-	187.5	1.99				
	.1139	.279	45.8	-	106.8	2.33				
	.220	.279	45.8	-	106.8	2.33				
	.1139	.208	34.1	-	80.6	2.35				
	.220	.208	34.1	-	78.2	2.29				
9/17	.119	0.84	6.71	0.110	17.4	2.59	.054	.11	.095	Pile Irradiation
	"	0.86	6.88	0.120	18.1	2.63	.054	.12	.10	
	"	3.90	31.2	9.7	70.3	2.26	.054	9.9	8.4	
	"	3.80	30.4	9.5	70.3	2.32	.054	9.6	8.2	
	"	7.20	57.5	20	136	2.37	.054	20	17.3	
	"	6.84	54.7	19	127	2.32	.054	19.3	16.4	
	"	4.78	38.2	13	87.0	2.28	.054	13.2	11.2	
	"	4.78	38.2	13	83.9	2.20	.054	13.2	11.2	
9/17	"	0.86	8.6	.120	22.1	2.57	.054	.153	.130	
	"	3.80	38.0	9.5	87.8	2.31	.054	12.1	10.3	
	"	6.84	68.4	19	149.8	2.19	.054	24	20.5	
	"	4.79	47.9	14	104.0	2.17	.054	17.8	15.1	
	.248	0.83	8.3	.105	21.4	2.57	.113	.23	.20	
	"	3.87	38.7	9.6	83.8	2.17	.113	21.5	18.3	
	"	7.20	72.0	20	160.2	2.23	.113	45	38	
	"	4.78	47.8	14	109.0	2.28	.113	32	27	

TABLE XVII

BENZENE-WATER-LITHIUM METABORATE

Date	$[LiBO_2]$ mol/Liter	Gamma Dose Rate Krep/Min.	Total Gamma Dose Krep	$\phi_T \times 10^{-9}$ Neut./cm^2 sec	$[P]_o$ mol/Liter	A_o mols/(Krep)(Lit)	Σ_a cm^{-1}	Neutron Capture Energy E_r (Kiloreps)	Neutron Capture Energy E_a (Kiloreps)	
9/6	0.154	.384	43.9	-	74.9	1.71	Co-60 Irradiation			
	"	.575	65.6	-	101	1.54				
	"	.279	31.8	-	52.8	1.66				
	0.102	.384	43.9	-	70.2	1.60				.027M H_2SO_4(pH = 5)
	"	.575	65.6	-	103.3	1.57				"
	"	.279	31.8	-	53.6	1.69				"
9/8	.165	.384	51.4	-	84.4	1.67	Co-60 Irradiation			
	"	.575	76.9	-	113	1.47				
	"	.279	37.3	-	60.5	1.62				
	"	.208	27.8	-	44.9	1.62				
	.110	.384	51.4	-	86.6	1.69				.0826M H_2BO_3(pH = 5)
	"	.279	37.3	-	63.8	1.71				"
	"	.575	76.9	-	110	1.43				.027M H_2SO_4
	"	.208	27.8	-	42.5	1.53				"
9/9	.165	.384	14.1	-	24.2	1.72	Co-60 Irradiation			
	"	.384	14.1	-	23.9	1.69				
	"	.575	21.1	-	36.2	1.72				
	"	.575	21.1	-	36.0	1.71				
	"	.279	10.2	-	17.1	1.67				
	"	.279	10.2	-	17.1	1.67				
	"	.208	7.62	-	12.6	1.65				
	"	.208	7.62	-	12.6	1.65				
9/19	.162	0.86	5.1	.120	10.3	2.0	.804	.14	.12	
	"	0.83	5.0	.105	10.0	2.0	.804	.12	.10	
	"	3.87	23.2	9.6	40.6	1.75	.804	10.8	9.3	
	"	3.80	22.8	9.5	37.9	1.66	.804	10.5	9.2	
	"	7.20	45.8	20	79.0	1.73	.804	22	19.3	
	"	6.84	41.2	19	69.5	1.69	.804	21	18.4	
	"	4.79	28.7	14	49.0	1.71	.804	15.5	13.5	
	"	4.78	28.3	14	48.2	1.71	.804	15.5	13.5	

X. NOMENCLATURE

A(X)	Micromols (μ mols) of component X formed per kilorep
A	Atomic weight
a	Avogadro's number
b	Jaffé's measure of the radius of the ionized column
C	Arbitrary constants or collected rate constants
CR	Cadmium ratio = $\frac{\text{activity of bare gold foil}}{\text{activity of cadmium covered gold foil}}$
D	Diffusion coefficient of radicals or thermal neutrons
D	Optical density
E	Energy
$\frac{dE}{dx}$	LET (linear energy transfer of ionizing radiation)(ev/$\mathring{A}$)
$\left(\frac{dE_\gamma}{dt}\right)_a$	Gamma dose rate
F	Dilution factor
G(X)	Molecule of component X formed per 100 ev absorbed
	(Fe^{3+}) designates the yield of the Fricke dosimeter
	(P) designates phenol; (PX) phenyl peroxide;
	(DP) diphenyl
	G(F) = 100 ev yield of $2H_2O \rightarrow H_2 + H_2O_2$
	G(E) = 100 ev yield of $2H_2O \rightarrow 2H + H_2O_2$
	G(R) = 100 ev yield of $H_2O \rightarrow H + OH$
G_i	Instantaneous G value
I_o, I_1, K_o, K_1	Bessel functions
k	Reaction rate constant (subscript refers to particular reaction defined in text)

NOMENCLATURE (CONT'D)

L	Mean free path
(MW)	Molecular weight
M	Atoms or molecules/cm^3
m	Mole fraction
$\mathcal{m}$	Molarity (mols/liter)
N_o	Radical pairs formed initially/cm.
N_∞	Radical pairs remaining after spur is dissipated
n	Radicals of one kind/cm^3
$(\bar{n}_c/\bar{n}_m)$	Relative number of neutron captures in a cylinder
P	Reactor power level (kilowatts)
p	Path length of transmission cell
Q	Slowing down density (neutrons/cm^3/sec)
R	Radius
$\bar{R}$	Average path of a particle in the reaction system
r	Radial coordinate
$\bar{r}_o$	Initial spur radius
S	Neutron utilization, molecules reacted/neutron capture
t	Time
V	Volume of experimental system
W	Work to form an ion pair (ev/ion pair)
w	Weight fraction
x	Average fraction of the initial energy of a neutron/collision
y	Fraction of the released energy that is absorbed in reacting system

NOMENCLATURE (CONT'D)

Greek Letters

α	Angle
β	Energy released per neutron capture
γ	$\sqrt{\Sigma_a/D}$
ϵ	Molar extinction coefficient (liter/mol/cm)
κ	Calibration constant for phenol analysis
μ	Gamma absorption coefficient
$\bar{\mu}$	Average cosine of the neutron scattering angle
ξ	Average logarithmic energy decrement/collision
ρ	Density (gm/cm^3)
Σ	Macroscopic cross-section
σ	Microscopic cross-section
Φ	Neutron flux (neut.-cm/cm^3/sec)

Subscripts

a	Absorption
avg	Average
c	Cylinder
F	Fast
f	Final
n	Neutron
o	Initial
r	Released
t	Total
T	Thermal
W	Water
γ	Gamma photon

XI. BIBLIOGRAPHY

1. Allen, A.O., MDDC-962 (AEC Publication, undated).

2. Allen, A.O., Radiation Research, 1, 85 (1954).

3. Allen, A.O., Proc. Geneva Conference, 7, 513 (1955).

4. Allen, A.O., Schuler, R.H., J. Am. Chem. Soc., 77, 507 (1955)

5. Allen, A.O., Schuler, R.H., J. Am. Chem. Soc., 79, 1565 (1957)

6. Alyea, H.N., J. Am. Chem. Soc., 52, 2743 (1930).

7. Bamford, C.H., Jenkins, A.D., Proc. Roy. Soc. (London) A228, 220 (1955).

8. Baxendale, J.H., Magee, J., Discussions Faraday Soc., 14, 160 (1953).

9. Baxendale, J.H., Smithies, D., J. Chem. Phys., 23, 604 (1955).

10. Benedict, M., Pigford, T.H., Nuclear Chemical Engineering, McGraw-Hill Book Company, Inc., New York (1957).

11. Bevington, J.C., Eaves, D.E., Nature, 178, 1112 (1956).

12. Birks, J.B., J. Chem. Phys., 20, 1655 (1952).

13. Bonét-Maurey, P., Brit. J. Radiol, 24, 422 (1951)

14. Bopp, C.D., Sisman, O., Nucleonics, 14 (1), 46 (1956).

15. Braid, T.H., Phys. Rev., 102, 1109-23 (1956)

16. Bray, B.G., "The Effects of Gamma Radiation on Several Polysulfone Reactions" Ph.D. Dissertation, Univ. of Mich., Ann Arbor, (1957).

17. Burton, M., J. Phys. & Colloid Chem., 51, 611 (1947).

18. Burton, M., J. Phys. & Colloid Chem., 51, 786 (1947).

19. Burton, M., J. Phys. & Colloid Chem., 52, 564 (1948).

20. Burton, M., J. Phys. & Colloid Chem., 52, 810 (1948).

21. Collinson, E., Dainton, F.S., Discussions Faraday Soc., 12, 212 (1952).

BIBLIOGRAPHY (CONT'D)

22. Collinson, E., Swallow, A.J., Chem. Rev., 56, 471 (1956).

23. Collinson, E., et al., Trans. Faraday Soc., 53, 357 (1957).

24. Coulson, C.A., J. Chem. Soc., 778 (1956).

25. Dainton, F.S., J. Phys. & Colloid Chem., 52, 490 (1948).

26. Dainton, F.S., Ann. Rev. Phys. Chem., 2, 112 (1951).

27. Daniels, M., Scholes, G., Weiss, J., J. Chem. Soc., 832 (1956).

28. Day, M.J., Stein, G., Nature, 164, 671 (1949).

29. Dewhurst, H.A., J. Chem. Phys., 19, 1329 (1951).

30. Dewhurst, H.A., Trans. Faraday Soc., 48, 905 (1952).

31. Dewhurst, H.A., Samuel, A.H., Magee, J.L., Radiation Research, 1, 62 (1954).

32. Dorfman, L.M., Shipko, F.J., KAPL 1337 (AEC Publication, 1955).

33. Dyne, P.J., Can. J. Chem., 33, 1109 (1955).

34. Ehrenburg, L., Saeland, E., JENER 8 (Joint Establishment for Nuclear Energy Research, Norway, 1954).

35. Eyring, H., Herschfelder, J.O., Taylor, H.S., J. Chem. Phys., 4, 570 (1936).

36. Fenstermacher, C.A., et al., Phys. Rev., 107, 1650 (1957).

37. Fluharty, R.G., Nucleonics, 2, (5), 28 (1948).

38. Folin, O., Looney, J.M., J. Biol. Chem., 51, 421 (1922).

39. Franck, J., Rabinowitsch, E., Trans. Faraday Soc., 30, 120 (1934).

40. Freeman, G.R., van Cleave, A.B., Spinks, J.W.T., Can. J. Chem., 21, 448, (1953).

41. Fricke, H., Ann. N.Y. Acad. Sci., 59, 567 (1955).

42. Ganguly, A.K., Magee, J.L., J. Chem. Phys., 25, 129 (1956).

43. Ghormley, J.A., Radiation Research, 5, 247 (1956).

44. Glasstone, S., Edlund, M.C., The Elements of Nuclear Reactor Theory, D. Van Nostrand Co. Inc., New York (1955).

BIBLIOGRAPHY (CONT'D)

45. Hardwick, T.J., Can. J. Chem., 30, 17 (1952).

46. Hart, E.J., ANL 4636 (AEC Publication, 1951).

47. Hart, E.J., Radiation Research 1, 53 (1954).

48. Hirschfelder, J.O., J. Phys. & Colloid Chem., 52, 447 (1948).

49. Hochanadel, C.J., David, T.W., Proc. Geneva Conference, 7, 521 (1955).

50. Hochanadel, C.J., Ghormely, J.A., J. Chem. Phys., 21, 880 (1953).

51. Hughes, D.J., Pile Neutron Research, Addison Wesley Co., Cambridge, Mass., (1953).

52. Jaffé, G., Ann. Physik, 42, 303 (1913).

53. Johnson, E.B., et al., ORNL-1871 (AEC Publication, 1955).

54. Johnson, E.R., Allen, A.O., J. Am. Chem. Soc., 74, 4147 (1952).

55. Keene, J.P., Radiation Research, 6, 424 (1957).

56. Kelly, P., Rigg, T., Weiss, J., Nature, 173, 1130 (1954).

57. Lazo, R.M., Dewhurst, H.A., Burton, M., J. Chem. Phys., 22, 1370, (1954).

58. Lea, D.E., Brit. J. Radiol Supplement, 1, 59 (1947).

59. Lea, D.E., Actions of Radiations on Living Cells, The Macmillan Company, New York (1947).

60. Lefort, M., Ann. Rev. Phys. Chem., 9, 123 (1958).

61. Lind, S.C., J. Phys. Chem., 16, 564 (1912).

62. Lind, S.C., J. Am. Chem. Soc., 47, 2675 (1925).

63. Lind, S.C., Bardwell, D.C., J. Am. Chem. Soc., 48, 2335 (1926).

64. Lind, S.C., Bardwell, D.C., Perry, J.H., J. Am. Chem. Soc., 48, 1556 (1926).

65. Lind, S.C., Bardwell, D.C., Perry, J.H., J. Am. Chem. Soc., 48, 1575 (1926).

66. Loeble, H., Stein, G., Weiss, J., J. Chem. Soc., 2704 (1950).

BIBLIOGRAPHY (CONT'D)

67. Magee, J.L., Burton, M., J. Am. Chem. Soc., 72, 1965 (1950).

68. Magee, J.L , Burton, M., J. Am. Chem. Soc., 73, 523 (1951).

69. Majury, T.G., J. Polymer Sci., 15, 297 (1955).

70. Manion, J.P., Burton, M , J. Phys. Chem., 56, 560 (1952).

71. McDonell, W.R., UCRL 1378 (AEC Publication, 1951).

72. McDonell, W.R., ANL 4949 (AEC Publication, 1952).

73. McDonell, W.R , ANL 5205 (AEC Publication, 1954).

74. Meisels, G.G., Hamill, W.H., Williams, R.R., J. Chem. Phys., 25, 790 (1956).

75. Mellor, J.H., A Comprehensive Treatise on Inorganic and Theoretical Chemistry, 5, 52-53, Longmans, Green and Co., New York (1937).

76. Mesrobian, R.B., Ander, P., Ballantine, D S., Dienes, G.J., J. Chem. Phys., 22, 565 (1954).

77. Miley, G.H., Use of Nuclear Reactor Radiation to Promote Chemical Reactions, Ph.D. Dissertation, Univ. of Mich., Ann Arbor (1958).

78. Miller, N., J. Chem. Phys., 18, 79 (1950).

79. Miller, N., Wilkinson, J., Discussions Faraday Soc., 12, 50 (1952).

80. Monchick, L., Magee, J.L., Samuel, A.H., J Chem. Phys., 26, 935 (1957).

81. Noyes, R.M., J. Am. Chem. Soc., 77, 2042 (1955).

82. Oldenburg, O., J. Chem. Phys., 2, 713 (1934).

83. Patrick, W N., Burton, M., J. Am. Chem. Soc., 76, 2626 (1954).

84. Phung, P.V., Burton, M., Radiation Research, 7, 199 (1957).

85. Platzman, R.L., Radiation Research, 2, 1 (1955).

86. Prevost-Bernas, A., et al., Discussions Faraday Soc., 12, 98 (1952).

87. Pringle, B.D , Phys. Rev., 87, 1016 (1952).

88. Reed, J., Brit. J. Radiol., 23, 621 (1950).

89. Rigg, T., Stein, G., Weiss, J., Proc. Roy. Soc. (London) A211, 375 (1952).

BIBLIOGRAPHY (CONT'D)

90. Saeland, E., Proc. Geneva Conference, 7, 610 (1955).

91. Samuel, A.H., Magee, J.L., J. Chem. Phys., 21, 1080 (1953).

92. Schoepfle, C.S., Fellows, C.H., Ind. & Eng. Chem., 23, 1396 (1931).

93. Schuler, R.H., Allen, A.O., J. Chem. Phys., 24, 56 (1956).

94. Schuler, R.H., Barr, N.F., J. Am. Chem. Soc., 78, 5756, (1956).

95. Schuler, R.H., Petry, R.C., J. Am. Chem. Soc., 78, 3954 (1956).

96. Schulte, J.W., Suttle, J.F., Wilhelm, R., J. Am. Chem. Soc., 75, 2222 (1953).

97. Schwarz, H., J. Am. Chem. Soc., 77, 4960 (1955).

98. Selke, W.A., et al., NYO 3328 (AEC Publication, 1952).

99. Sheppard, C.W., Burton, V.L., J. Am. Chem. Soc., 68, 1636 (1946).

100. Shields, N.P., Bolt, R.O., Carroll, J.G., Nucleonics, 14, (8), 54 (1956).

101. Spencer, L.V., Attix, F.H., Radiation Research, 3, 239 (1955).

102. Spiers, F.W., Discussions Faraday Soc., 12, 13 (1952).

103. Steacie, W.R., J. Phys. & Colloid Chem., 52, 441 (1948).

104. Stein, G., Weiss, J., Nature, 161, 650 (1948).

105. Stein, G., Weiss, J., J. Chem. Soc., 3245 ff (1949).

106. Stein, G , Weiss, J., Nature, 166, 1104 (1950).

107. Sutton, J., Draganic, I., Hering, H., CEA 414 (French AEC Publication, 1955).

108. Sworski, T.J., J. Chem. Phys., 20, 1817 (1952).

109. Sworski, T.J., Radiation Research, 1, 231 (1954).

110. Tolbert, B.M., Lemmon, R.M., Radiation Research, 3, 52, (1955).

111. Trice, J.B., Nucleonics, 16, (7), 81-83 (1958).

112. Weiss, J., Nature, 153, 748 (1944).

BIBLIOGRAPHY (CONT'D)

113. Weiss, J , Nucleonics, 10 (7), 28-31 (1952).

114. Weiss, J., Nature, 174, 78 (1954).

115. Weiss, J., Experientia, 12, 280 (1956).

116. AECD-3647, The Reactor Handbook, Vol. 3, Sec. 1 (AEC Publication, 1955).

117. A.S.M.E. Boiler and Pressure Vessel Code, Vol. 8 (1952).

118. The Ford Nuclear Reactor - Description and Operation, Univ. of Mich., Ann Arbor (1957).

119. Initial Calibration of the Ford Nuclear Reactor, Univ. of Mich., Ann Arbor (1958).

120. International Critical Tables, Vol. 3, 257, McGraw-Hill Book Co., New York (1926).

121. Handbook of Chemistry and Physics, Chemical Rubber Publishing Co., Cleveland, Ohio (1951).

122. Calkins, V. P., Chemical Engineering Symposium Series, 50 (12), 28 (1954).